Supplementary Information

for

Peptide foldamer-based inhibitors of the SARS-CoV-2 S protein - human ACE2 interaction

Violeta Marković, Jeelan Basha Shaik, Katarzyna Ożga, Agnieszka Ciesiołkiewicz, Juan Lizandra Perez, Ewa Rudzińska-Szostak, Łukasz Berlicki*

Table of contents   **page**

Table S1. Analytical data of ACEa1 and their analogues

Name	MS calculated	MS found	analytical HPLC		preparative HPLC	
			Retention time (min)	gradient	Retention time (min)	gradient
ACEα1	934.7869 [M + 3H$^+$]	934.7861 [M + 3H$^+$]	13.29	A	19.76	A
A1	950.1515 [M + 3H$^+$]	950.1512 [M + 3H$^+$]	17.26	A	23.85	A
A1a	1212.6628 [M + H$^+$]	1212.6626 [M + H$^+$]	14.86	A	16.89	A
A1b	626.3138 [M + 2H$^+$]	626.3176 [M + 2H$^+$]	13.59	A	14.19	A
A1c	650.3044 [M + 2H$^+$]	650.3006 [M + 2H$^+$]	20.65	A	17.61	A
A1_v1	961.5113 [M + 3H$^+$]	961.5126 [M + 3H$^+$]	15.20	A	23.83	A
A1_v2	1453.7725 [M + 2H$^+$]	1453.7930 [M + 2H$^+$]	16.13	A	24.91	A
A1_v3	970.1794 [M + 3H$^+$]	970.1803 [M + 3H$^+$]	15.98	A	25.43	A
A1_v4	1428.2338 [M + 2H$^+$]	1428.2454 [M + 2H$^+$]	15.67	A	25.11	A
A2	1395.7150 [M + 2H$^+$]	1395.7090 [M + 2H$^+$]	25.98	A	24.57	A
A2a	1155.6050 [M + H$^+$]	1155.6067 [M + H$^+$]	16.49	A	18.37	A
A2b	642.8266 [M + 2H$^+$]	642.8256 [M + 2H$^+$]	10.66	A	15.94	A
A2c	633.3123 [M + 2H$^+$]	633.3179 [M + 2H$^+$]	11.42	A	17.53	A
A2_v1	1412.7548 [M + 2H$^+$]	1412.8201 [M + 2H$^+$]	17.22	A	32.59	B
A2_v2	1424.2627 [M + 2H$^+$]	1424.3079 [M + 2H$^+$]	18.18	A	34.28	B
A2_v3	1425.7570 [M + 2H$^+$]	1425.7865 [M + 2H$^+$]	18.58	A	35.94	B
A2_v4	1399.2255 [M + 2H$^+$]	1399.2761 [M + 2H$^+$]	18.17	A	35.36	B
A3	949.4796 [M + 3H$^+$]	949.4785 [M + 2H$^+$]	15.50	A	33.74	A
A3a	1172.6316 [M + H$^+$]	1172.6313 [M + H$^+$]	13.02	A	15.34	A
A3b	1286.6169 [M + H$^+$]	1286.6163 [M + H$^+$]	7.92	B	15.26	A
A3c	1301.6166 [M + H$^+$]	1301.6171 [M + H$^+$]	12.90	A	19.53	A

Analytical HPLC program (eluent A: 0.05% TFA in H$_2$O, eluent B: 0.05% TFA in ACN, flow 0.9 mL/min, column: ReproSil Saphir 100 C18, 5μ, 150 x 4.6 mm):
A: t=0 min, 90 % A; t=2 min, 90% A; t=32 min, 10% A,
B: t=0 min, 90 % A; t=2 min, 90% A; t=20 min, 10% A.

Preparative HPLC programs (eluent A: 0.05% TFA in H₂O, eluent B: 0.05% TFA in ACN, flow 10 mL/min):

A: t=0 min, 90 % A; t=6 min, 90 % A; t=10 min, 75% A; t=20 min, 60% A; t=30 min, 60% A; t=35 min, 10 % A,

B: t=0 min, 90 % A; t=6 min, 90 % A; t=10 min, 75% A; t=40 min, 45% A; t=42 min, 10 % A.

Table S2. Analytical data of peptides **1-41**

Name	MS calculated	MS found	analytical HPLC		preparative HPLC	
			Retention time (min)	gradient	Retention time (min)	gradient
1	991.0601 [M + 2H⁺]	991.0590 [M + 2H⁺]	14.63	A	31.06	C
2	998.5693 [M + 2H⁺]	998.5263 [M + 2H⁺]	13.58	A	20.63	A
3	1034.5630 [M + 2H⁺]	1034.4657 [M + 2H⁺]	13.57	A	20.40	A
4	1035.0670 [M + 2H⁺]	1035.0679 [M + 2H⁺]	13.38	A	20.28	A
5	1091.4665 [M K⁺+ H⁺]	1091. 4868 [M + K⁺ + H⁺]	16.63	A	26.17	A
6	1135.5807 [M + 2H⁺]	1135.5791 [M + 2H⁺]	18.85	A	46.00	E
7	1079.0386 [M + 2H⁺]	1079.0906 [M + 2H⁺]	15.08	A	27.117	B
8	1116.0313 [M + 2H⁺]	1116.0376 [M + 2H⁺]	15.29	A	27.507	B
9	1115.5363 [M + 2H⁺]	1115.5863 [M + 2H⁺]	14.84	A	26.233	B
10	1151.5323 [M + 2H⁺]	1151.5377 [M + 2H⁺]	15.00	A	26.407	B
11	1147.5337 [M + 2H⁺]	1147.5325 [M + 2H⁺]	16.65	A	26.177	B
12	1161.5549 [M + 2H⁺]	1161.5541 [M + 2H⁺]	15.43	A	28.007	B
13	1139.0078 [M + 2H⁺]	1139.0553 [M + 2H⁺]	14.24	A	24.517	B
14	1160.0131 [M + 2H⁺]	1160.0117 [M + 2H⁺]	16.34	A	31.773	B
15	1184.0313 [M + 2H⁺]	1184.0369 [M + 2H⁺]	14.51	A	24.89	B
16	1176.0338 [M + 2H⁺]	1176.0411 [M + 2H⁺]	15.68	A	27.203	B
17	1158.5402 [M + 2H⁺]	1158.5487 [M + 2H⁺]	14.98	A	32.353	B
18	1151.5419 [M + 2H⁺]	1151.5477 [M + 2H⁺]	15.05	A	32.127	B
19	1184.5653 [M + 2H⁺]	1184.5657 [M + 2H⁺]	16.62	A	33.000	B

20	1167.5731 [M + 2H⁺]	1167.5747 [M + 2H⁺]	16.52	A	33.383	B
20	1167.5731 [M + 2H$^+$]	1167.5747 [M + 2H$^+$]	16.52	A	33.383	B
21	1167.5731 [M + 2H$^+$]	1167.5735 [M + 2H$^+$]	16.71	A	31.04	B
22	1142.0494 [M + 2H$^+$]	1142.0483 [M + 2H$^+$]	15.27	A	26.483	B
23	1150.0470 [M + 2H$^+$]	1150.0481 [M + 2H$^+$]	15.09	A	26.89	B
24	1125.0574 [M + 2H$^+$]	1125.0574 [M + 2H$^+$]	15.3	A	27.117	B
25	1171.0760 [M + 2H$^+$]	1171.0754 [M + 2H$^+$]	15.25	A	29.48	B
26	1173.0629 [M + 2H$^+$]	1173.0623 [M + 2H$^+$]	15.89	A	27.22	B
27	1182.5840 [M + 2H$^+$]	1182.5743 [M + 2H$^+$]	15.02	A	32.71	C
28	1178.56 [M + 2H$^+$]	1178.56 [M + 2H$^+$]	15.75	A	28.25	B
29	1168.5627 [M + 2H$^+$]	1168.5641 [M + 2H$^+$]	15.7	A	27.00	B
30	1168.5627 [M + 2H$^+$]	1168.5638 [M + 2H$^+$]	15.82	A	26.89	B
31	1192.1051 [M + 2H$^+$]	1192.1146 [M + 2H$^+$]	14.79	A	25.01	C
32	1189.0903 [M + 2H$^+$]	1189.1252 [M + 2H$^+$]	15.16	A	27.99	C
33	1190.0933 [M + 2H$^+$]	1190.0872 [M + 2H$^+$]	15.58	A	32.23	B
34	1211.5868 [M + 2H$^+$]	1211.6257 [M + 2H$^+$]	15.14	A	33.43	E
35	1189.5918 [M + 2H$^+$]	1189.5957 [M + 2H$^+$]	15.50	A	33.40	E
36	1186.5922 [M + 2H$^+$]	1186.5850 [M + 2H$^+$]	14.18	A	23.49	C
37	1207.5974 [M + 2H$^+$]	1207.5916 [M + 2H$^+$]	14.68	A	27.32	C
38	1199.5762 [M + 2H$^+$]	1199.5793 [M + 2H$^+$]	15.05	A	29.77	B
39	1208.0751 [M + 2H$^+$]	1208.0784 [M + 2H$^+$]	14.46	A	28.32	C
40	1220.5997 [M + 2H$^+$]	1220.6147 [M + 2H$^+$]	15.91	A	28.80	D
41	1203.5894 [M + 2H$^+$]	1203.5493 [M + 2H$^+$]	15.68	A	27.15	D

Analytical HPLC program (eluent A: 0.05% TFA in H$_2$O, eluent B: 0.05% TFA in ACN, flow 0.9 mL/min):

A: t=0 min, 90 % A; t=2 min, 90% A; t=32 min, 10% A (ReproSil Saphir 100 C18, 5µ, 150 x 4.6 mm column).

Preparative HPLC programs (eluent A: 0.05% TFA in H$_2$O, eluent B: 0.05% TFA in ACN, flow 10 mL/min):

A: t=0 min, 90 % A; t=6 min, 90 % A; t=10 min, 75% A; t=20 min, 60% A; t=30 min, 60% A; t=35 min, 10 % A,

B: t=0 min, 90 % A; t=6 min, 90 % A; t=10 min, 75% A; t=40 min, 45% A; t=42 min, 10 % A,

C: t=0 min, 85 % A; t=6 min, 85 % A; t=10 min, 73% A; t=40 min, 50% A; t=42 min, 10 % A,
D: t=0 min, 85 % A; t=6 min, 85 % A; t=10 min, 65% A; t=40 min, 50% A; t=42 min, 10 % A,
E: t=0 min, 85 % A; t=6 min, 85 % A; t=10 min, 70% A; t=40 min, 50% A; t=42 min, 10 % A.

Table S3. Sequences of helix α1 of ACE2 (ACEα1) and their foldameric analogues. Residues interacting with protein S are marker in red. Mutated residues are shown in green and blue. *Trans*-(1*S*,2*S*)-2-aminocyclopentanecarboxylic acid residues are shown as black pentagons.

Entry	Peptide	Amino acid sequence
1	ACEα1	IEEQAKTFLDKFNHEAEDLFYQS-NH2
2	A1	I⬟EQ⬟KTF⬟DK⬟NHE⬟ED⬟FYQ⬟-NH2
3	A1a	I⬟EQ⬟KTF⬟D-NH2
4	A1b	F⬟DK⬟NHE⬟E-NH2
5	A1c	HE⬟ED⬟FYQ⬟-NH2
6	A1_v1	I⬟EQ⬟KHF⬟EY⬟NSE⬟HM⬟FRQ⬟-NH$_2$
7	A1_v2	I⬟EQ⬟KHF⬟EW⬟NSE⬟HM⬟FRQ⬟-NH$_2$
8	A1_v3	I⬟EQ⬟KYF⬟EY⬟NSE⬟HM⬟FRQ⬟-NH$_2$
9	A1_v4	I⬟EQ⬟KHF⬟EY⬟NSE⬟HM⬟FEQ⬟⁻NH$_2$
10	A2	I⬟EQA⬟TF⬟DKF⬟HE⬟EDL⬟YQ⬟-NH2
11	A2a	I⬟EQA⬟TF⬟D-NH2
12	A2b	F⬟DKF⬟HE⬟E-NH2
13	A2c	HE⬟EDL⬟YQ⬟-NH2
14	A2_v1	I⬟EQA⬟HF⬟EYF⬟SE⬟HML⬟RQ⬟-NH$_2$
15	A2_v2	I⬟EQA⬟HF⬟EWF⬟SE⬟HML⬟RQ⬟-NH$_2$
16	A2_v3	I⬟EQA⬟YF⬟EYF⬟SE⬟HML⬟RQ⬟-NH$_2$
17	A2_v4	I⬟EQA⬟HF⬟EYF⬟SE⬟HML⬟EQ⬟-NH$_2$
18	A3	I⬟EQAKTF⬟DKFNHE⬟EDLFYQ⬟-NH2
19	A3a	I⬟EQAKTF⬟D-NH2
20	A3b	F⬟DKFNHE⬟E-NH2
21	A3c	HE⬟EDLFYQ⬟-NH2
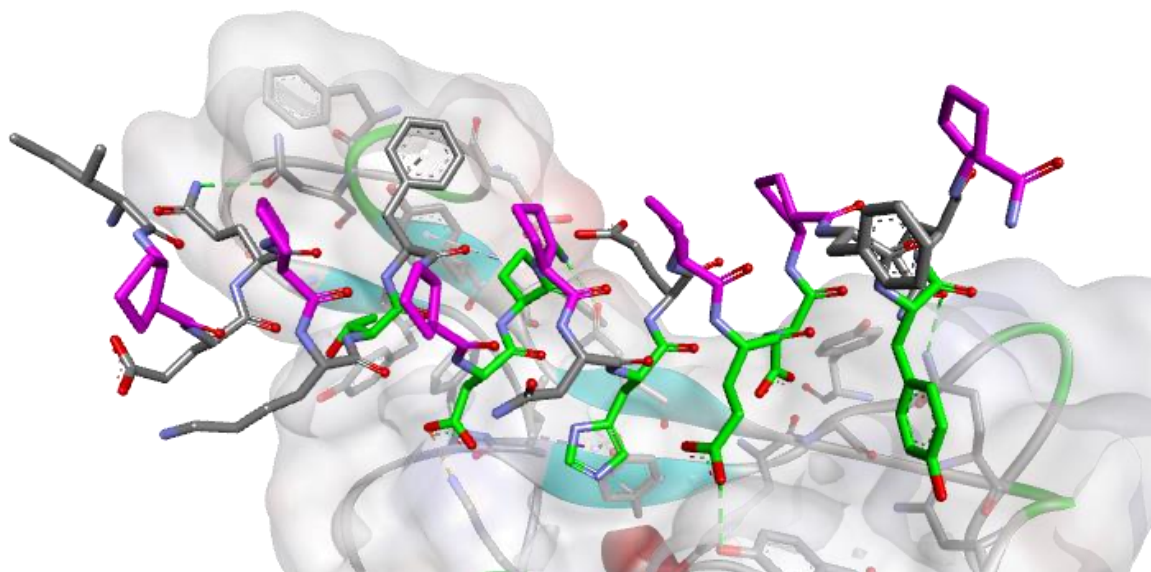
Figure S1. Modeled complex of peptide **A1** and the RBD domain of protein S (*trans*-ACPC residues forming "β-stripe" are colored pink).
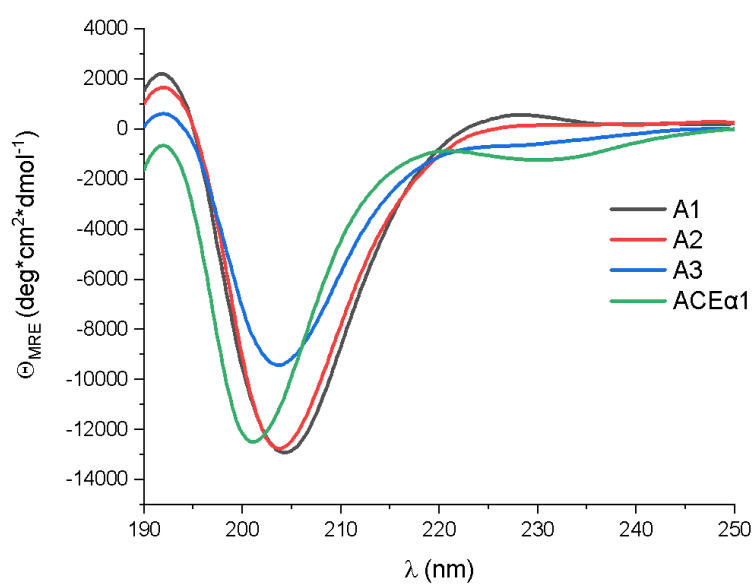
Figure S2. Comparison of CD spectra of peptides A1-3, and ACEα1 dissolved in potassium phosphate buffer, 50 mM, pH 7.5.
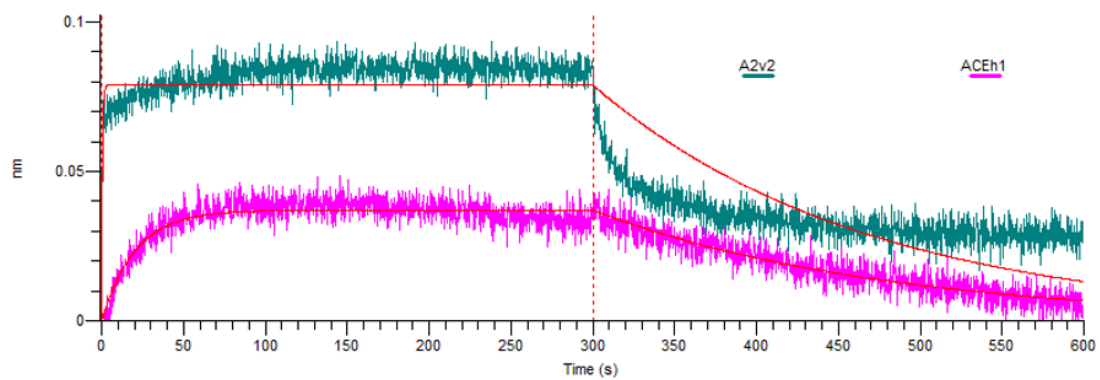
Figure S3. Comparison of BLI sensograms of peptides **ACEα1** and **A2_v2**.
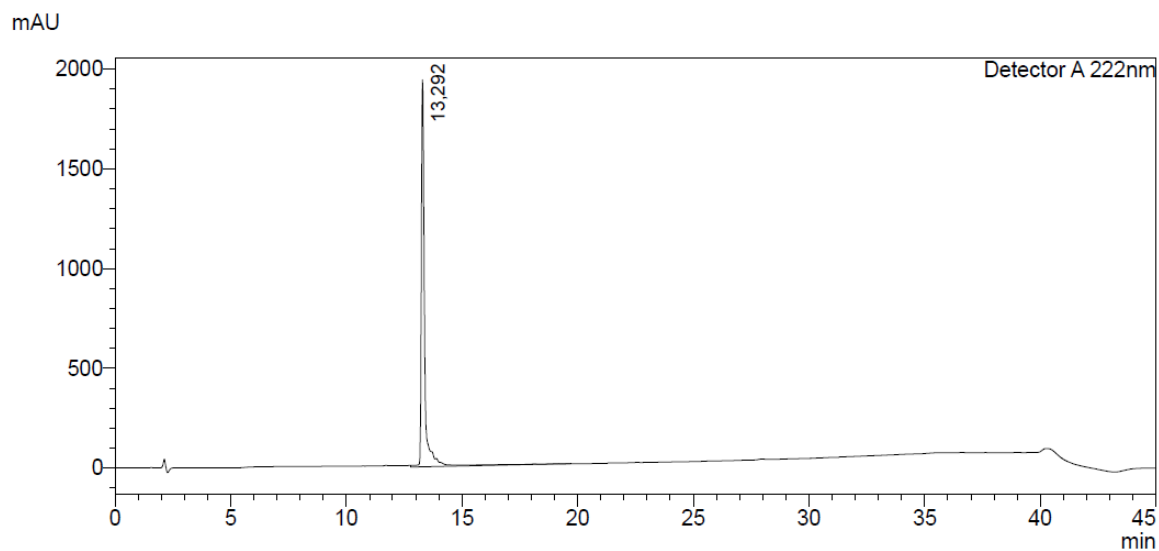
Figure S4. HPLC chromatogram of peptide **ACEα1**.
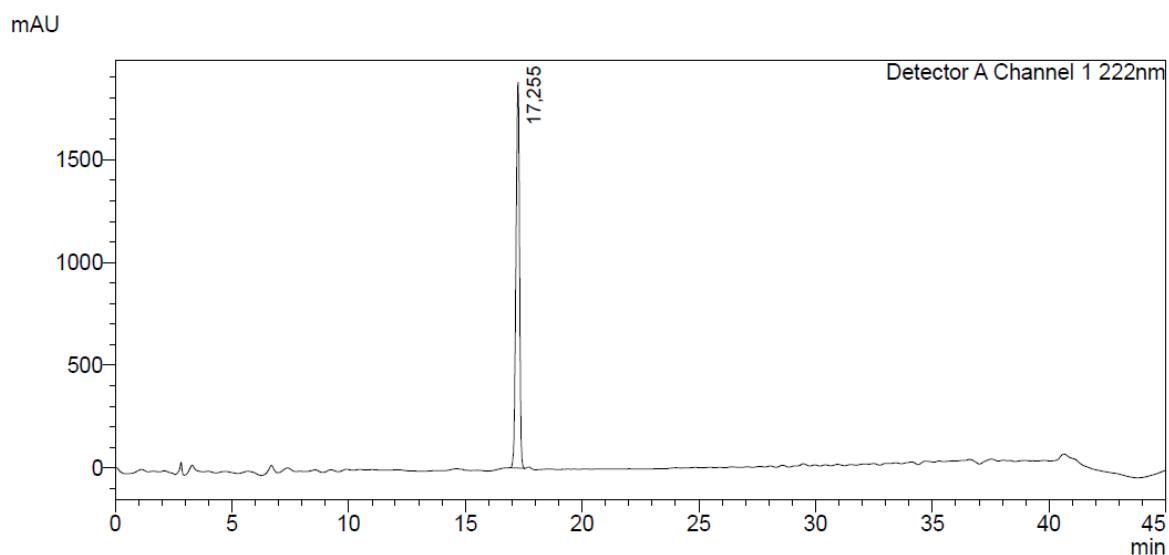
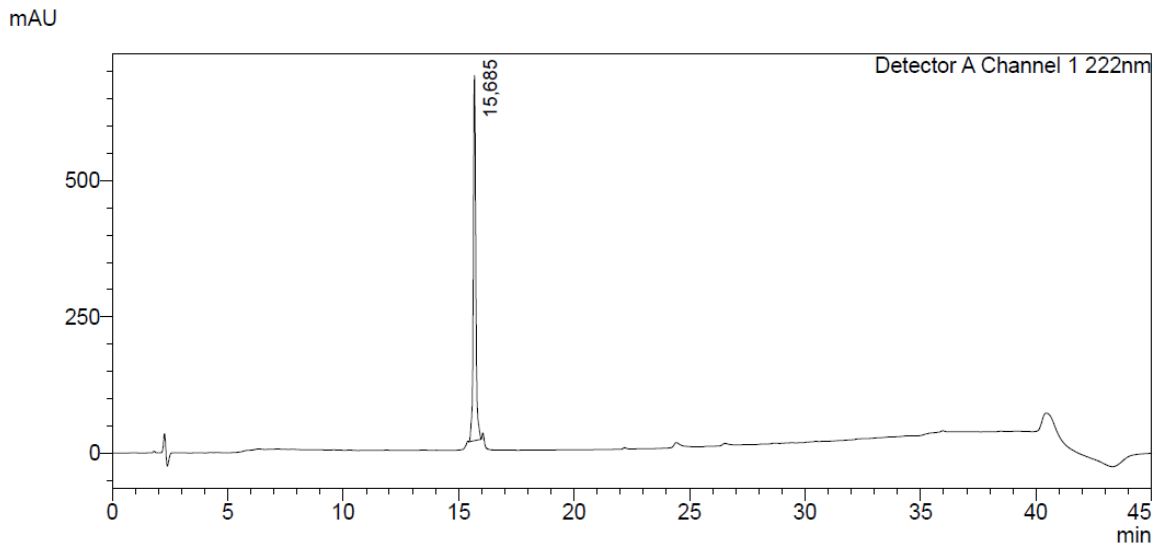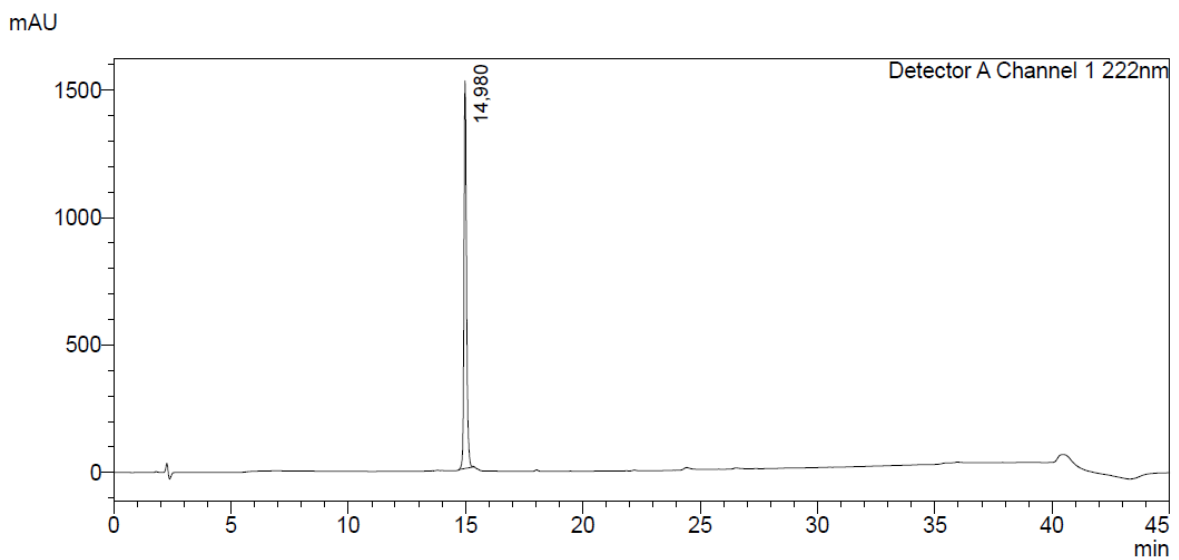**Figure S5**. HPLC chromatogram of peptide **A1**.
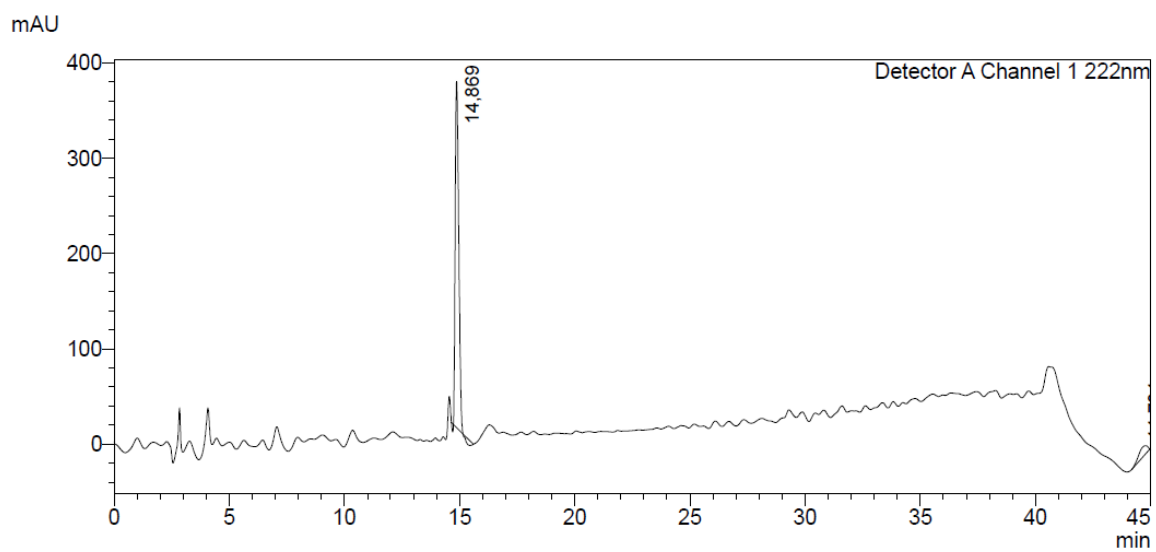
Figure S6. HPLC chromatogram of peptide **A1a**.
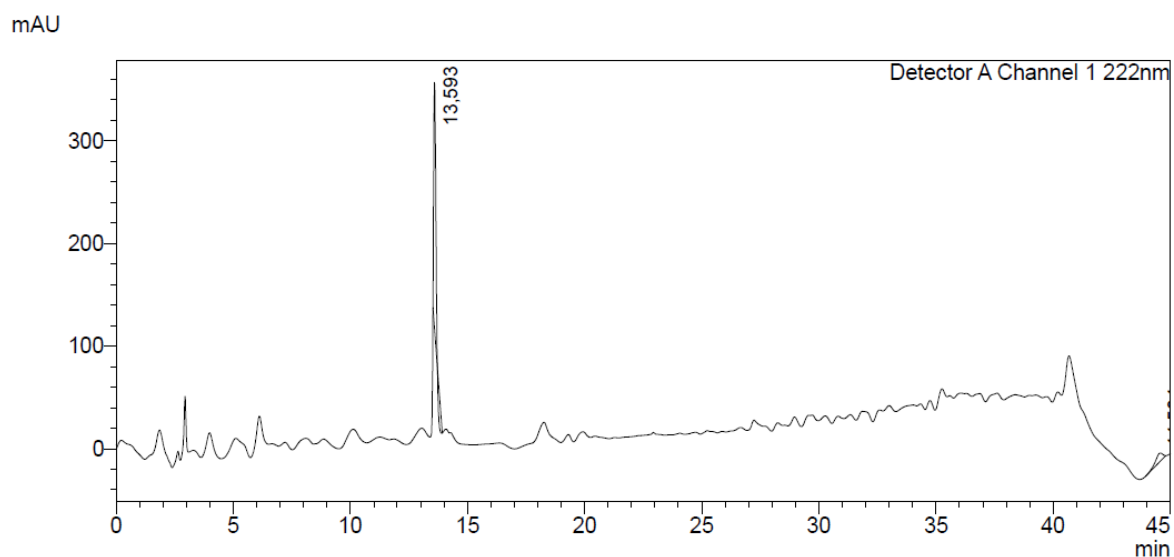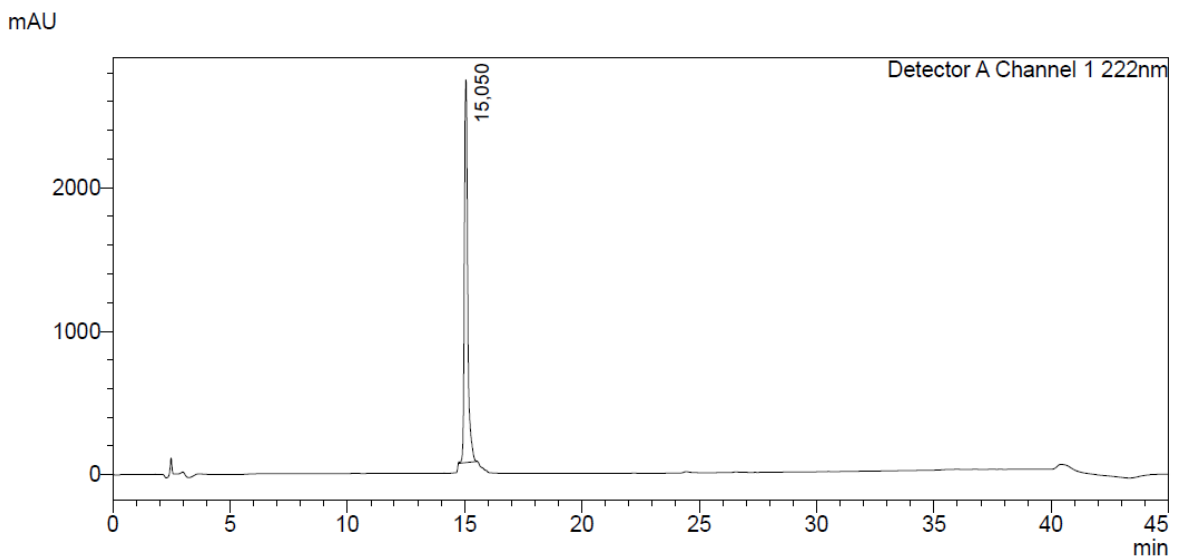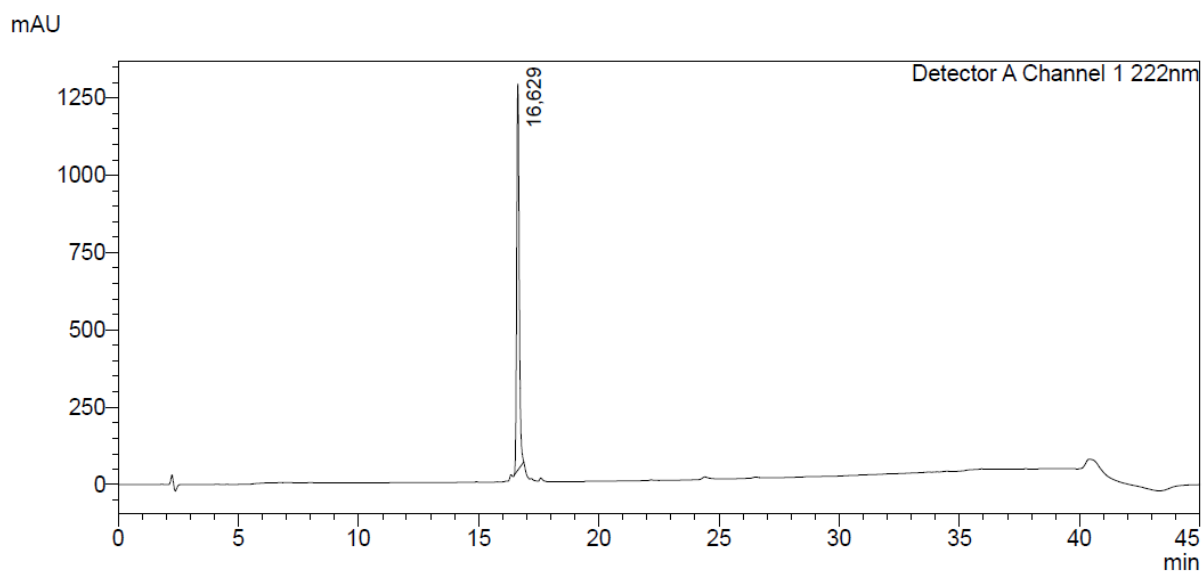
Figure S7. HPLC chromatogram of peptide **A1b**.
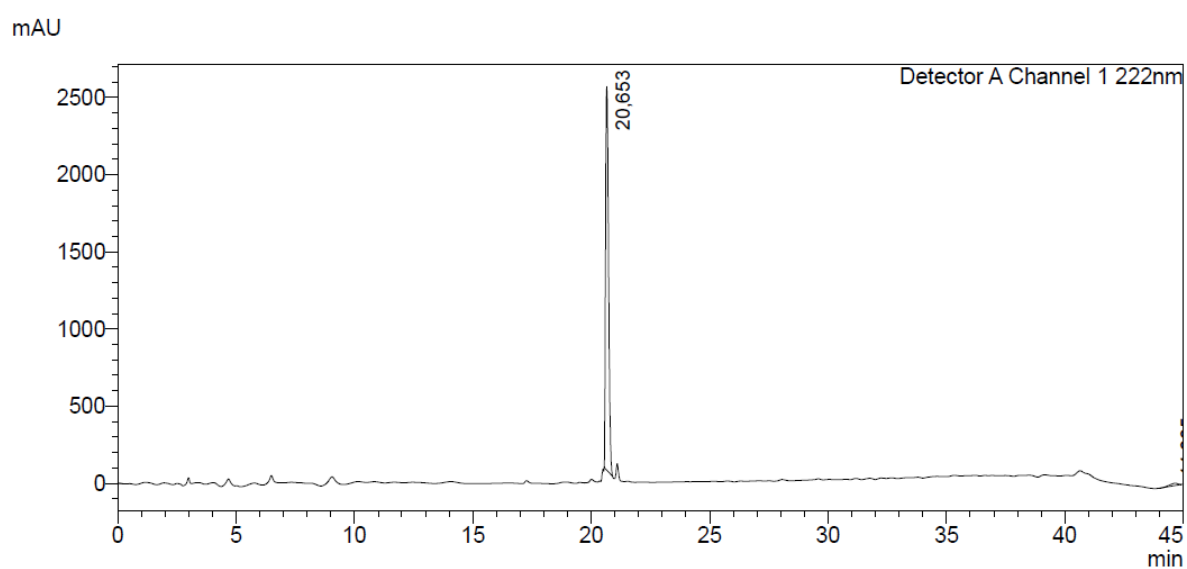
Figure S8. HPLC chromatogram of peptide **A1c**.
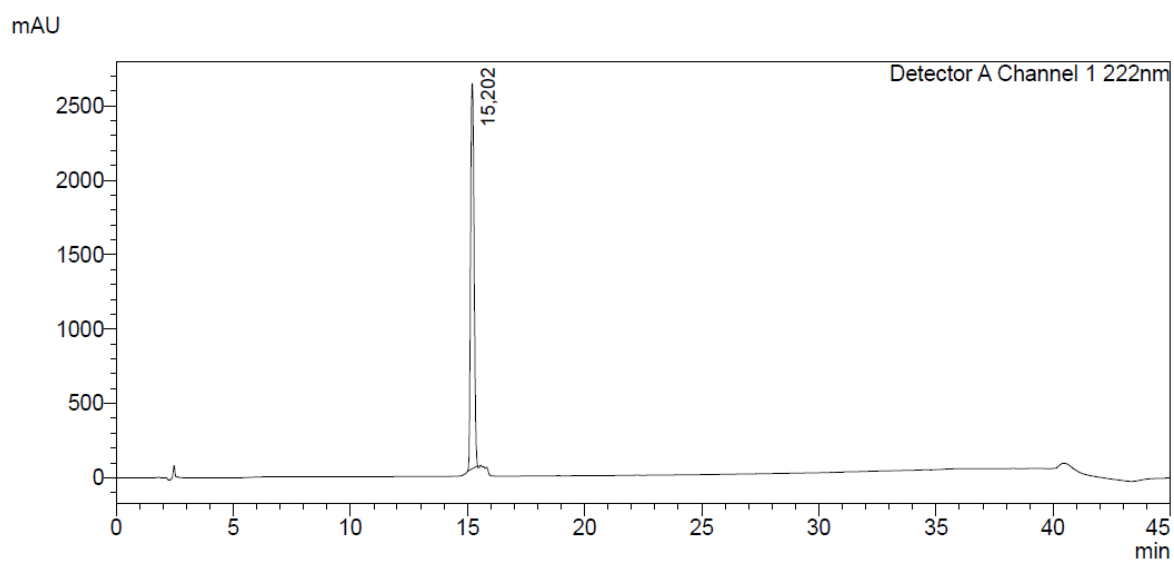
Figure S9. HPLC chromatogram of peptide **A1v1**.
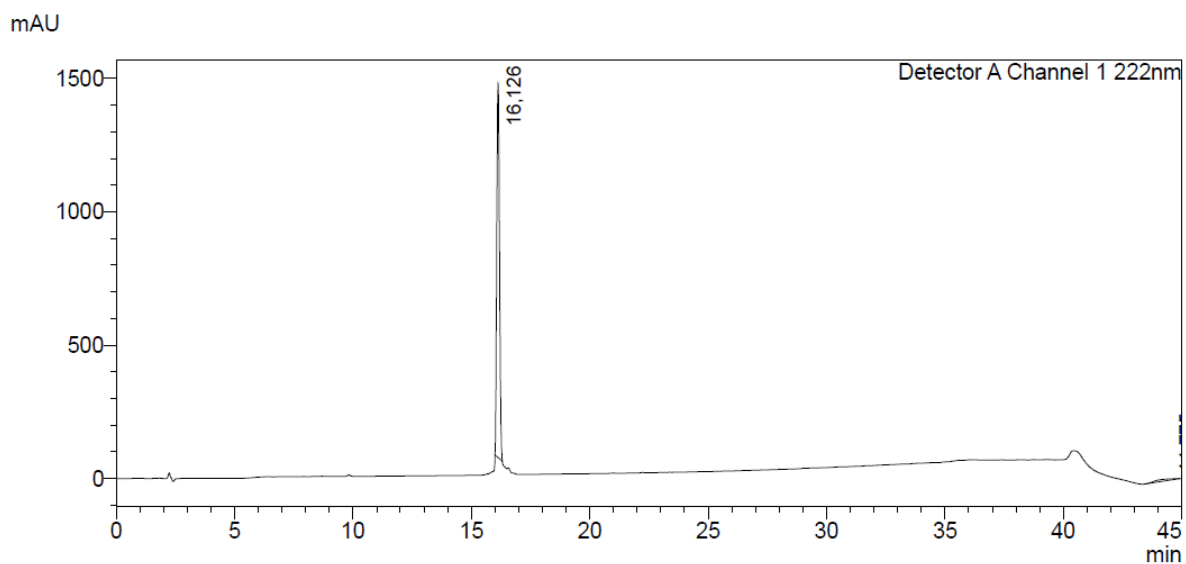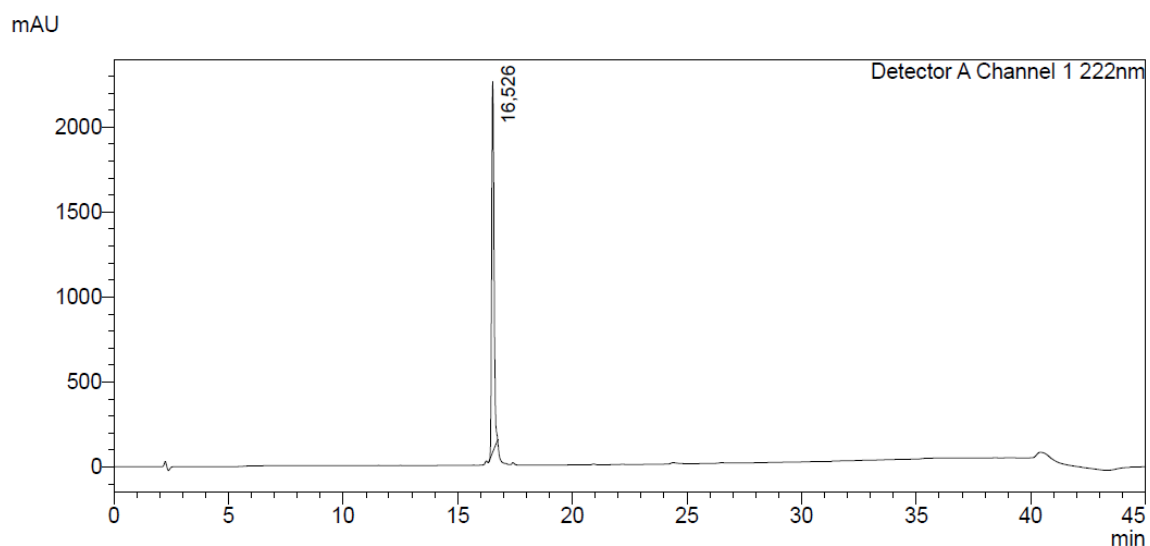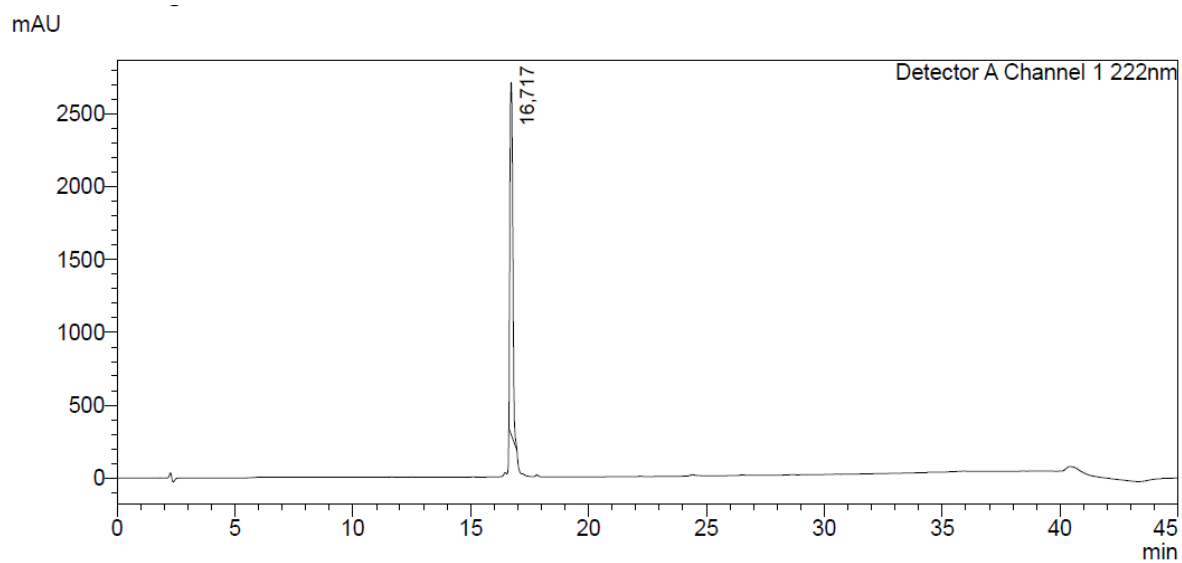
Figure S10. HPLC chromatogram of peptide **A1v2**.
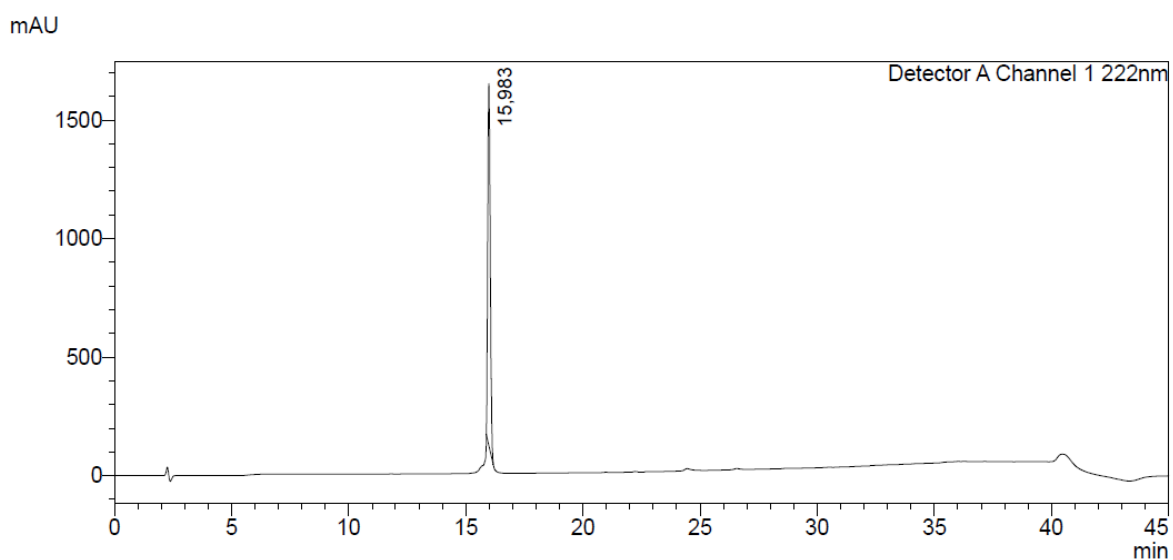
Figure S11. HPLC chromatogram of peptide **A1v3**.
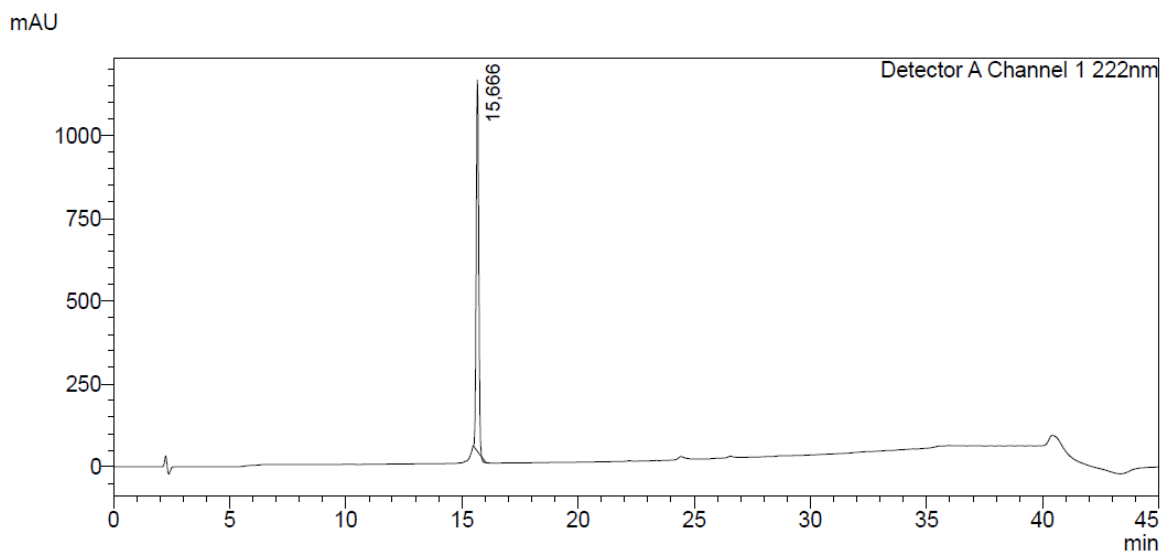
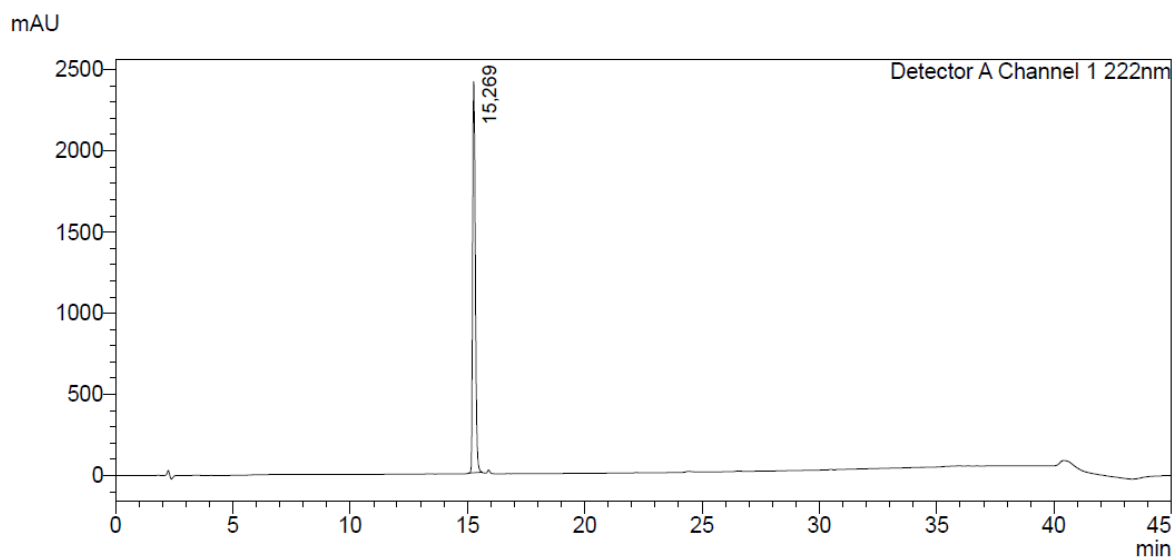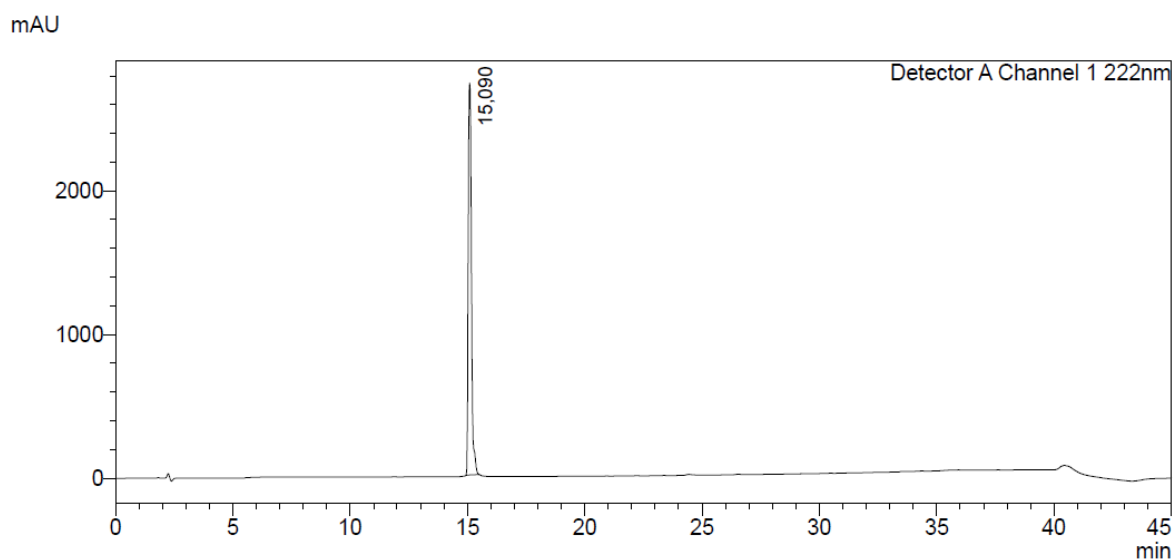**Figure S12**. HPLC chromatogram of peptide **A1v4**.
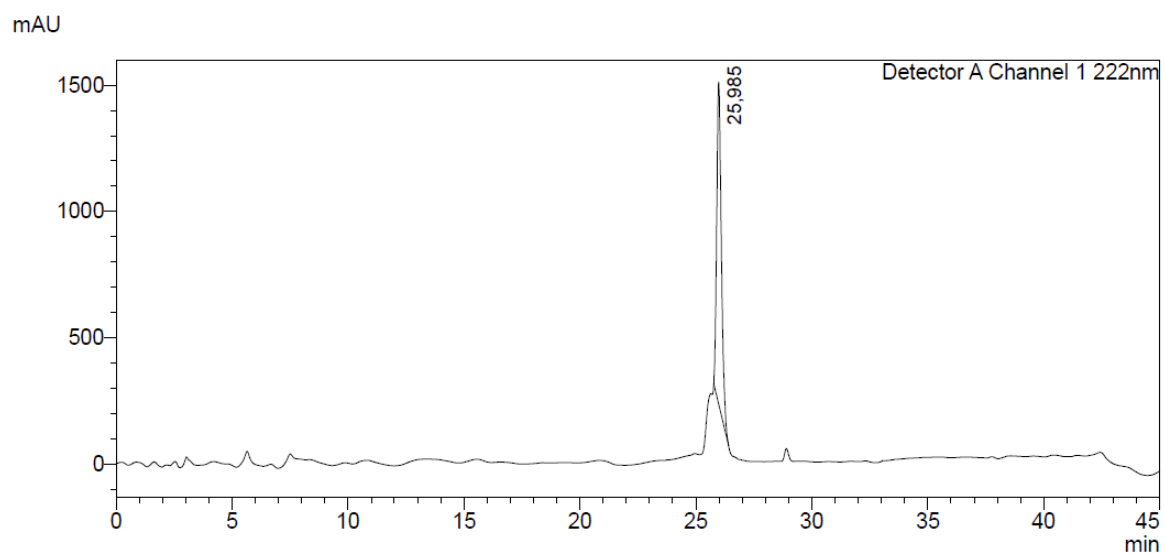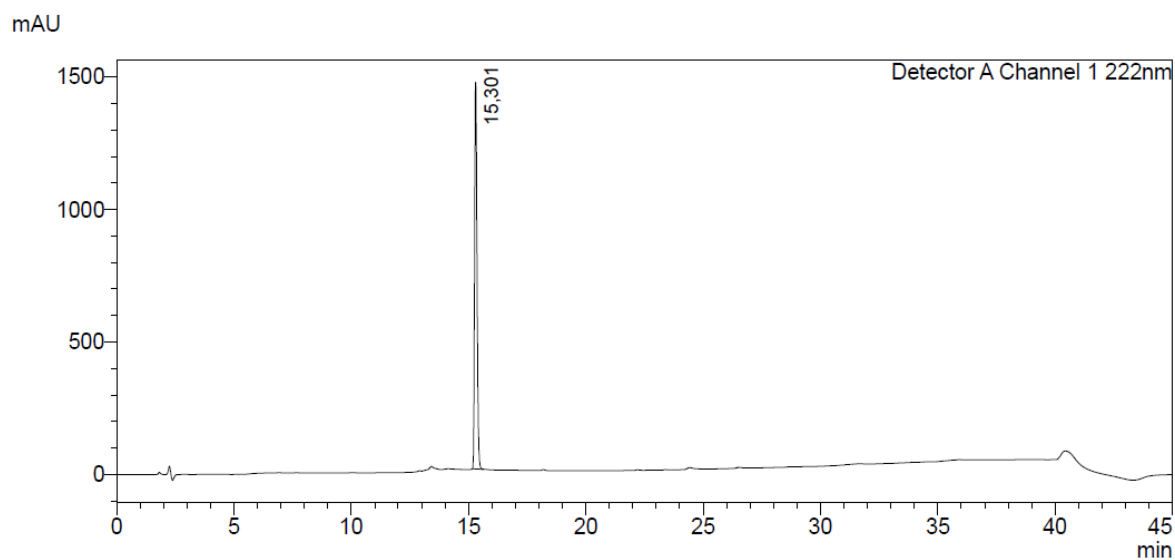
Figure S13. HPLC chromatogram of peptide **A2**.
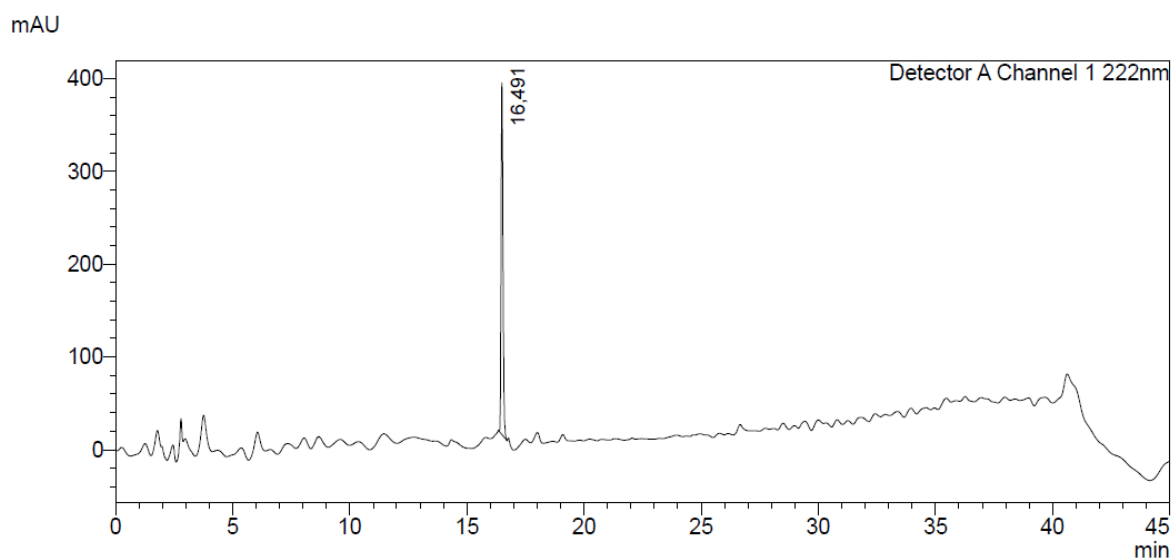
Figure S14. HPLC chromatogram of peptide **A2a**.
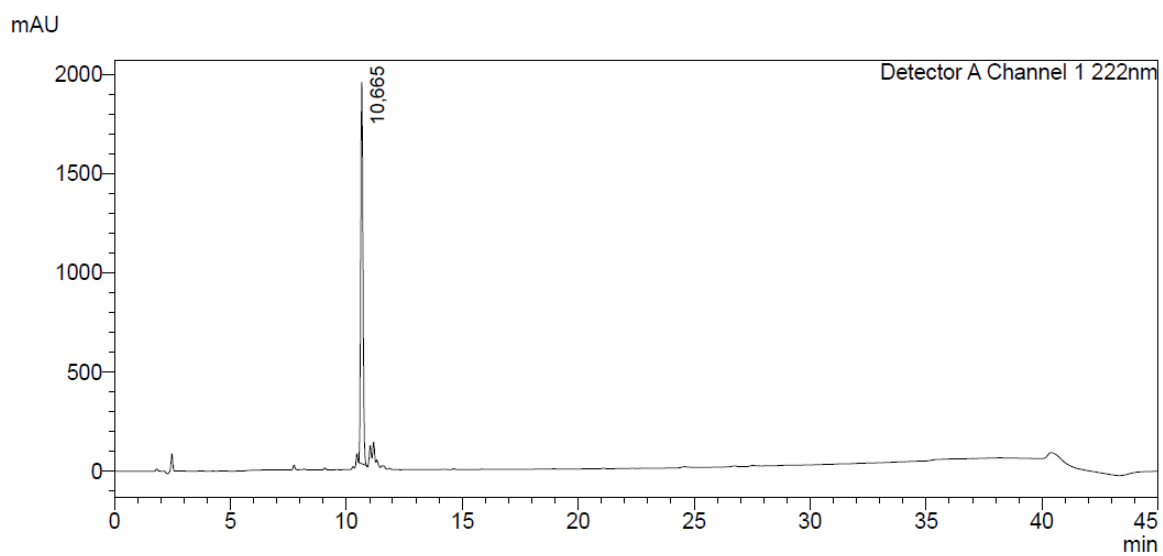
Figure S15. HPLC chromatogram of peptide **A2b**.
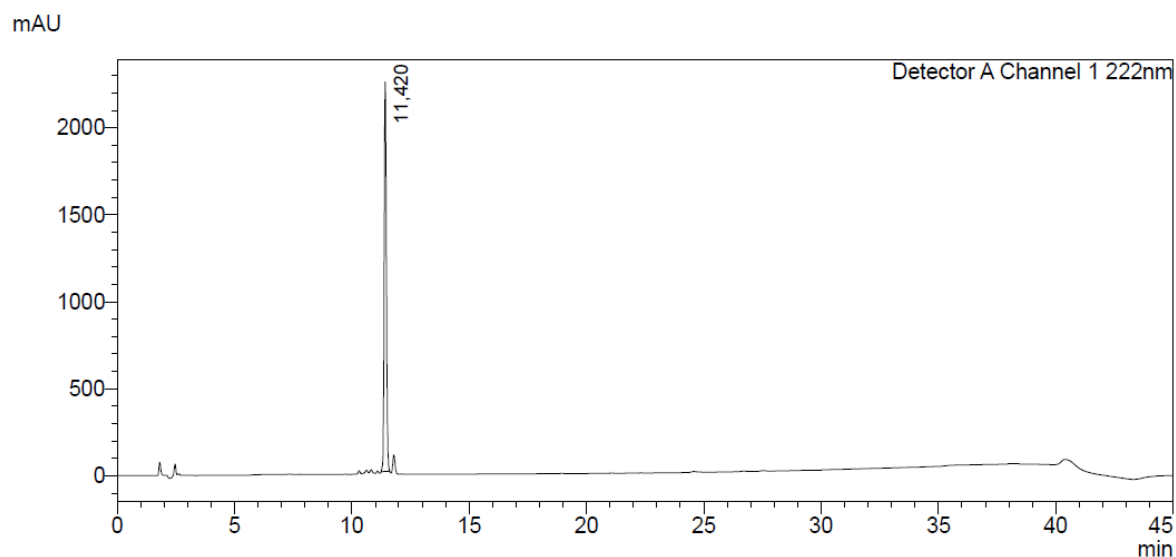
Figure S16. HPLC chromatogram of peptide **A2c**.
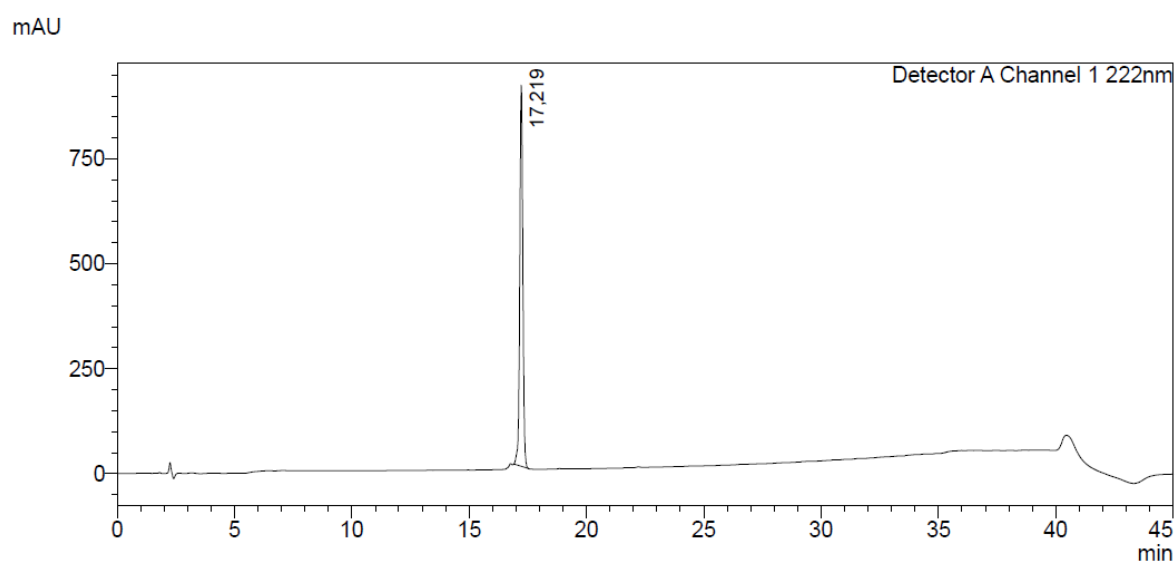
Figure S17. HPLC chromatogram of peptide **A2v1**.
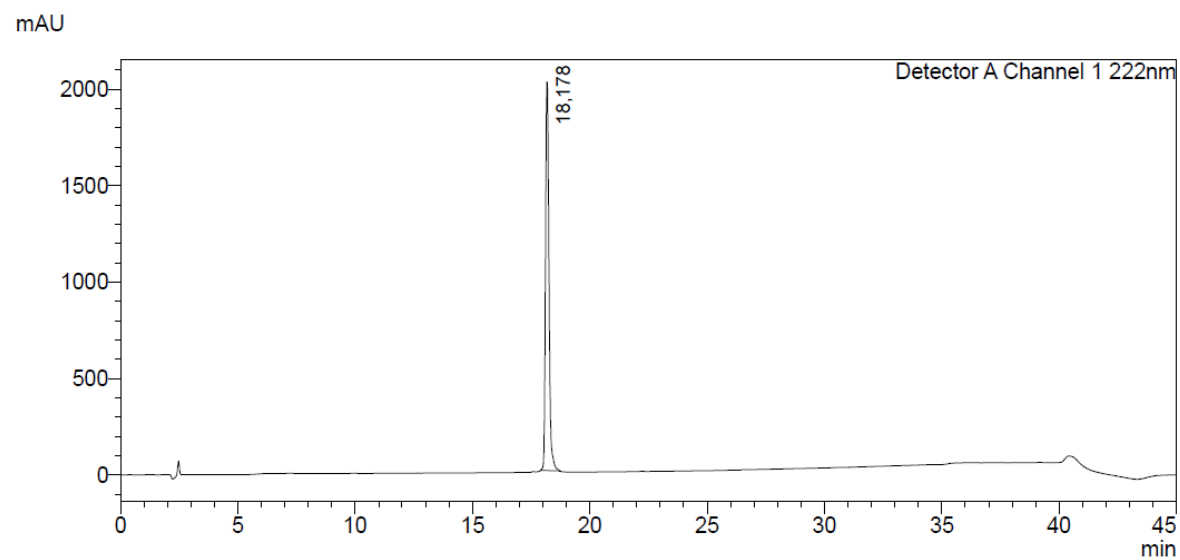
Figure S18. HPLC chromatogram of peptide **A2v2**.
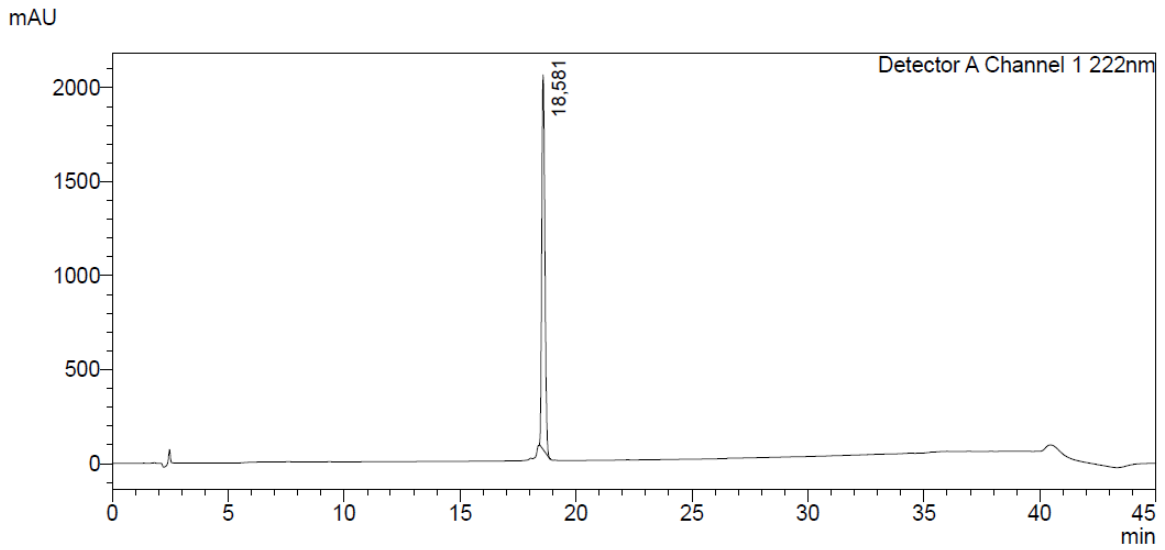
Figure S19. HPLC chromatogram of peptide **A2v3**.
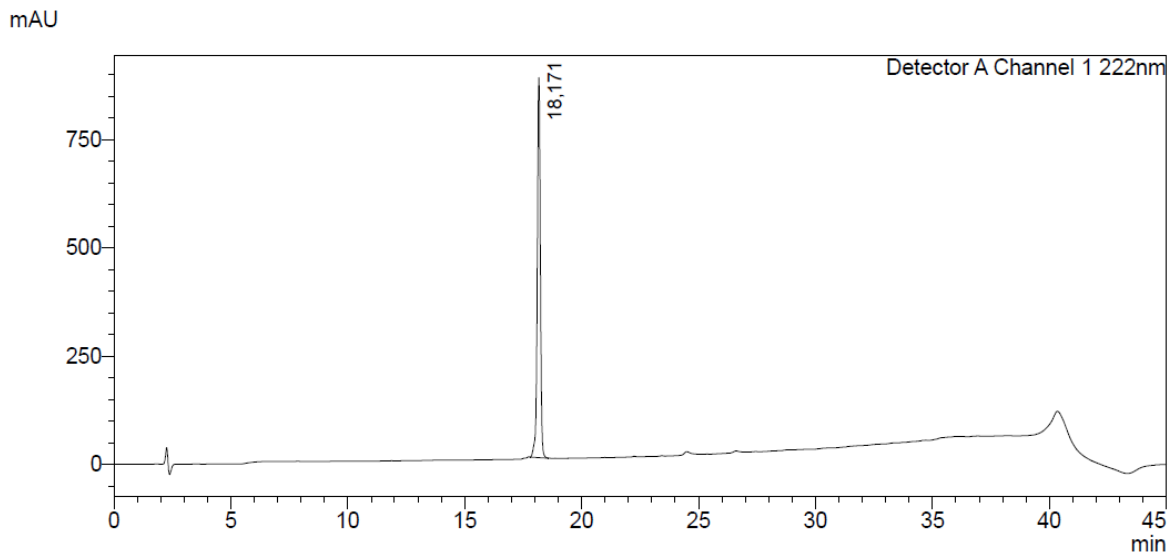
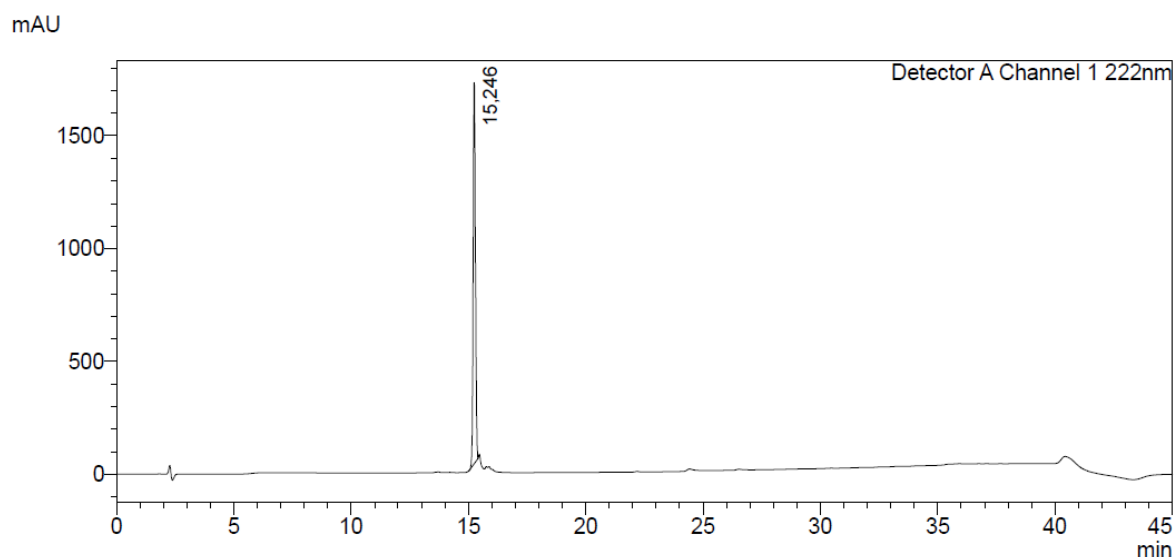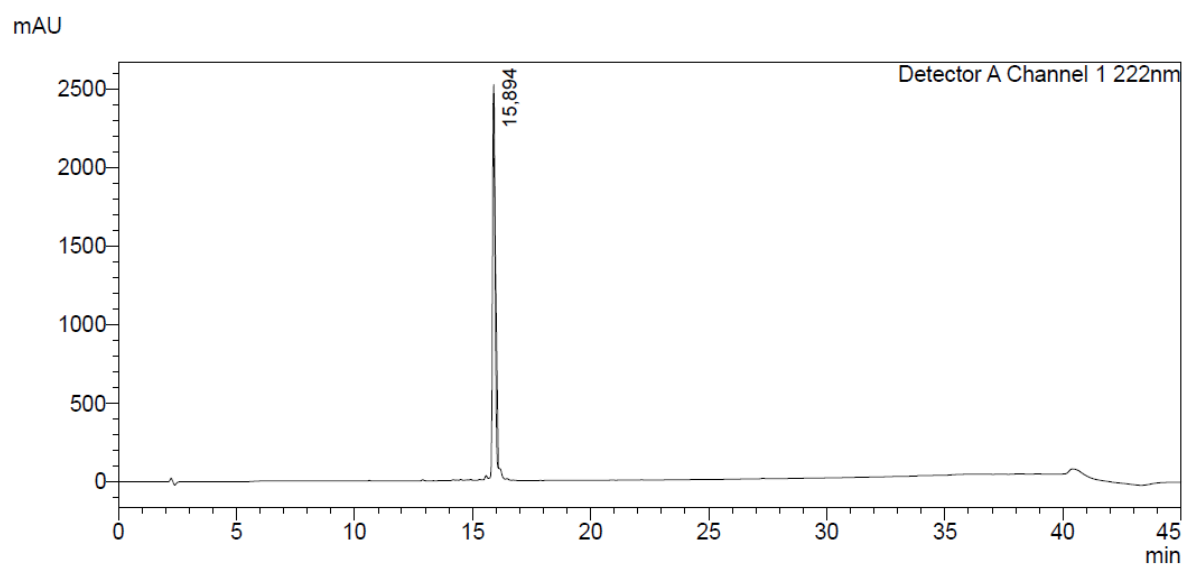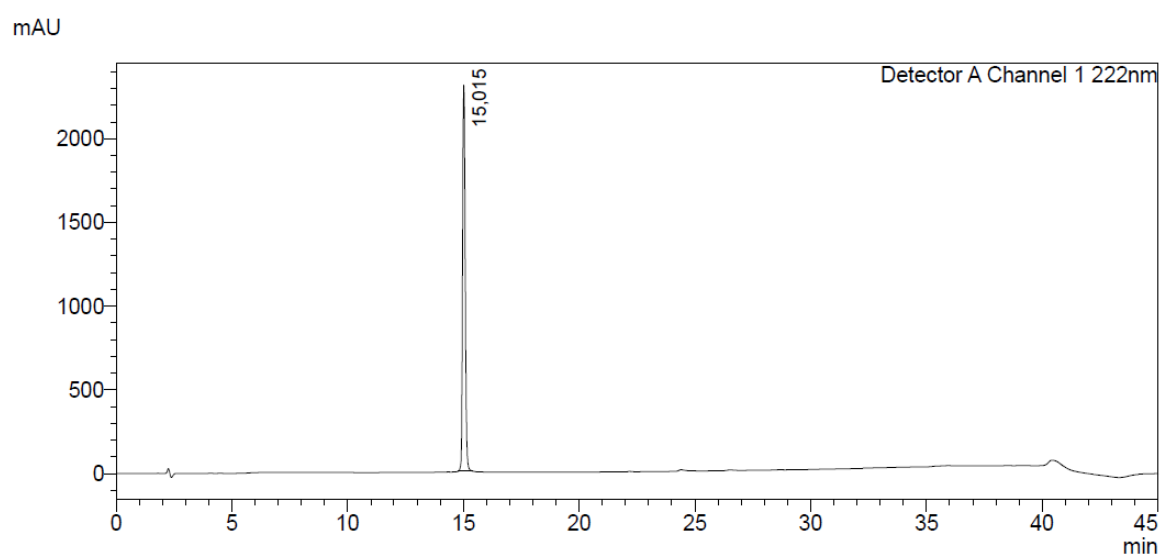**Figure S20**. HPLC chromatogram of peptide **A2v4**.
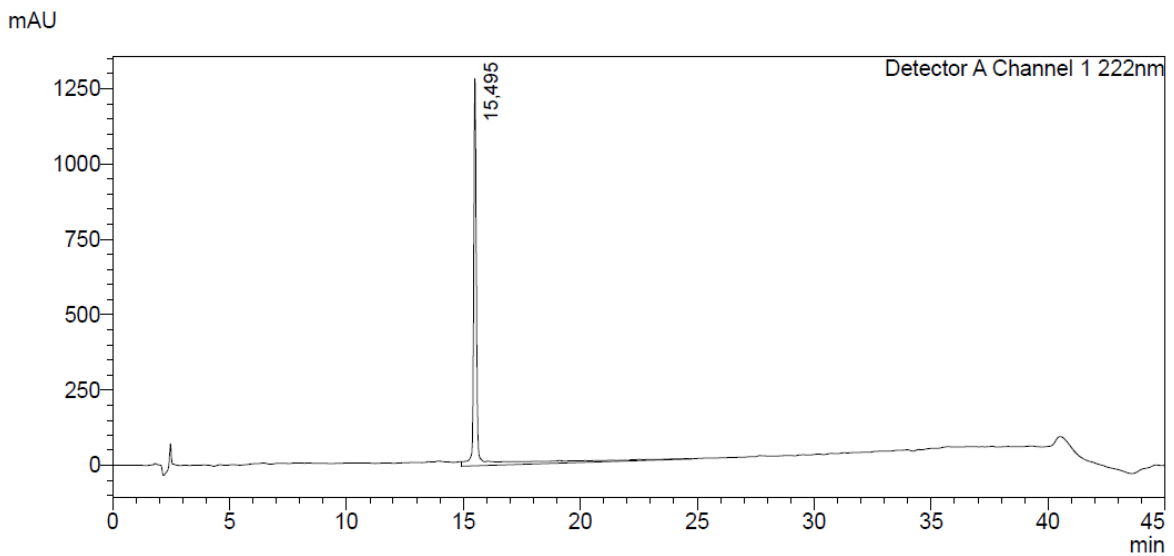
Figure S21. HPLC chromatogram of peptide **A3**.
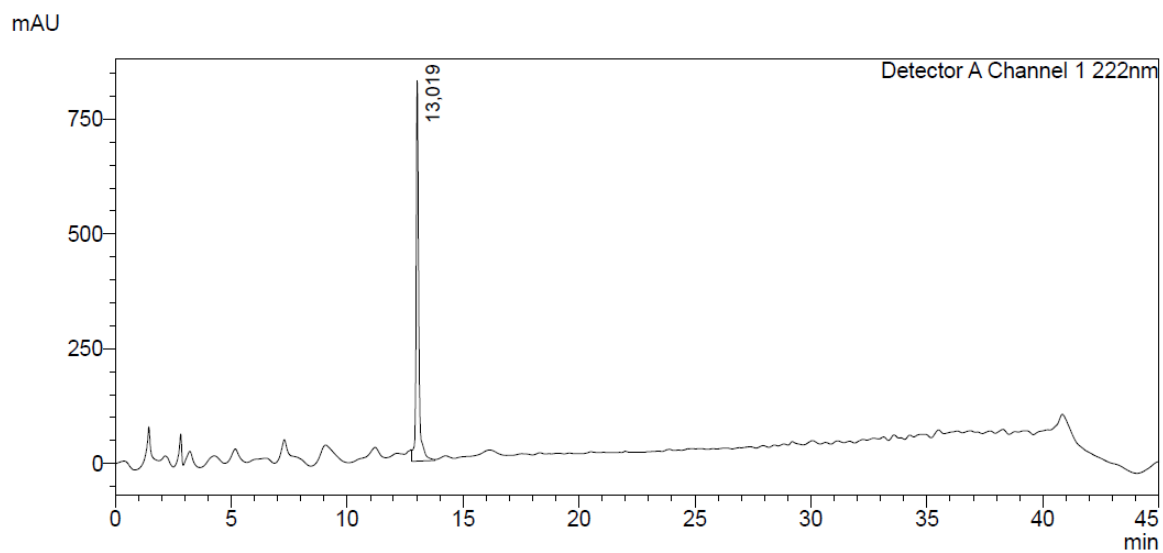
Figure S22. HPLC chromatogram of peptide **A3a**.
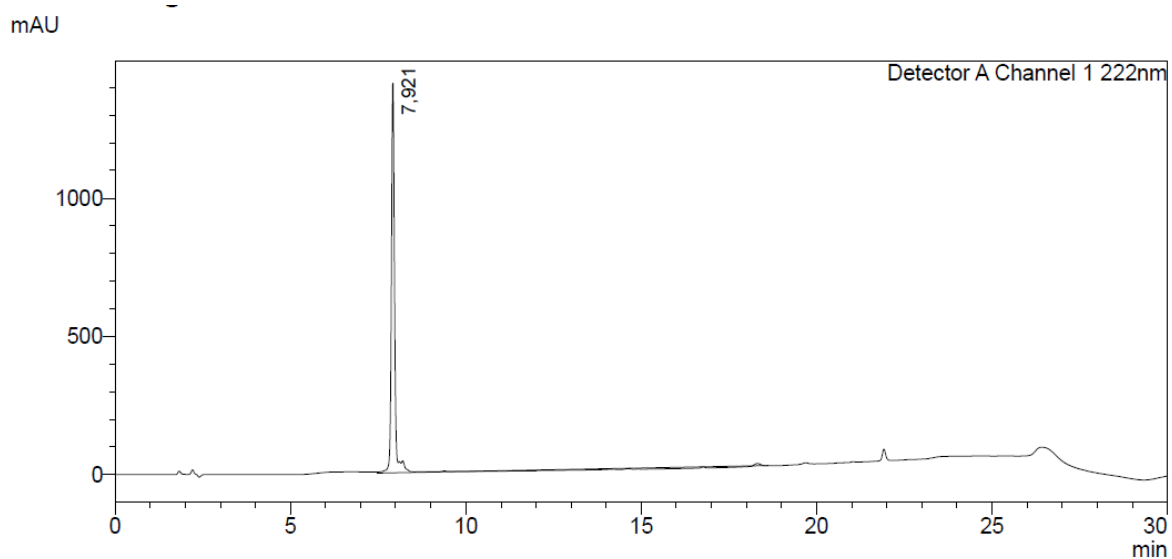
Figure S23. HPLC chromatogram of peptide **A3b**.
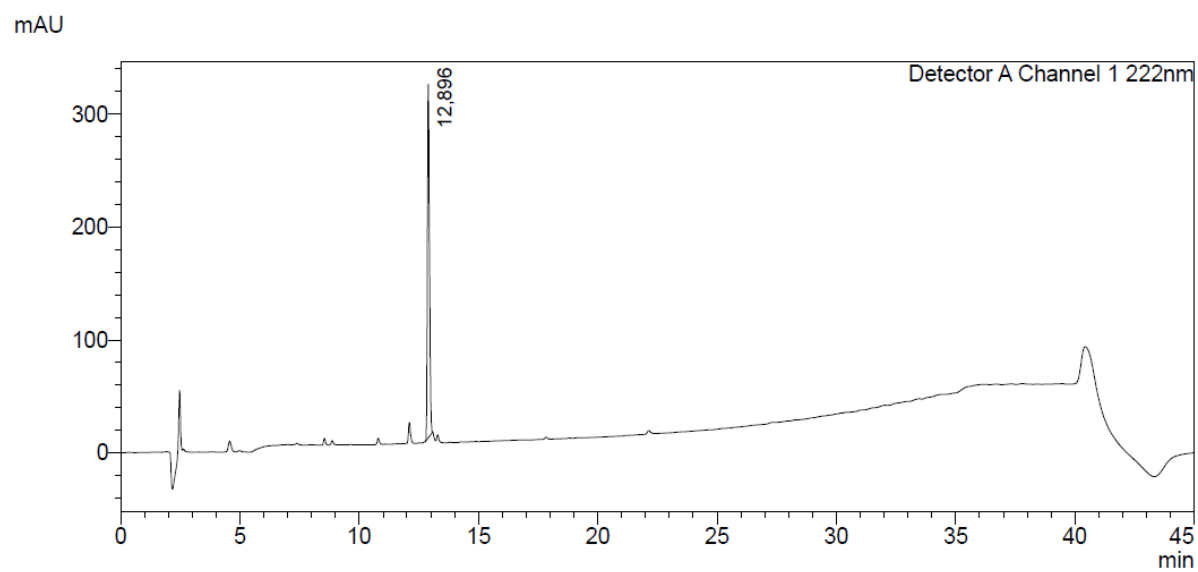
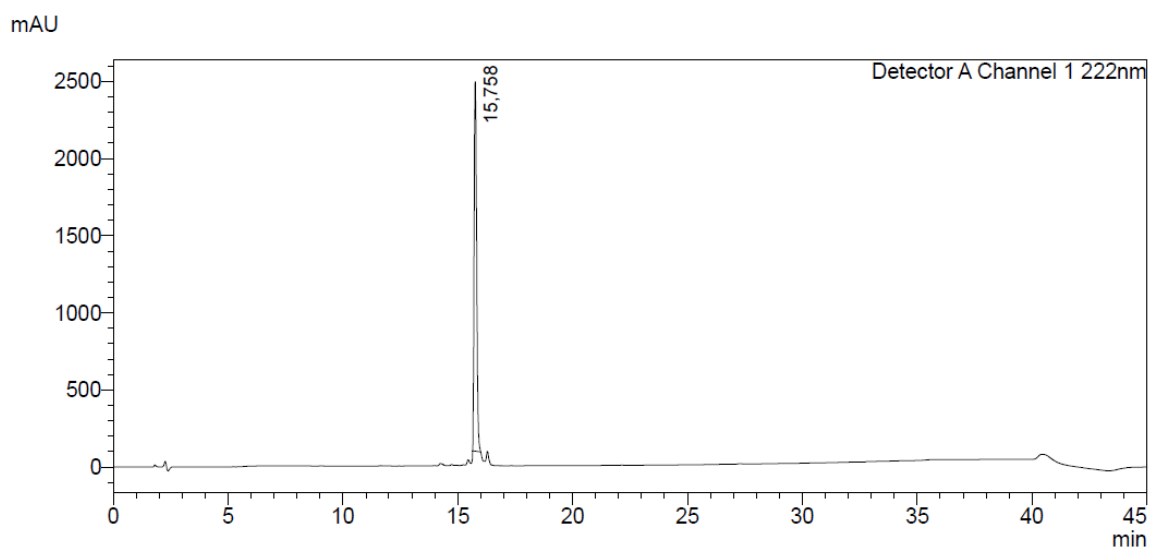**Figure S24**. HPLC chromatogram of peptide **A3c**.
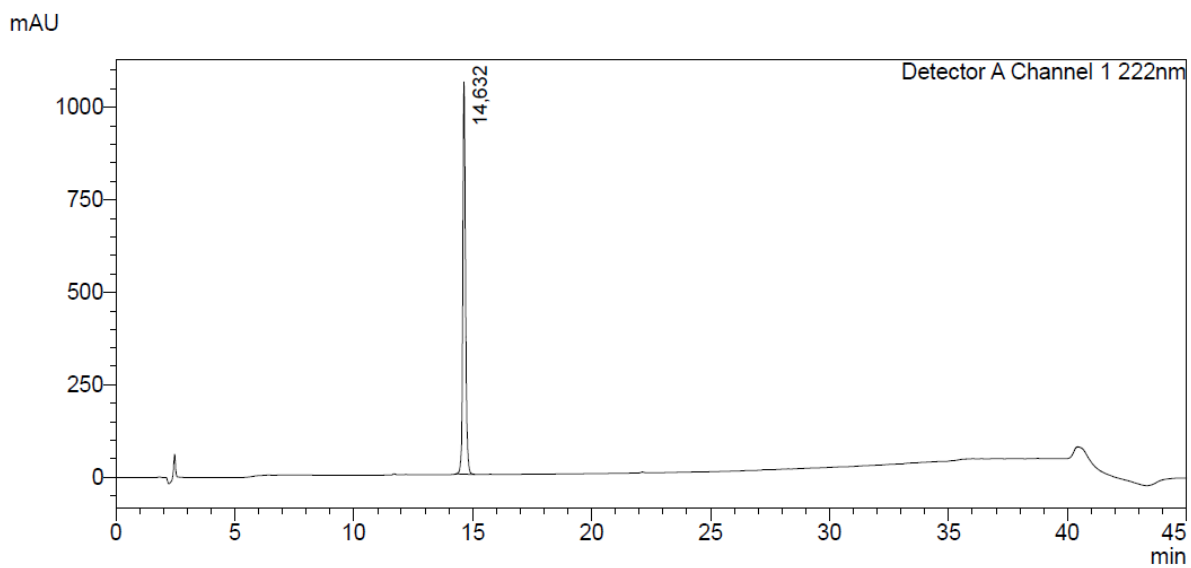
Figure S25. HPLC chromatogram of peptide **1**.
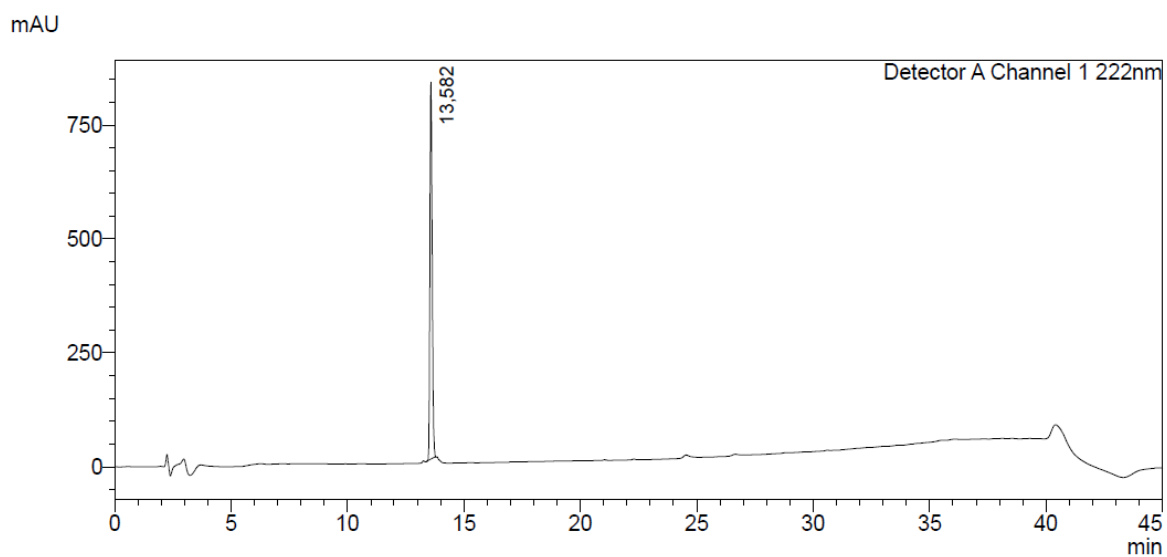
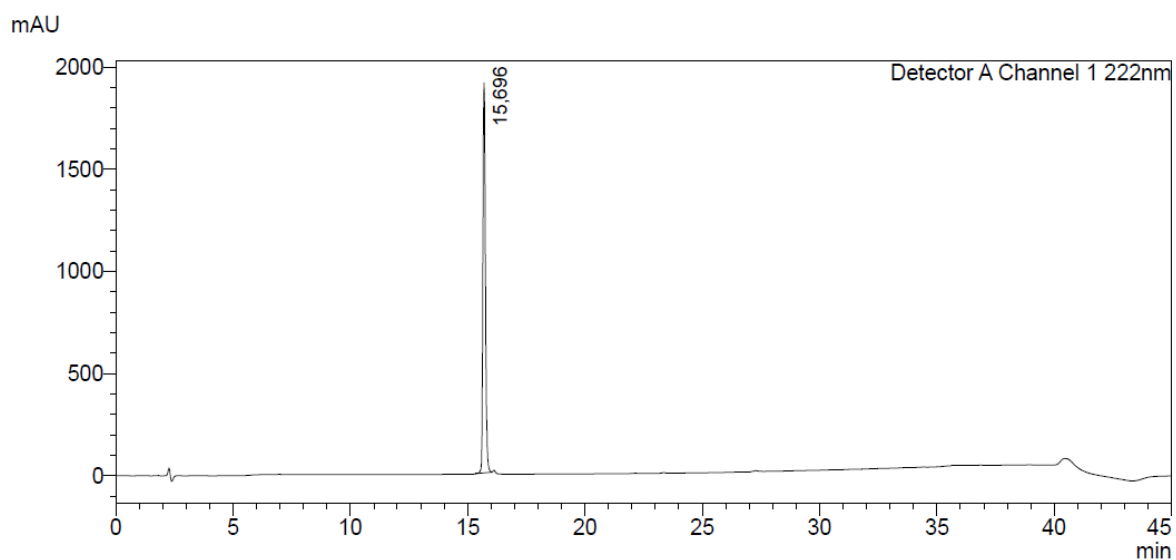**Figure S26**. HPLC chromatogram of peptide **2**.
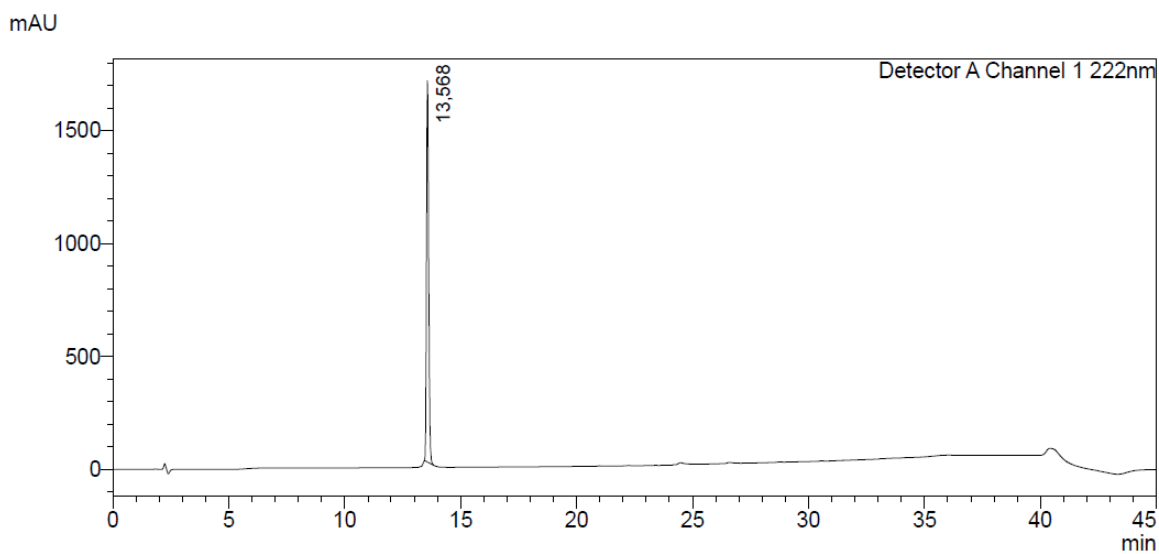
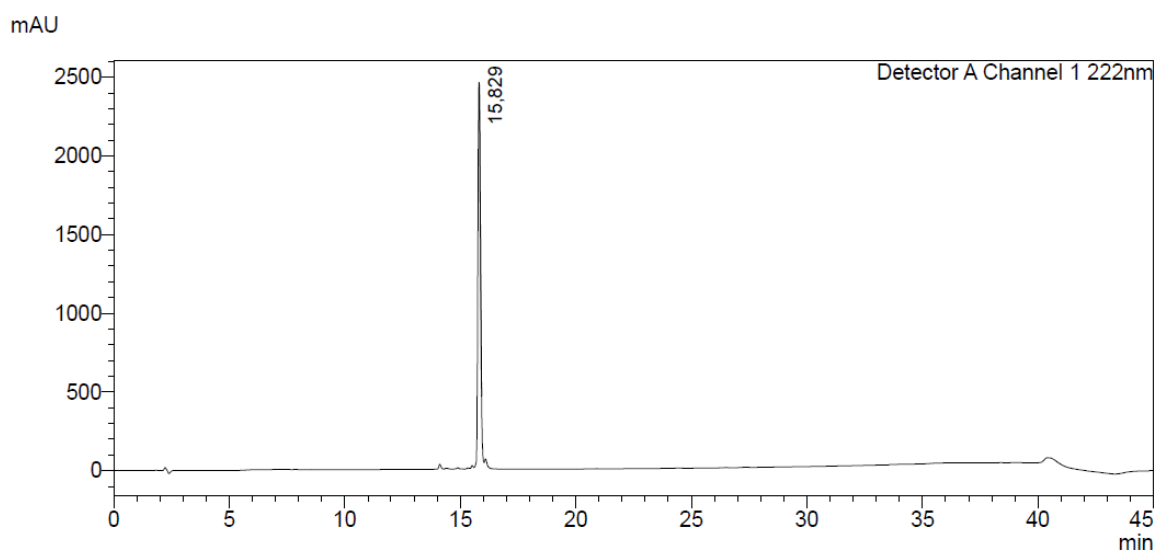**Figure S27**. HPLC chromatogram of peptide **3**.
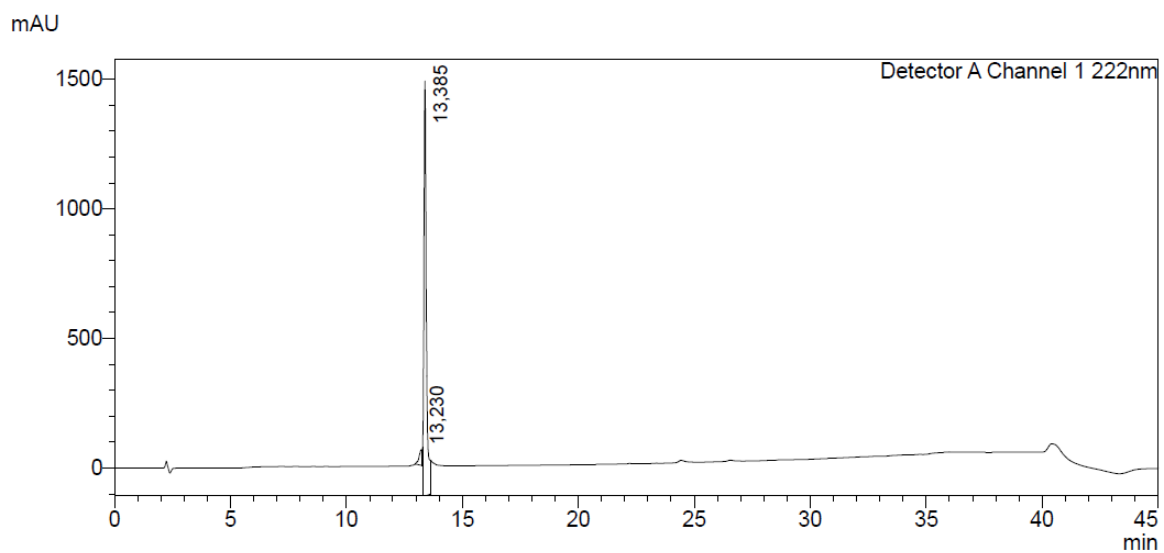
Figure S28. HPLC chromatogram of peptide **4**.
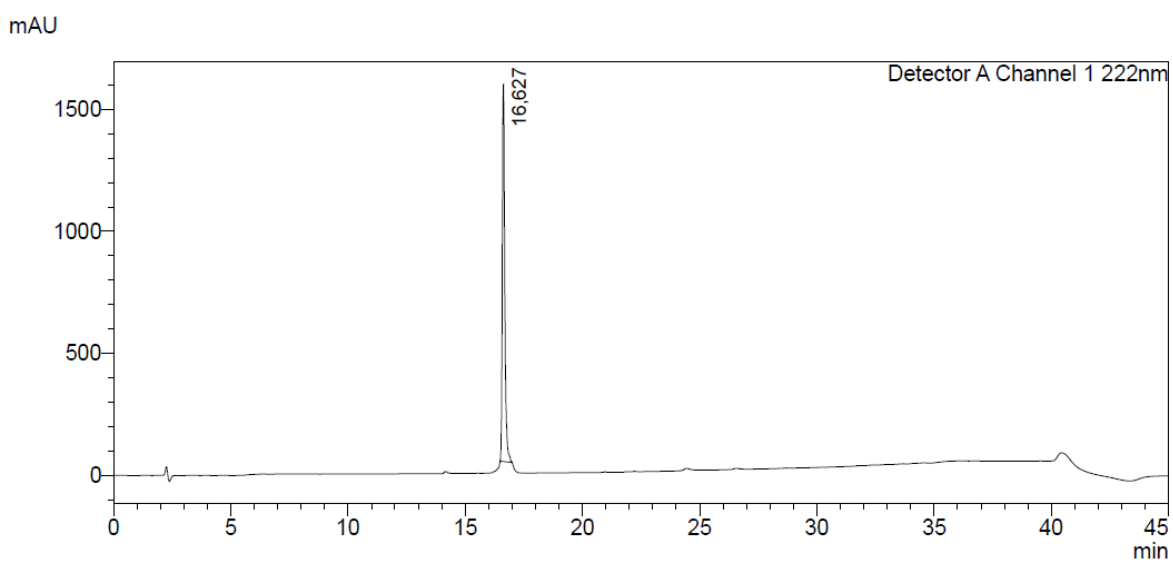
Figure S29. HPLC chromatogram of peptide **5**.
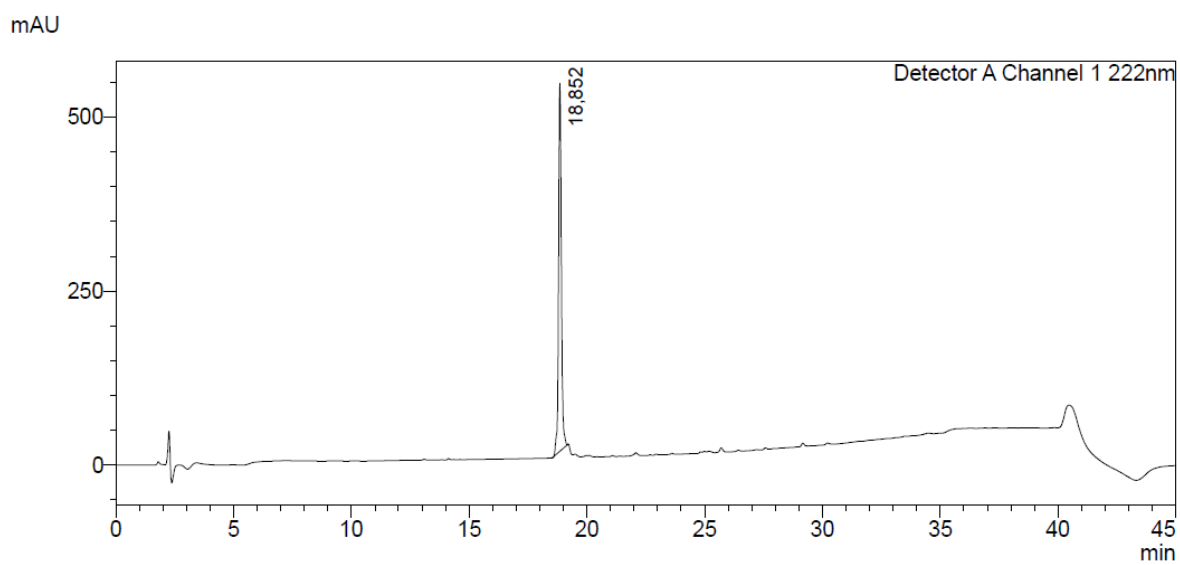
Figure S30. HPLC chromatogram of peptide **6**.
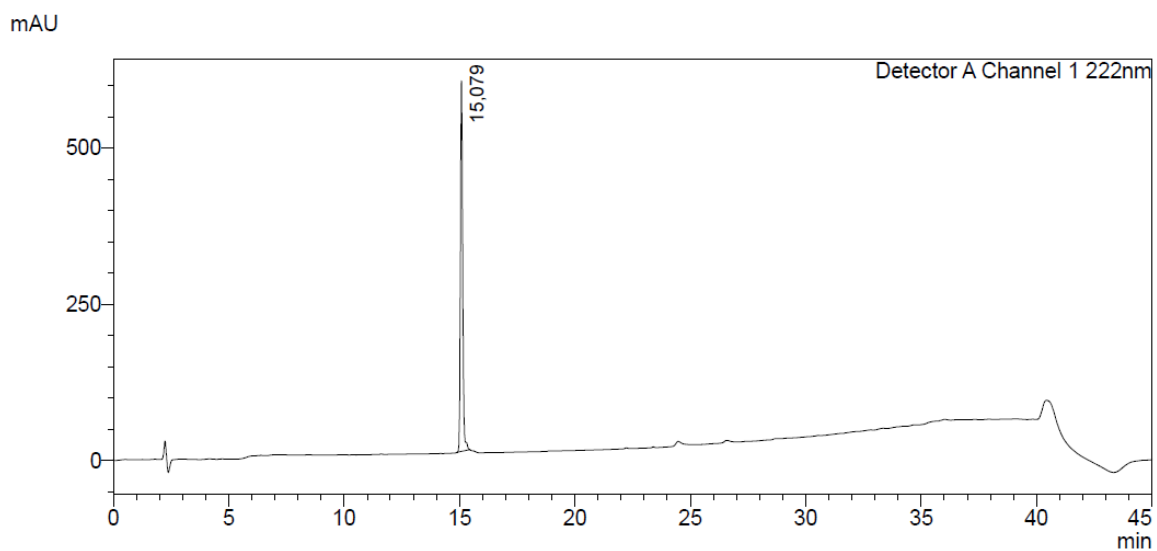
Figure S31. HPLC chromatogram of peptide **7**.
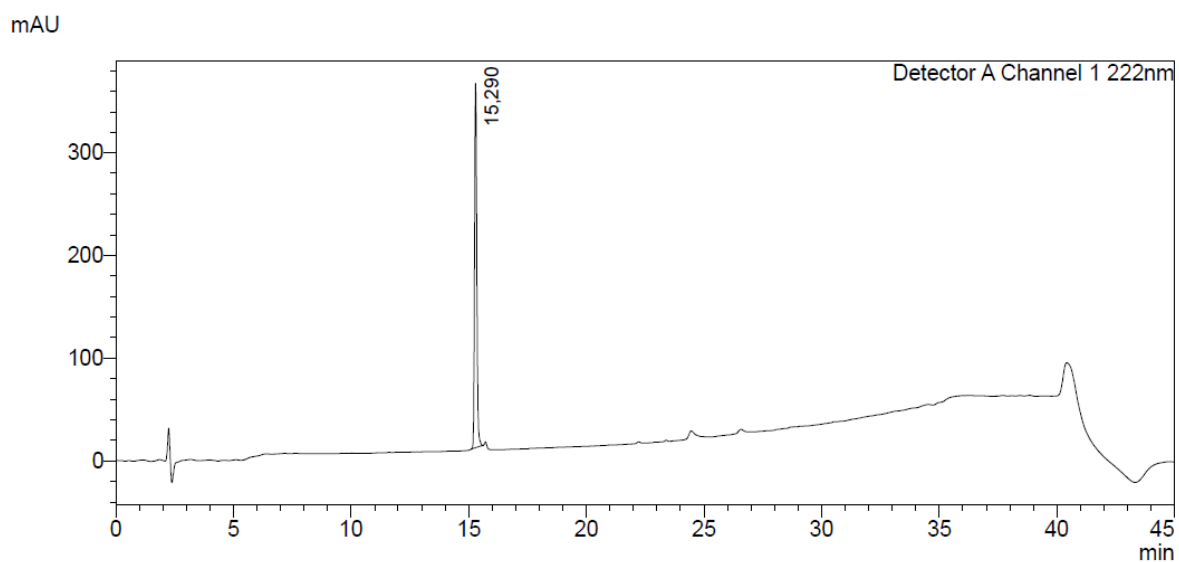
Figure S32. HPLC chromatogram of peptide **8**.
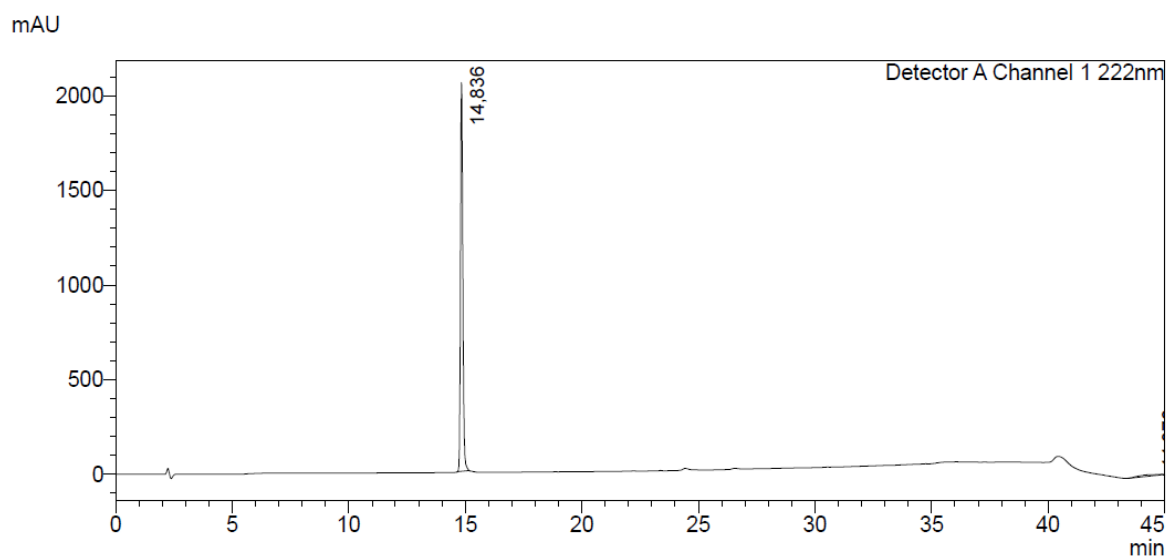
Figure S33. HPLC chromatogram of peptide **9**.
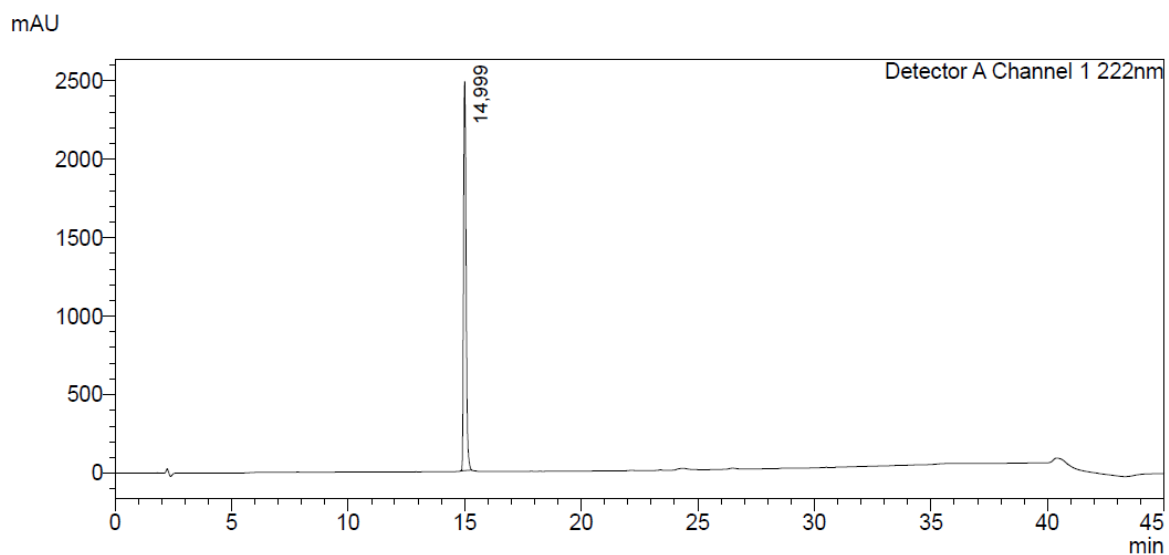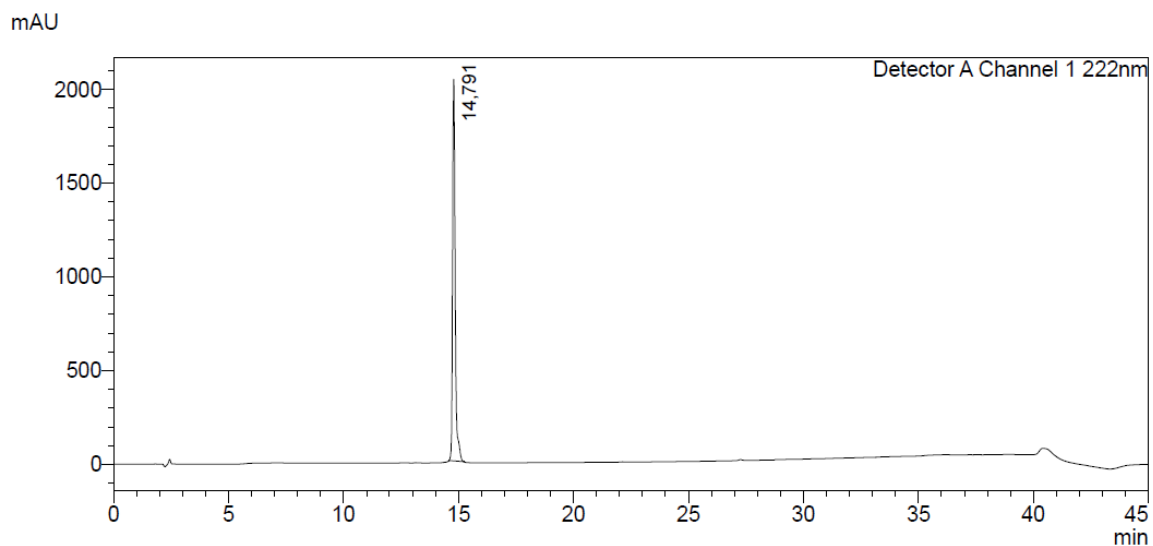
Figure S34. HPLC chromatogram of peptide **10**.
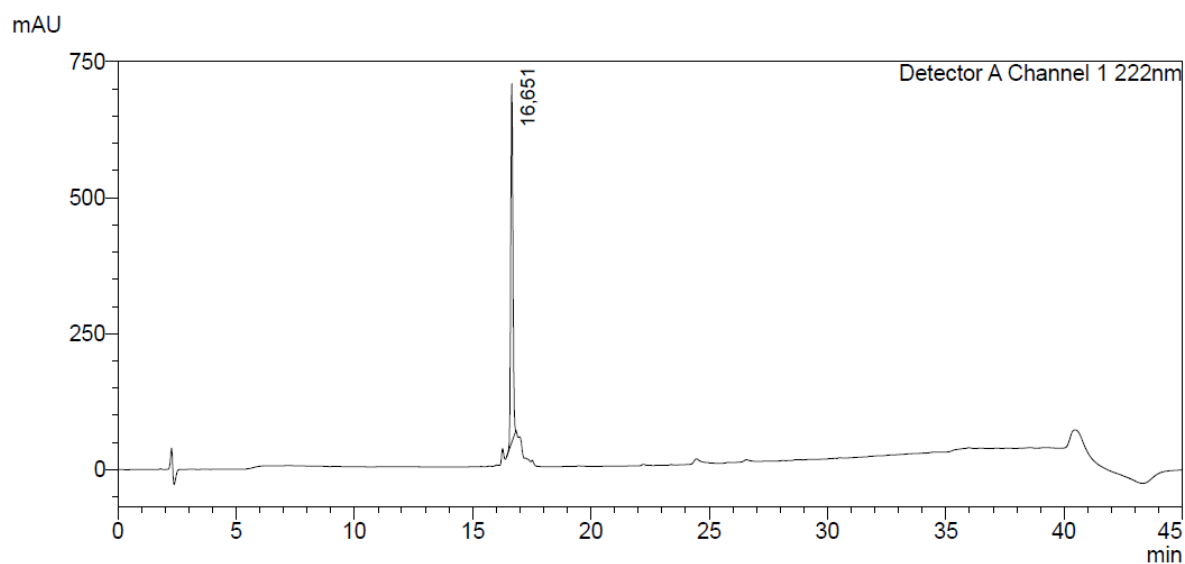
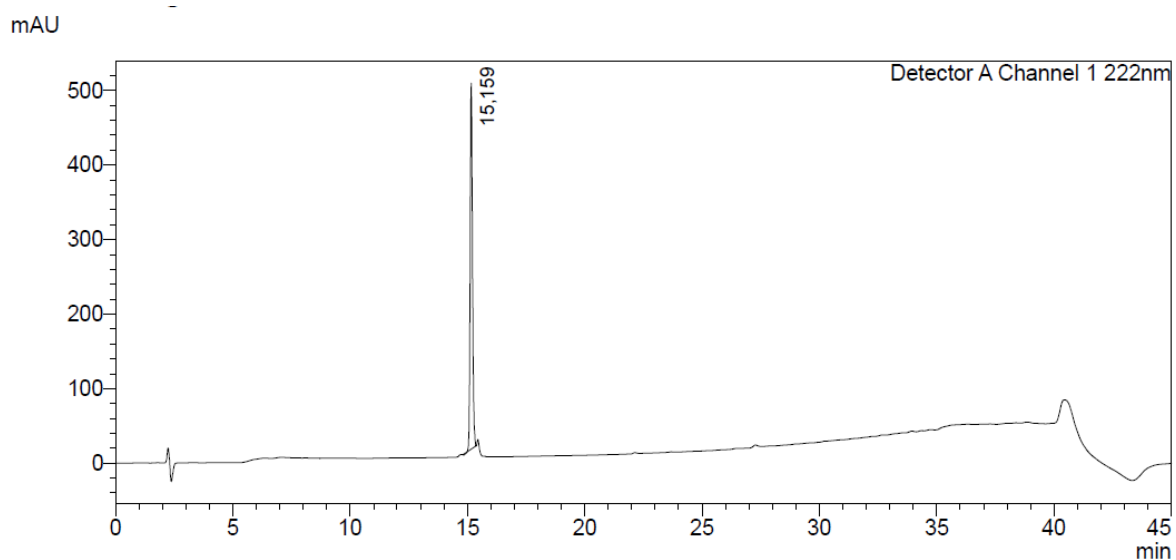
Figure S35. HPLC chromatogram of peptide **11**.
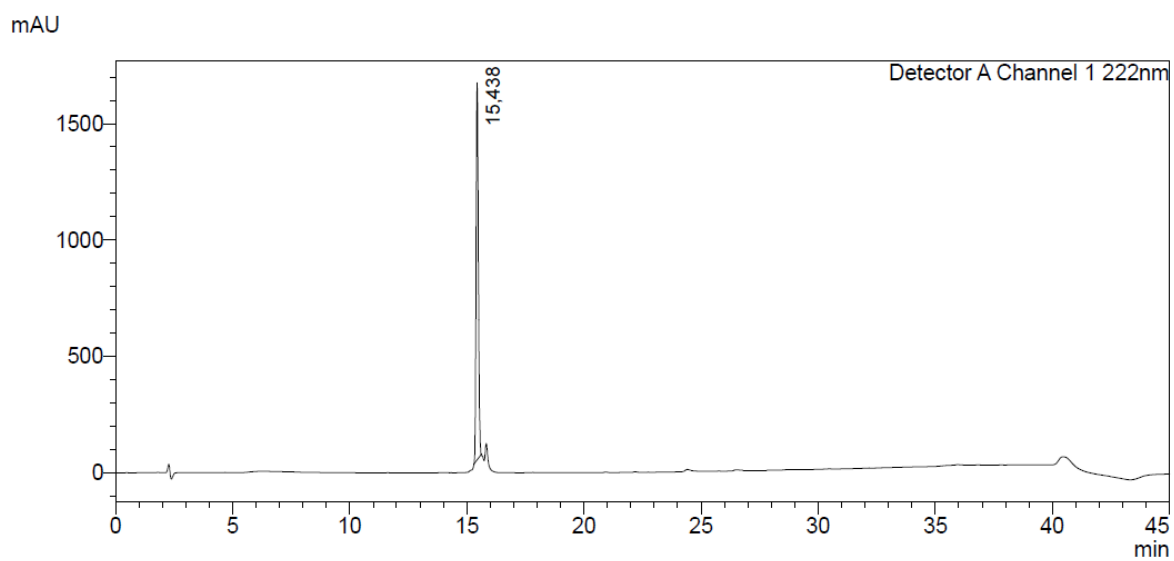
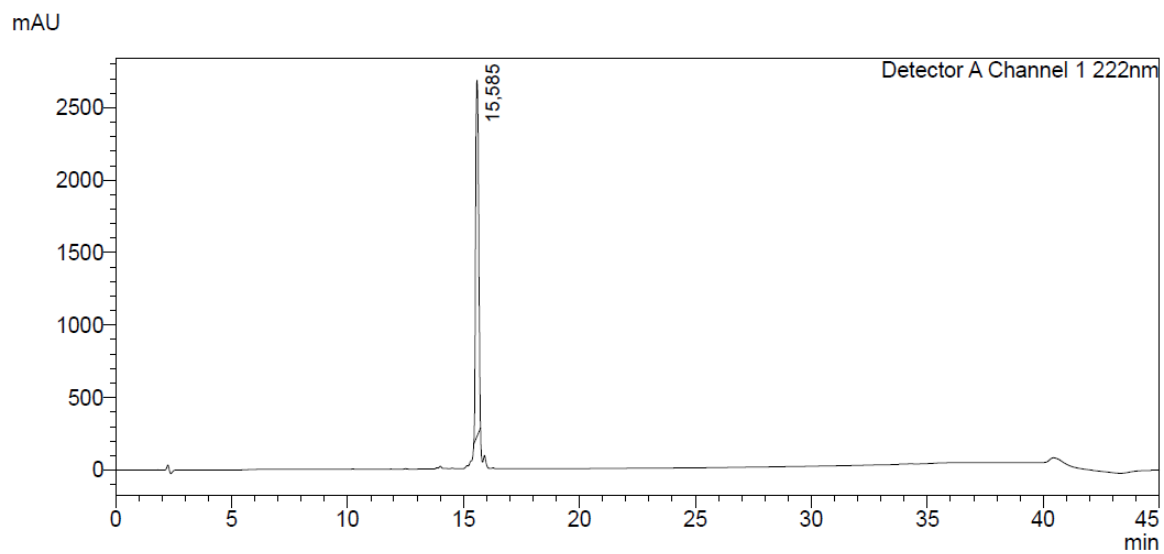**Figure S36**. HPLC chromatogram of peptide **12**.
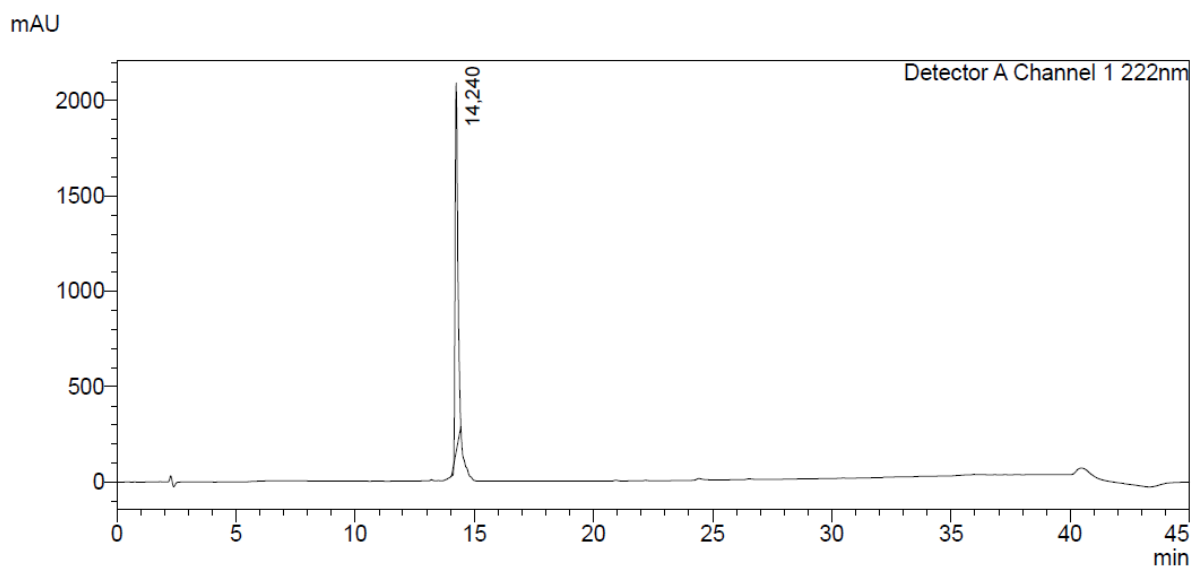
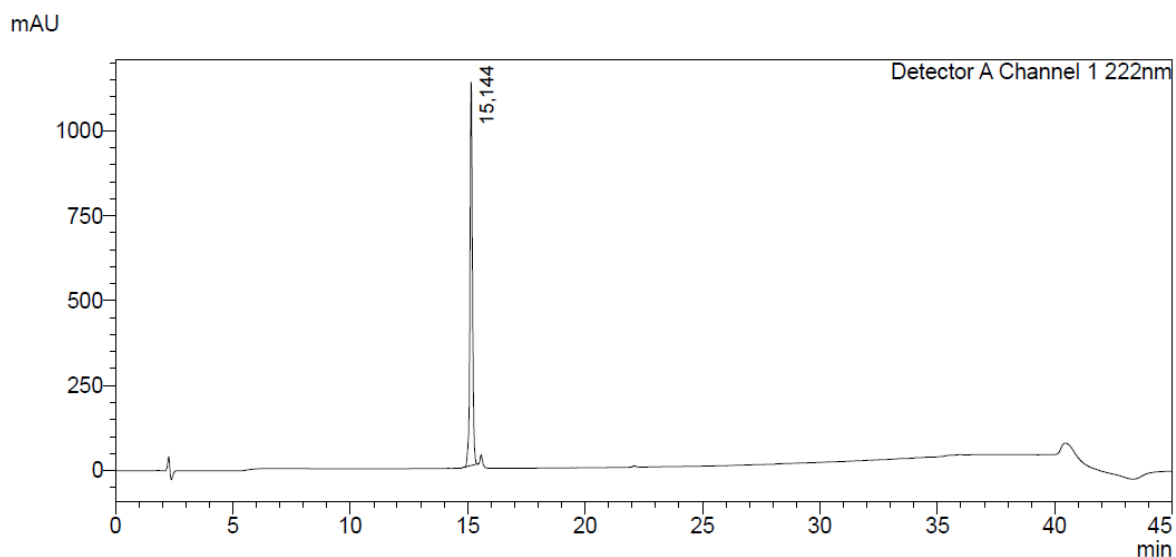**Figure S37**. HPLC chromatogram of peptide **13**.
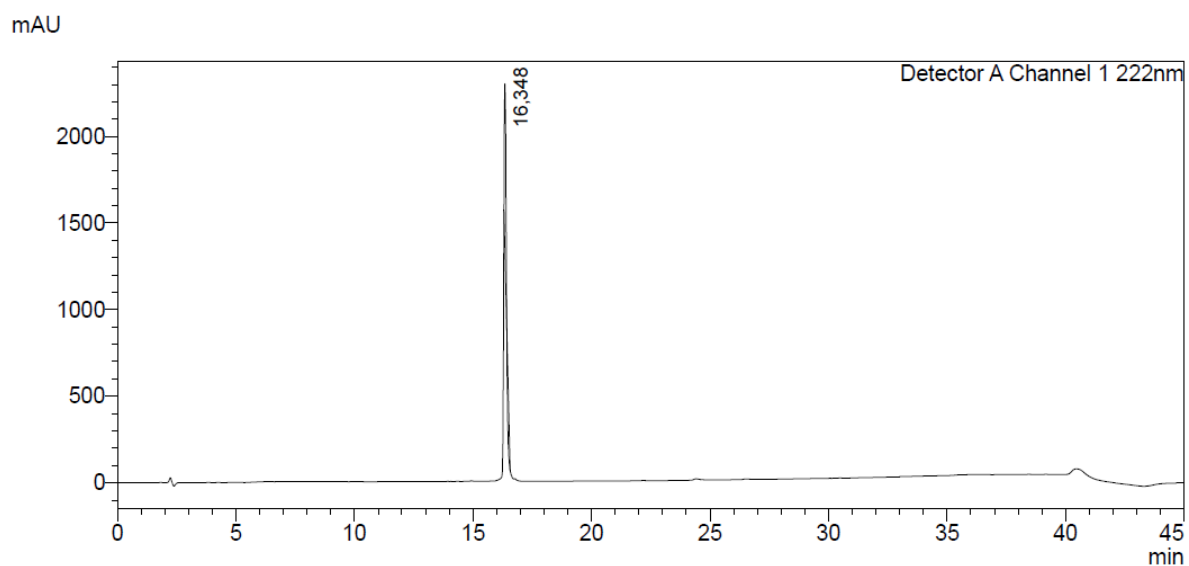
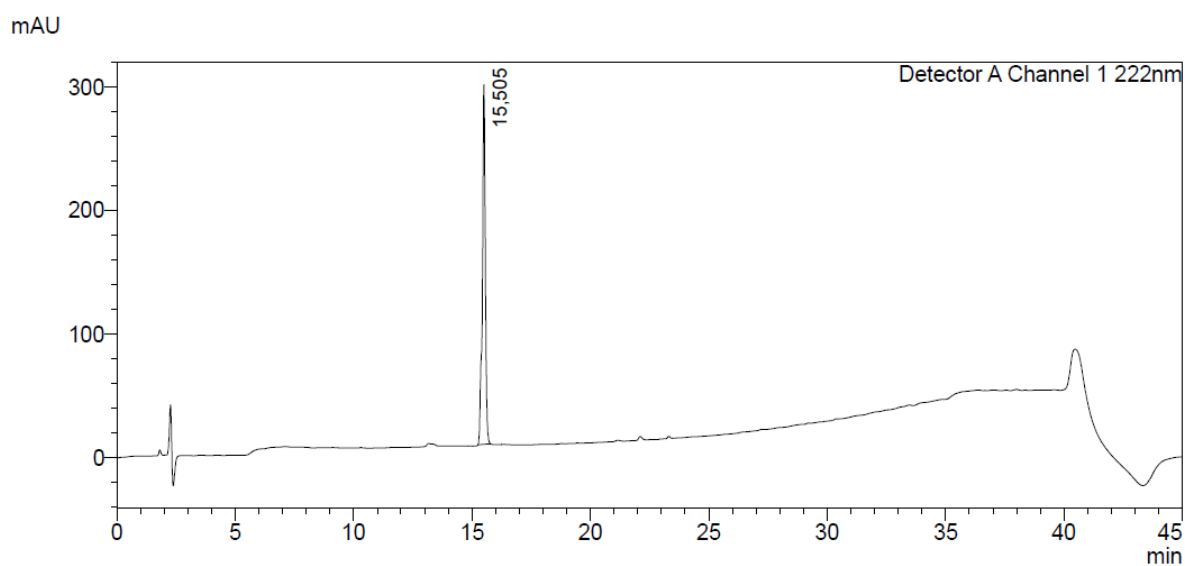**Figure S38**. HPLC chromatogram of peptide **14**.
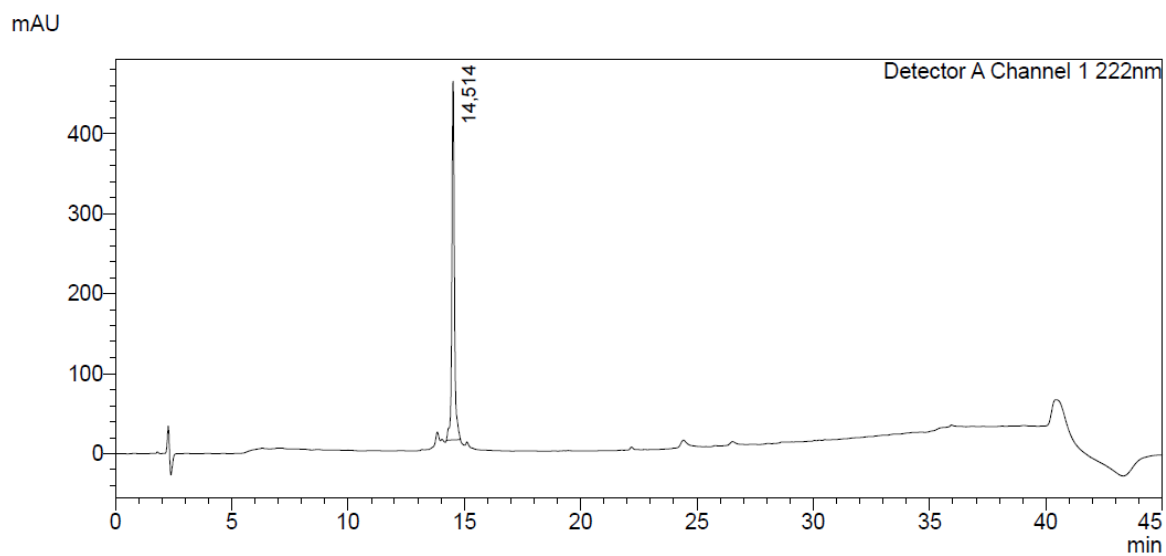
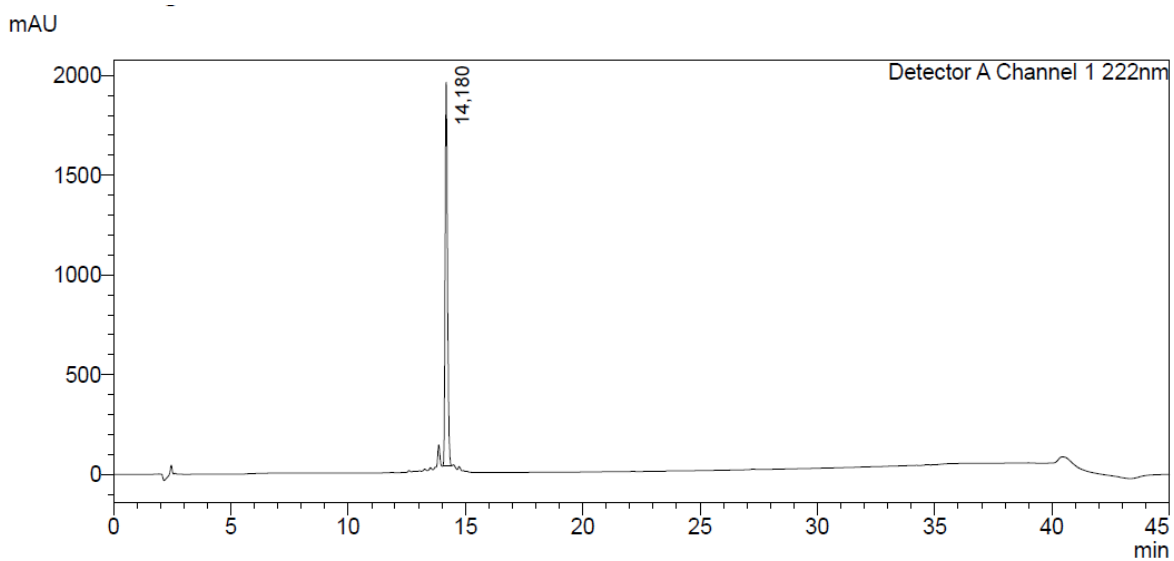**Figure S39**. HPLC chromatogram of peptide **15**.

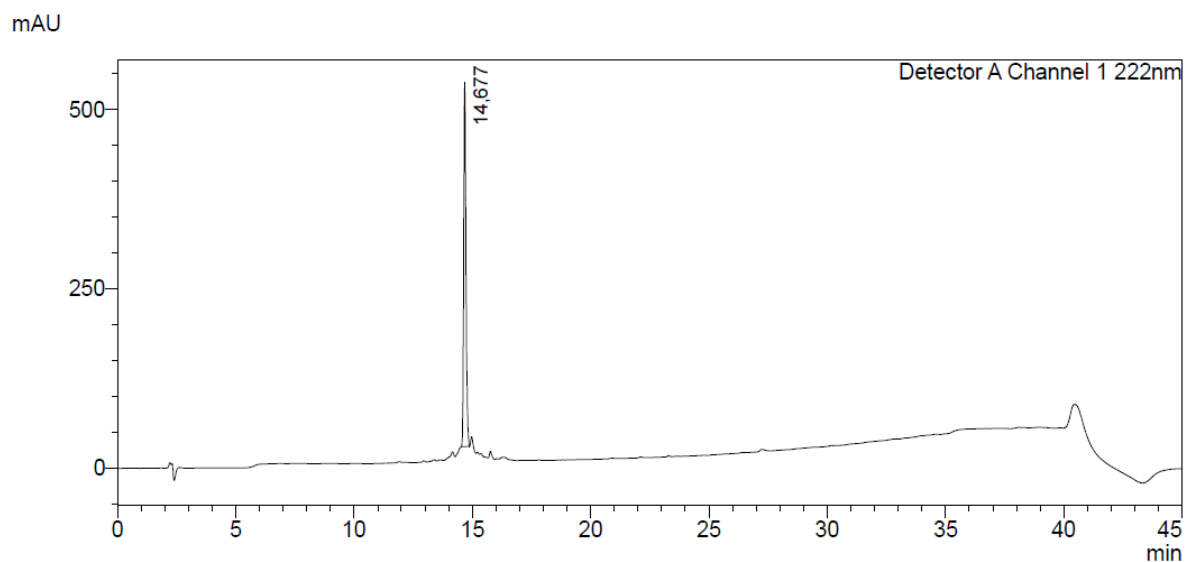**Figure S40**. HPLC chromatogram of peptide **16**.

Figure S41. HPLC chromatogram of peptide **17**.

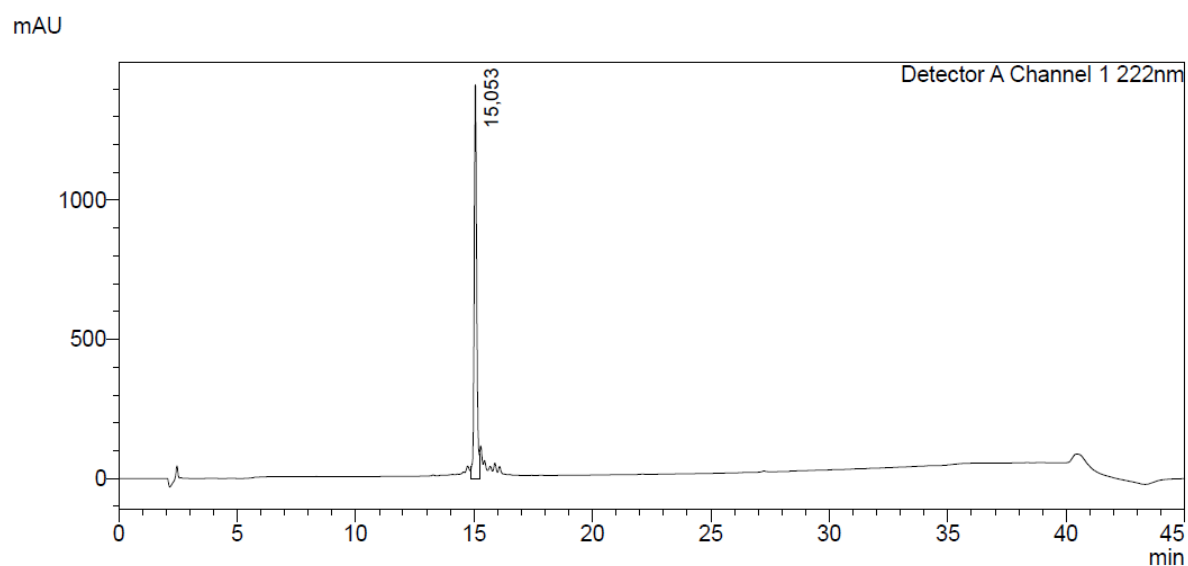**Figure S42**. HPLC chromatogram of peptide **18**.

Figure S43. HPLC chromatogram of peptide **19**.

Figure S44. HPLC chromatogram of peptide **20**.

Figure S45. HPLC chromatogram of peptide **21**.

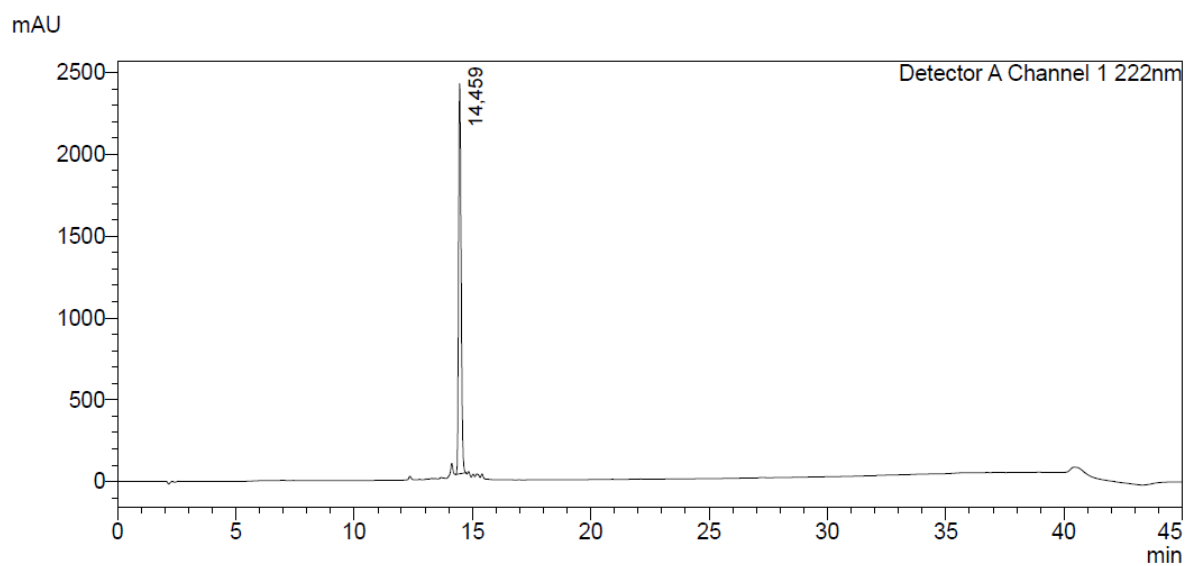**Figure S46**. HPLC chromatogram of peptide **22**.

Figure S47. HPLC chromatogram of peptide **23**.

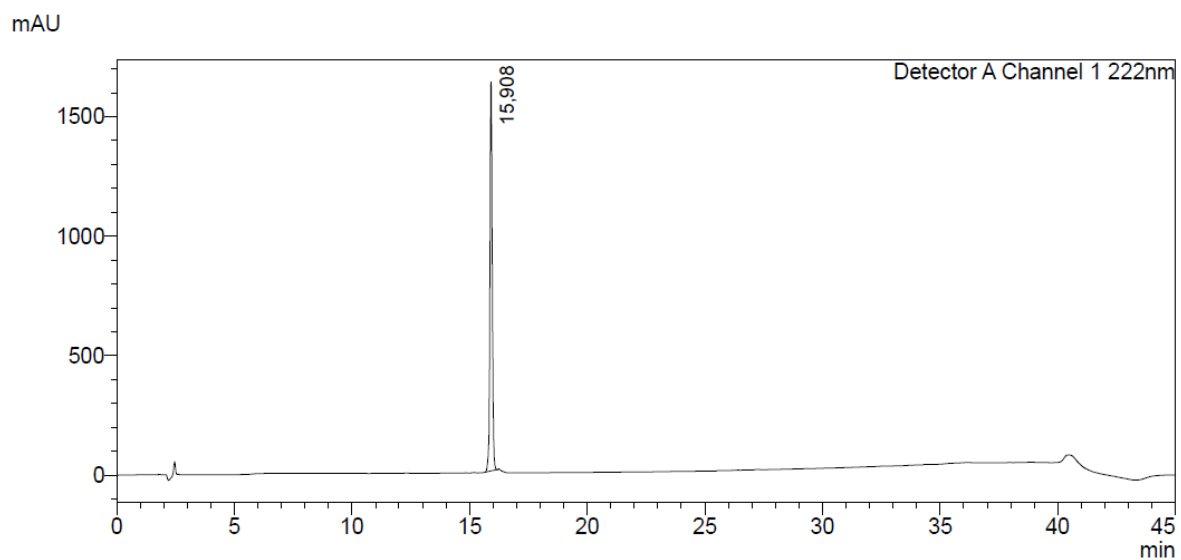
Figure S48. HPLC chromatogram of peptide **24**.

Figure S49. HPLC chromatogram of peptide **25**.

Figure S50. HPLC chromatogram of peptide **26**.

Figure S51. HPLC chromatogram of peptide **27**.

Figure S52. HPLC chromatogram of peptide **28**.

Figure S53. HPLC chromatogram of peptide **29**.

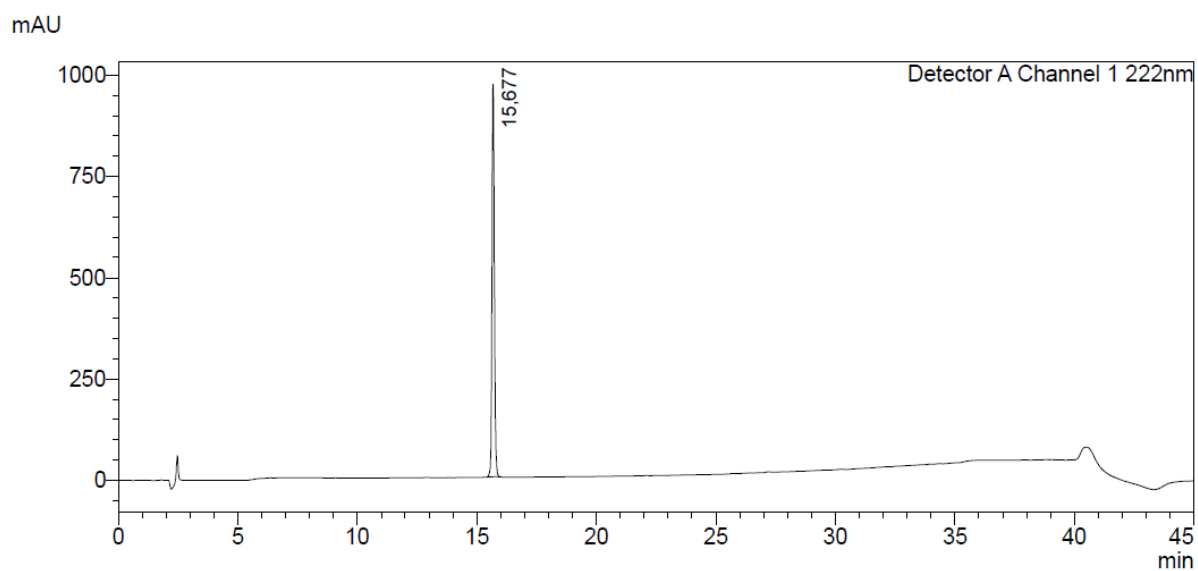**Figure S54**. HPLC chromatogram of peptide **30**.

Figure S55. HPLC chromatogram of peptide **31**.

Figure S56. HPLC chromatogram of peptide **32**.

Figure S57. HPLC chromatogram of peptide **33**.

Figure S58. HPLC chromatogram of peptide **34**.

Figure S59. HPLC chromatogram of peptide **35**.

Figure S60. HPLC chromatogram of peptide **36**.

Figure S61. HPLC chromatogram of peptide **37**.

Figure S62. HPLC chromatogram of peptide **38**.

Figure S63. HPLC chromatogram of peptide **39**.

Figure S64. HPLC chromatogram of peptide **40**.

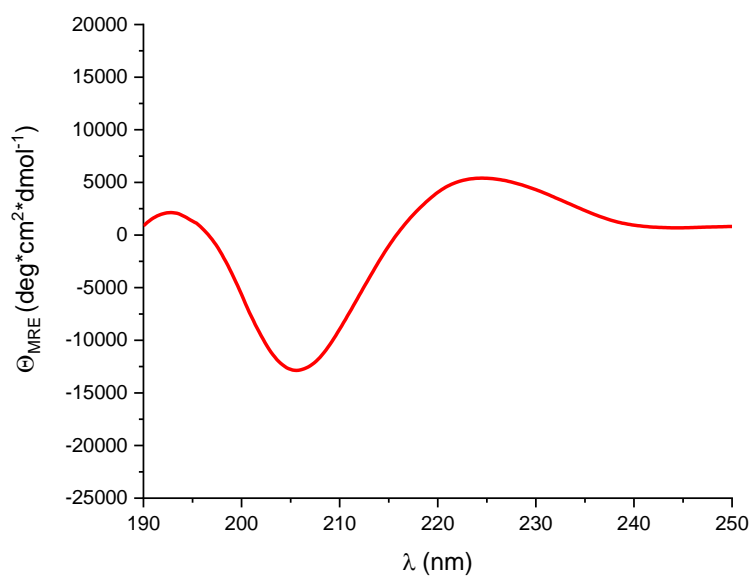**Figure S65**. HPLC chromatogram of peptide **41**.
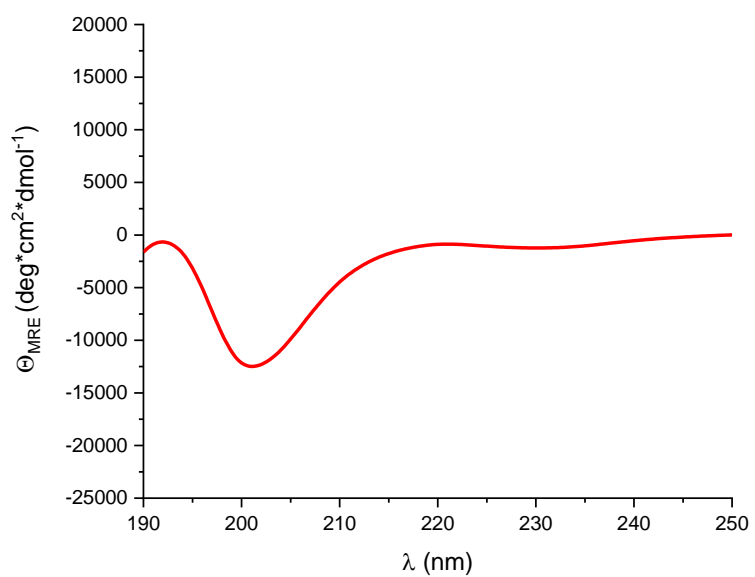
Figure S66. CD spectrum of peptide **ACEα1**.
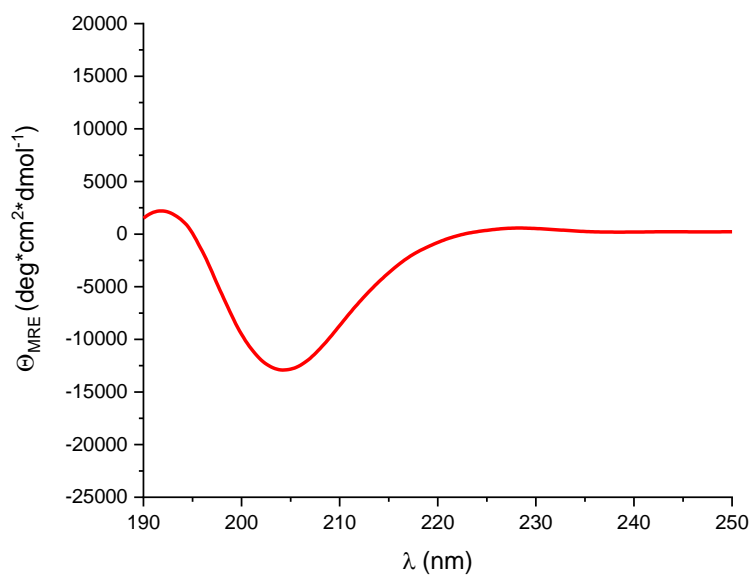
Figure S67. CD spectrum of peptide **A1**.
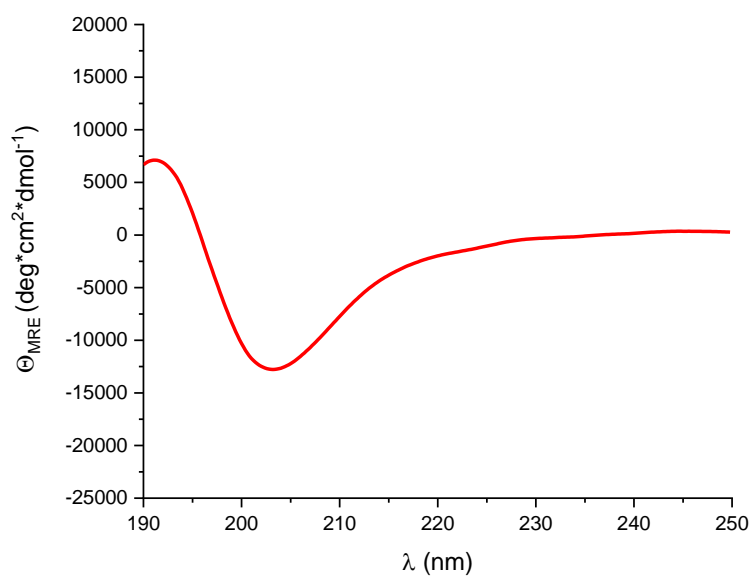
Figure S68. CD spectrum of peptide **A1a**.
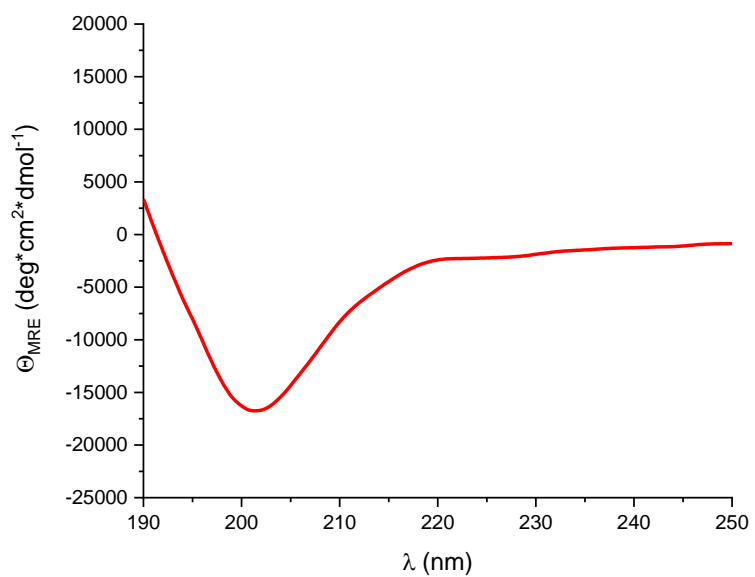
Figure S69. CD spectrum of peptide **A1b**.

Figure S70. CD spectrum of peptide **A1c**.
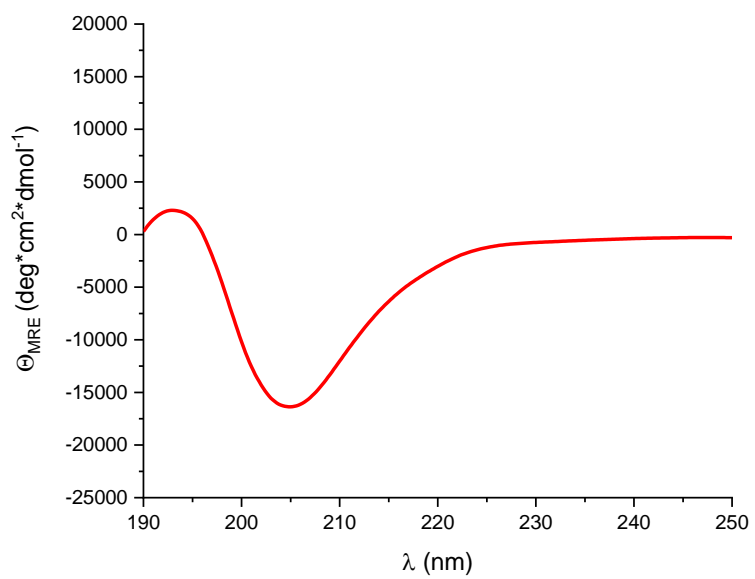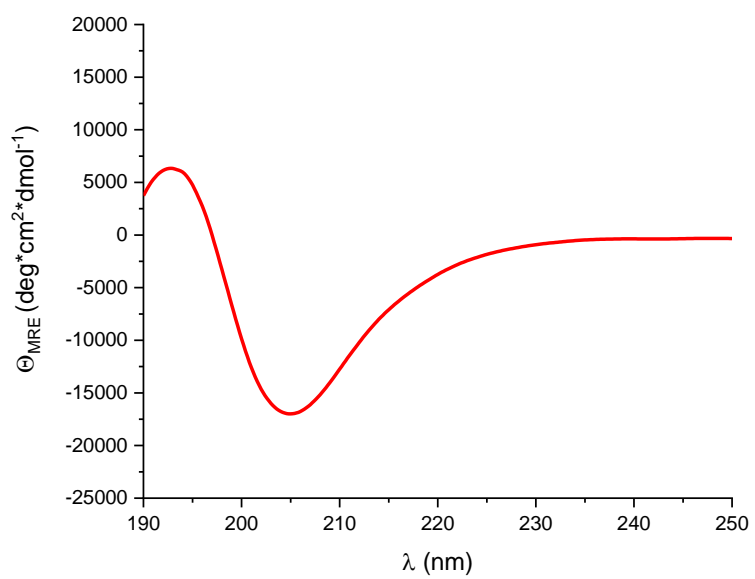

Figure S71. CD spectrum of peptide **A1v1**.
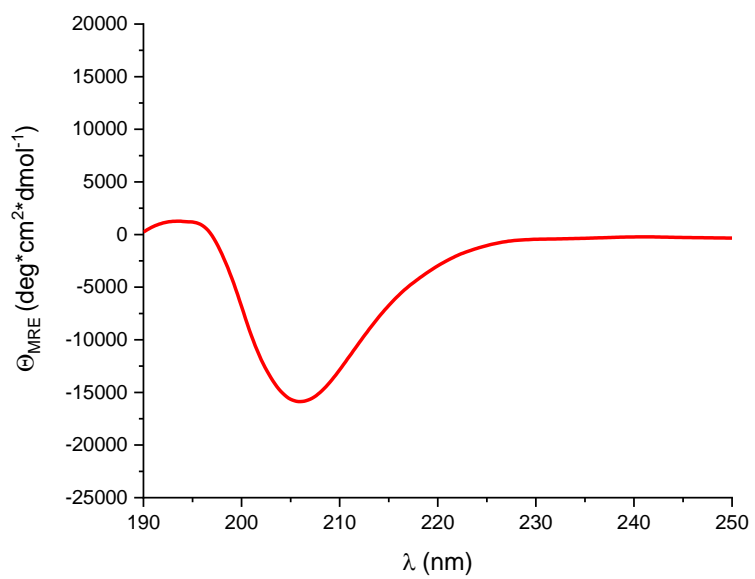
Figure S72. CD spectrum of peptide **A1v2**.

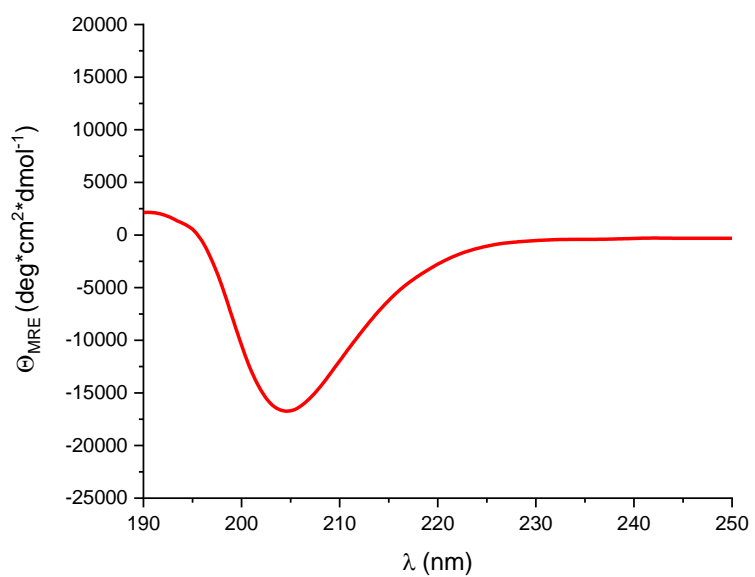**Figure S73**. CD spectrum of peptide **A1v3**.
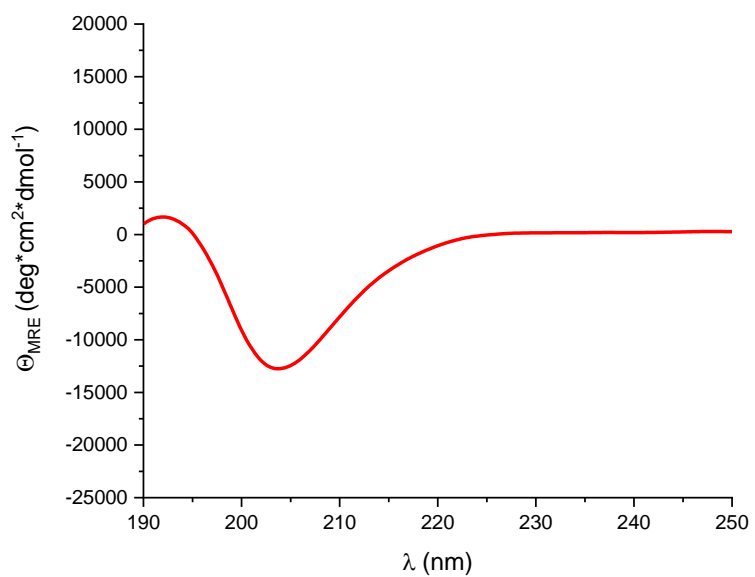
Figure S74. CD spectrum of peptide **A1v4**.

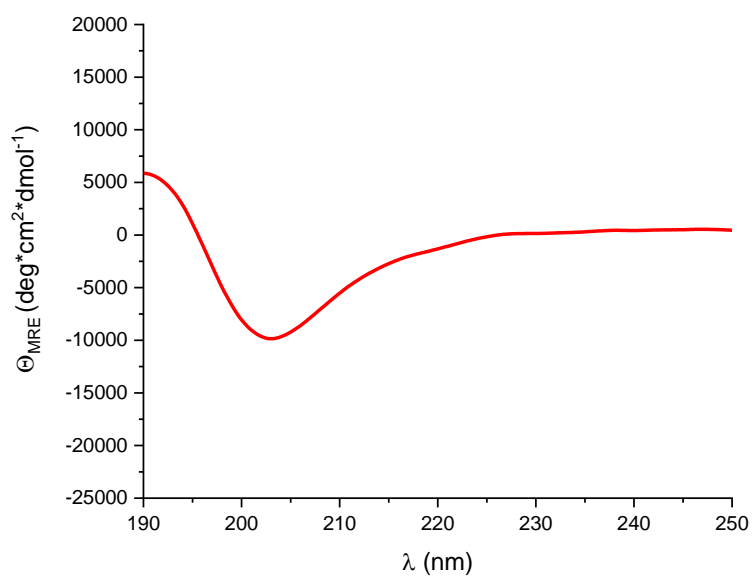**Figure S75**. CD spectrum of peptide **A2**.

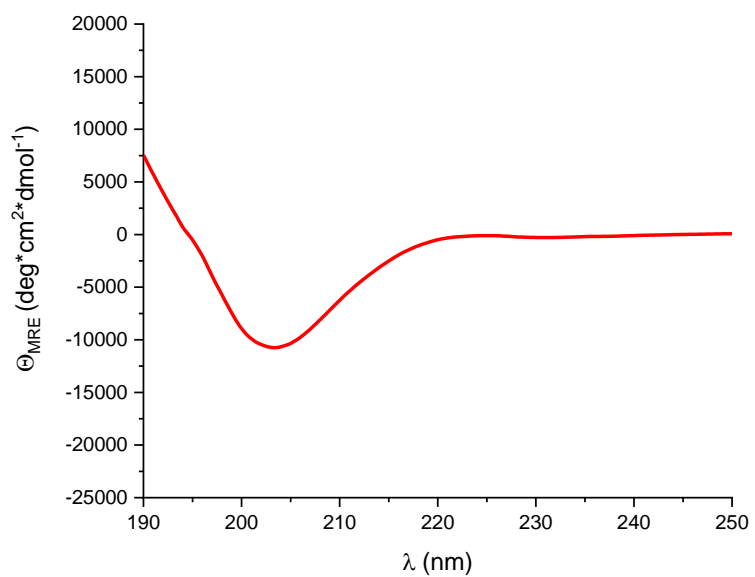**Figure S76**. CD spectrum of peptide **A2a**.

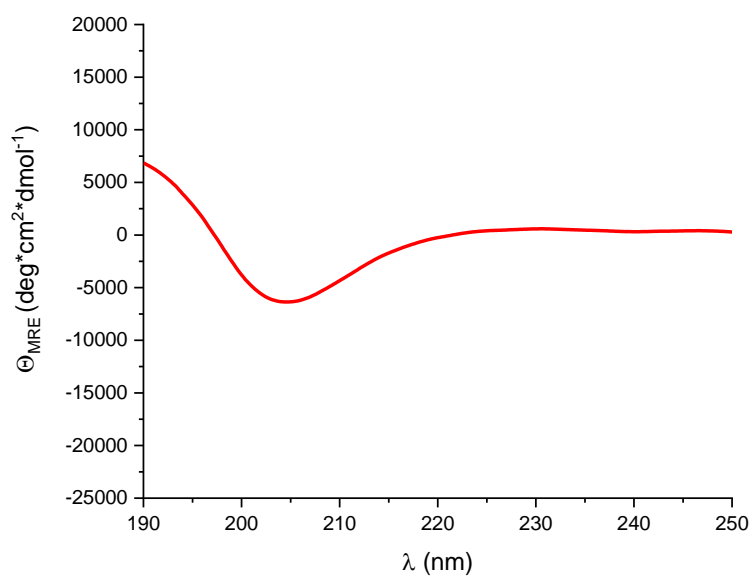**Figure S77**. CD spectrum of peptide **A2b**.
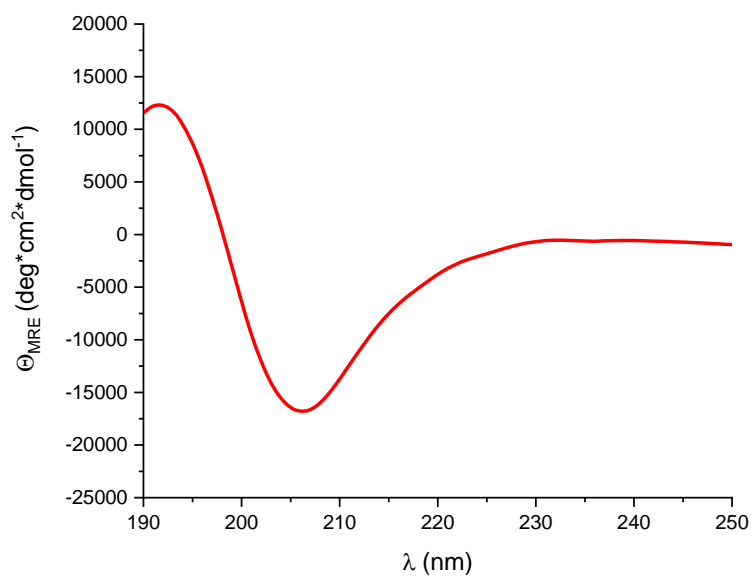
Figure S78. CD spectrum of peptide **A2c**.
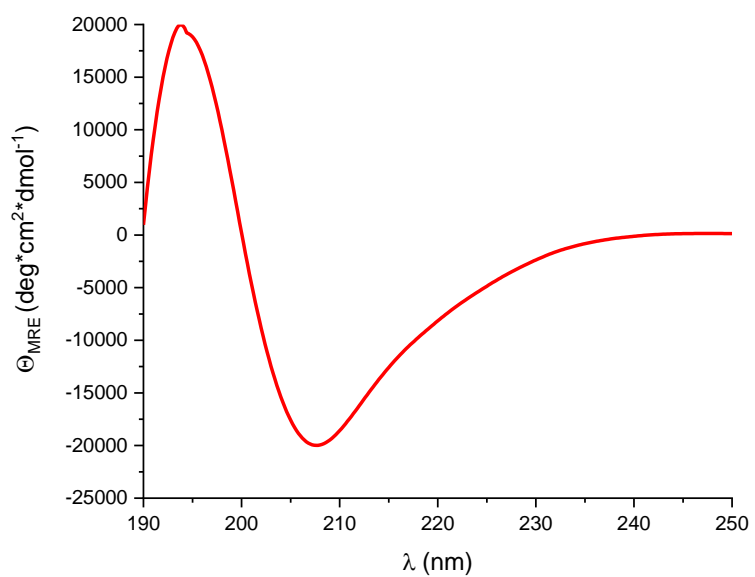

Figure S79. CD spectrum of peptide **A2v1**.

Figure S80. CD spectrum of peptide **A2v2**.
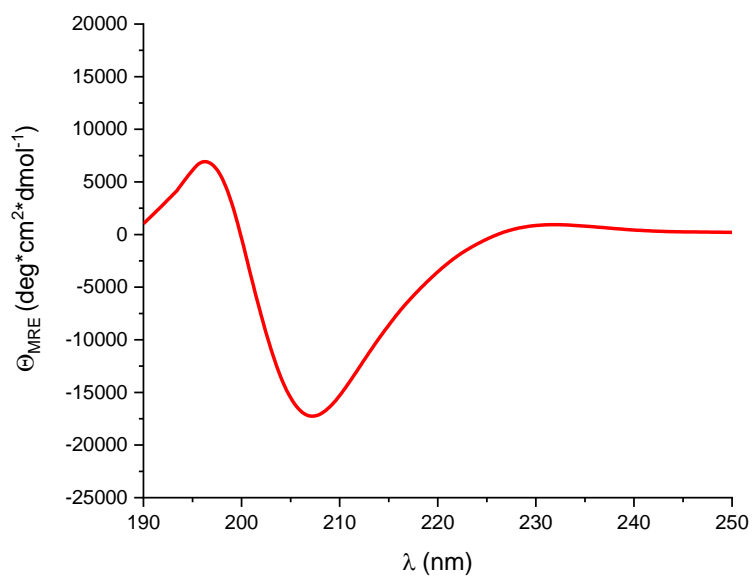

Figure S81. CD spectrum of peptide **A2v3**.

Figure S82. CD spectrum of peptide **A2v4**.

Figure S83. CD spectrum of peptide **A3**.

Figure S84. CD spectrum of peptide **A3a**.

Figure S85. CD spectrum of peptide **A3b**.

Figure S86. CD spectrum of peptide **A3c**.

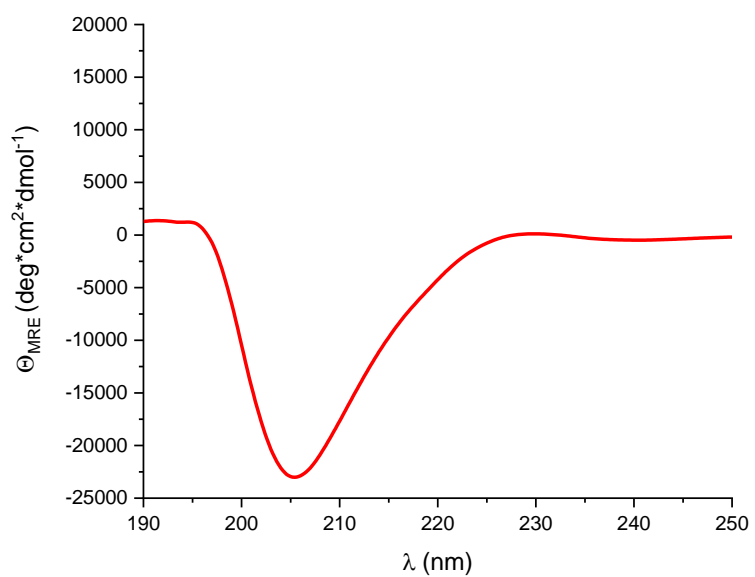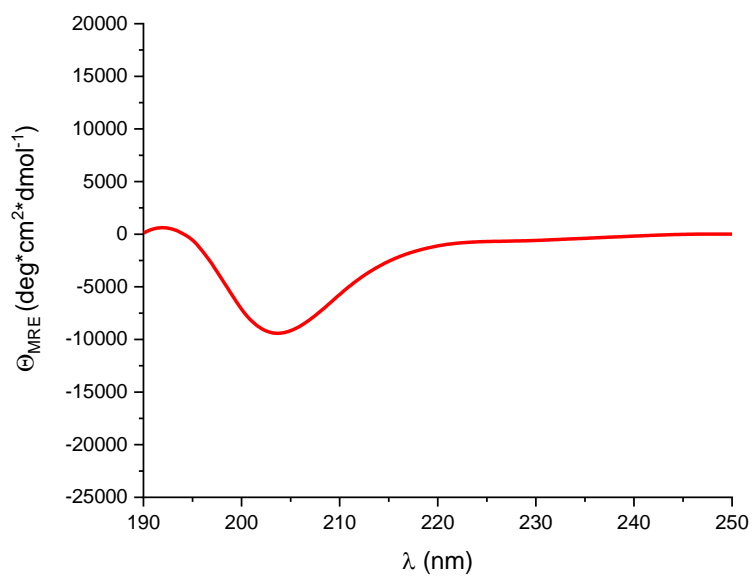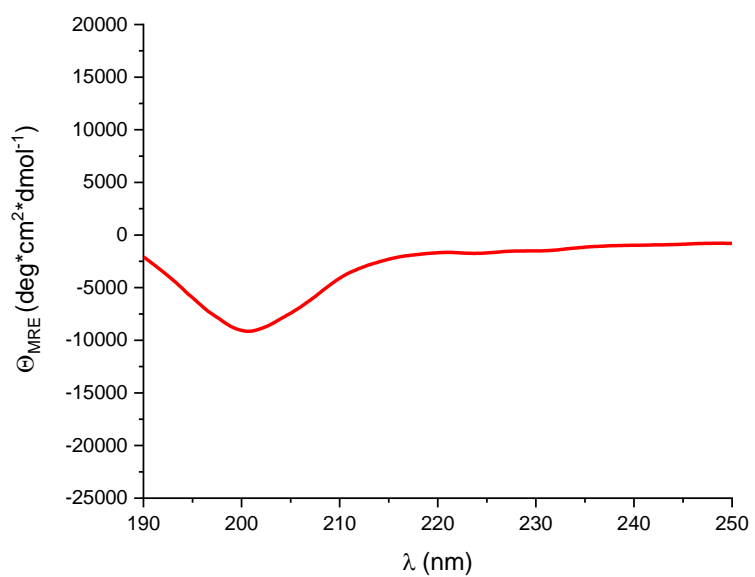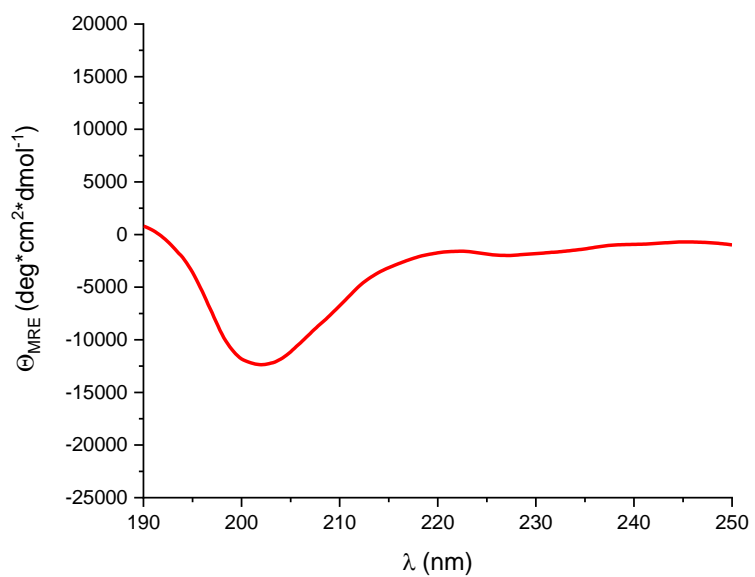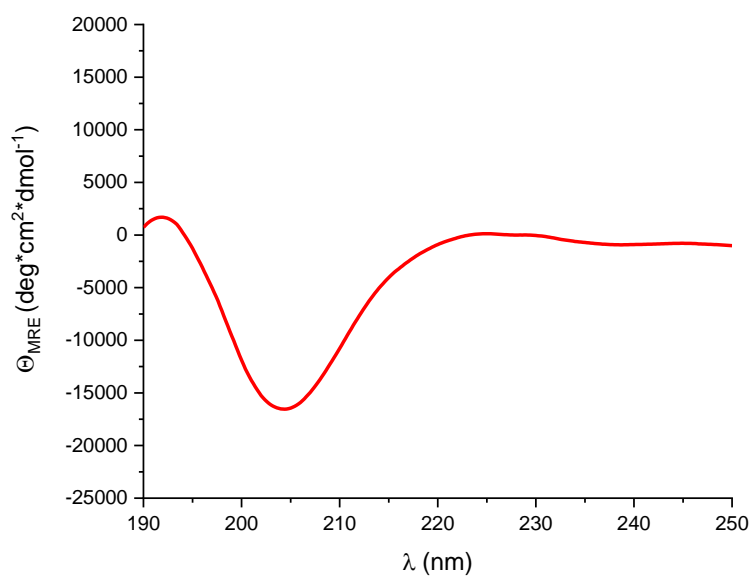**Figure S87**. CD spectrum of peptide **1**.
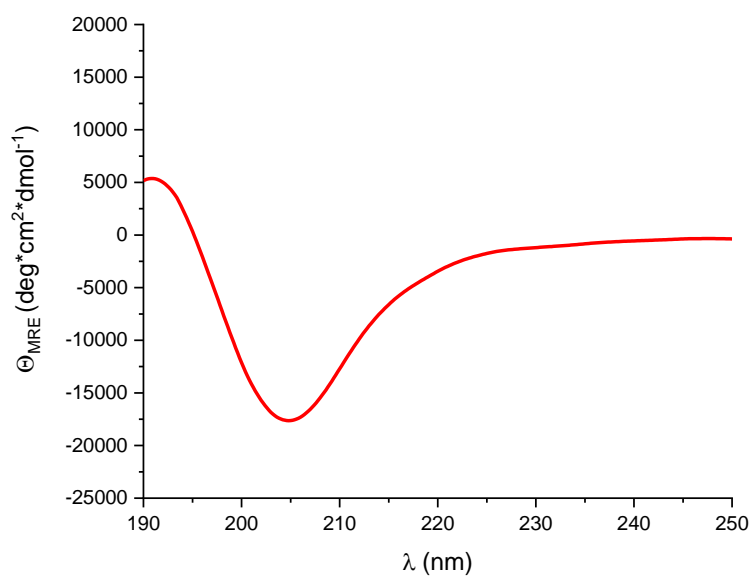
Figure S88. CD spectrum of peptide **2**.
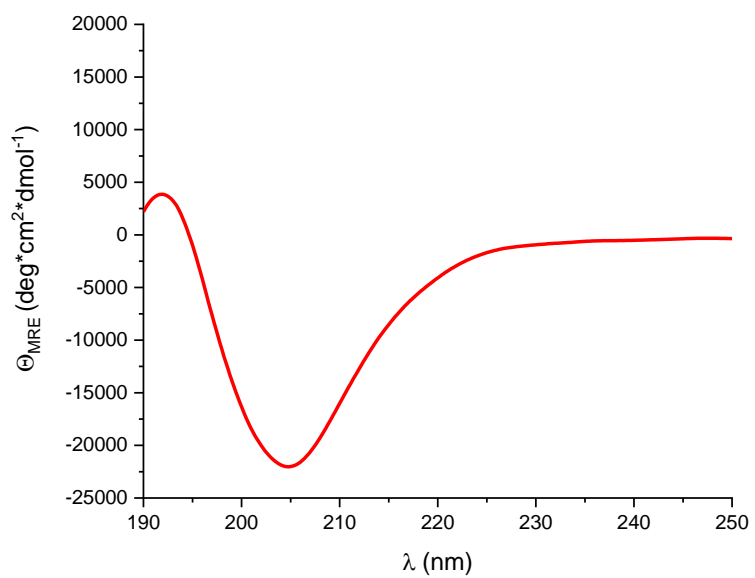
Figure S89. CD spectrum of peptide **3**.
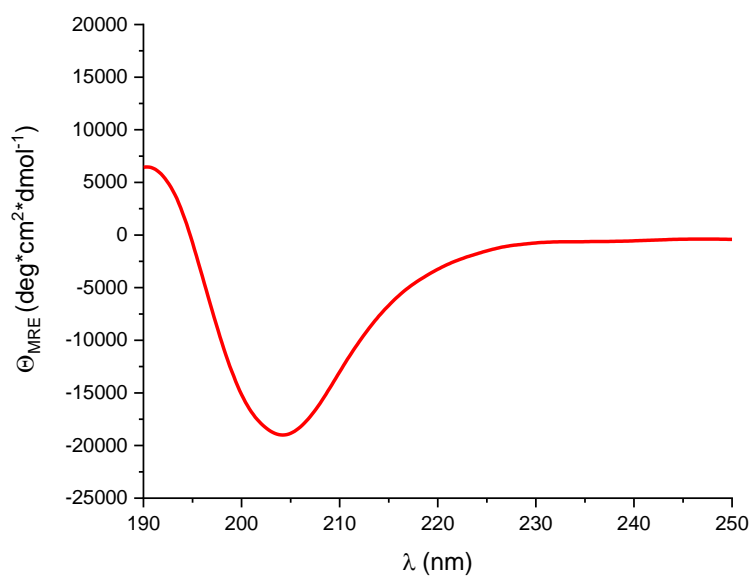
Figure S90. CD spectrum of peptide **4**.
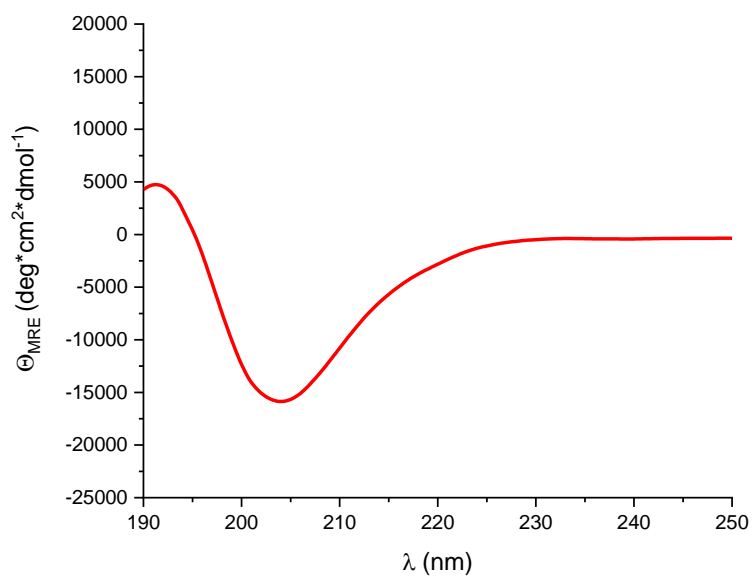
Figure S91. CD spectrum of peptide **5**.

Figure S92. CD spectrum of peptide **6**.

Figure S93. CD spectrum of peptide **7**.

Figure S94. CD spectrum of peptide **8**.

Figure S95. CD spectrum of peptide **9**.

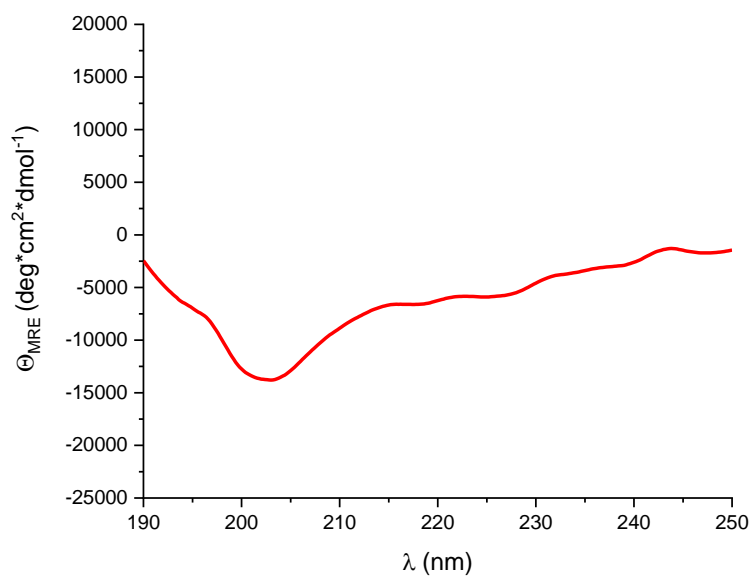**Figure S96**. CD spectrum of peptide **10**.

Figure S97. CD spectrum of peptide **11**.

Figure S98. CD spectrum of peptide **12**.
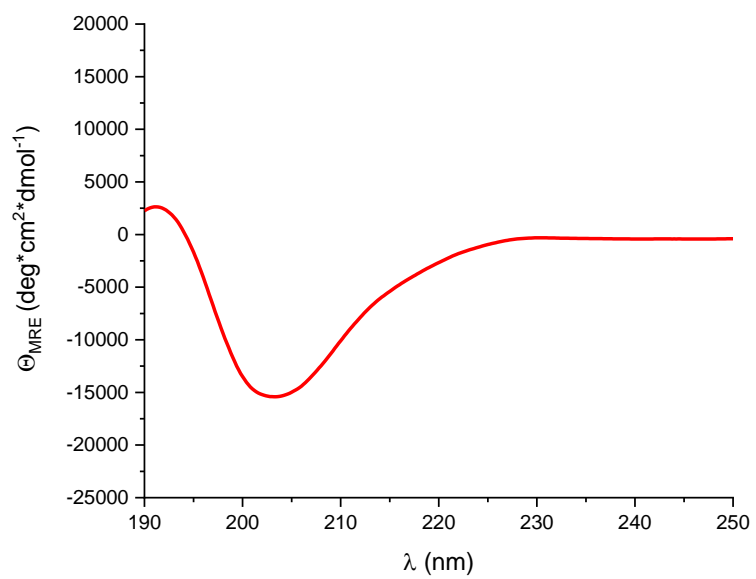
Figure S99. CD spectrum of peptide **13**.
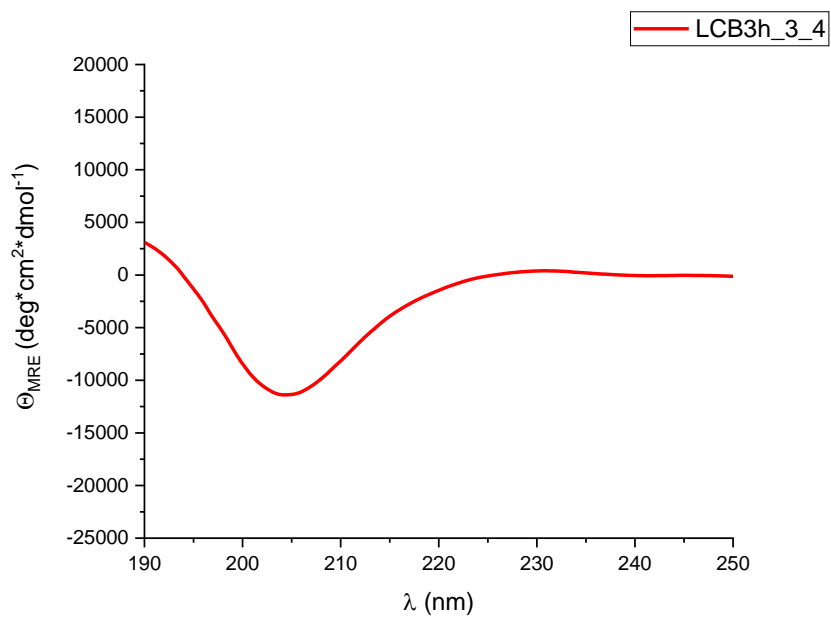
Figure S100. CD spectrum of peptide **14**.
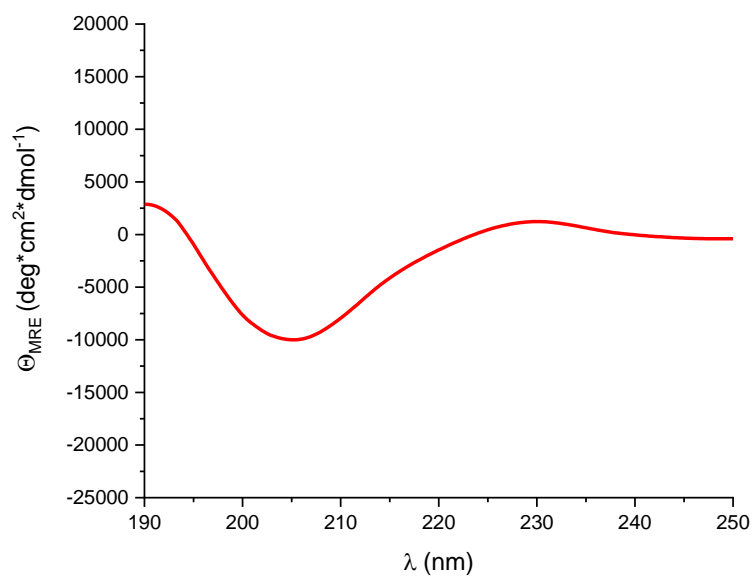
Figure S101. CD spectrum of peptide **15**.
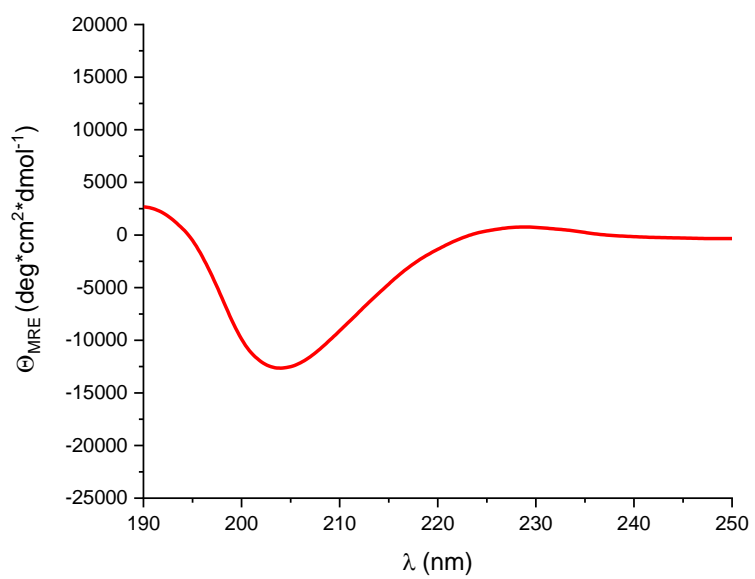
Figure S102. CD spectrum of peptide **16**.
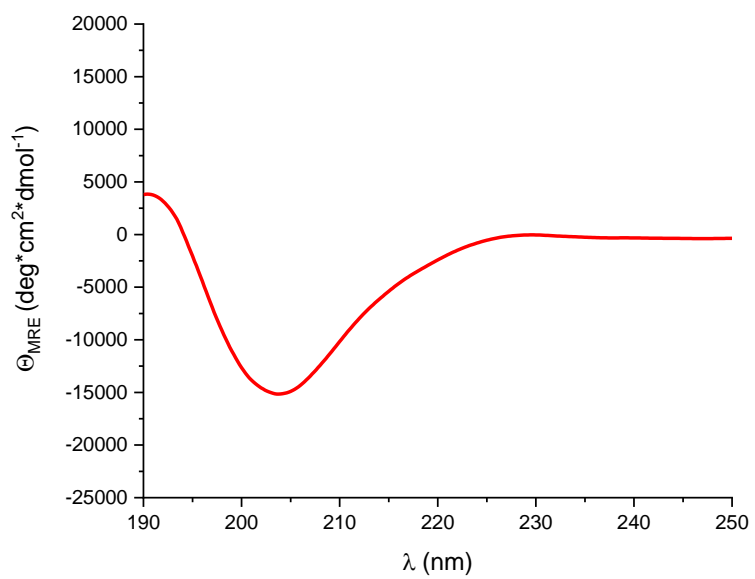
Figure S103. CD spectrum of peptide **17**.
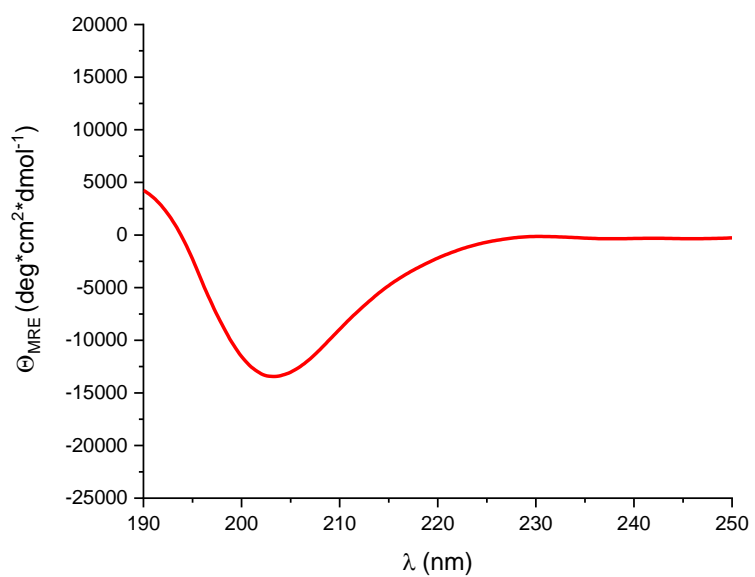
Figure S104. CD spectrum of peptide **18**.

Figure S105. CD spectrum of peptide **19**.
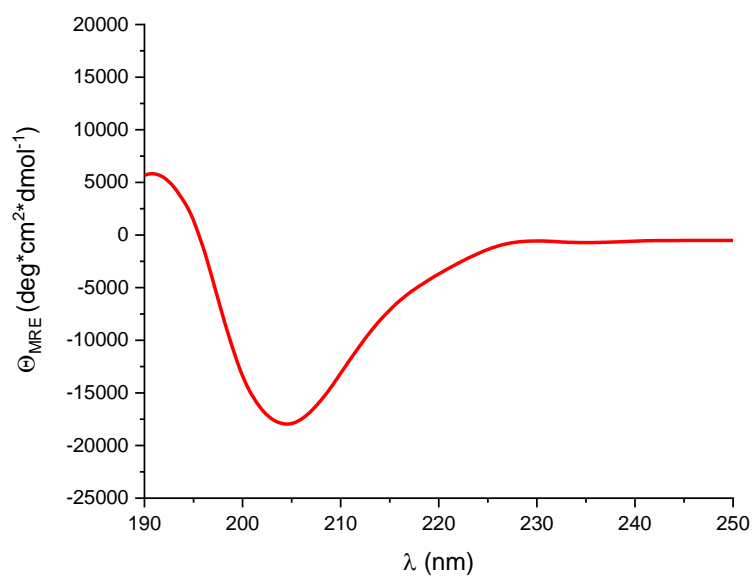
Figure S106. CD spectrum of peptide **20**.
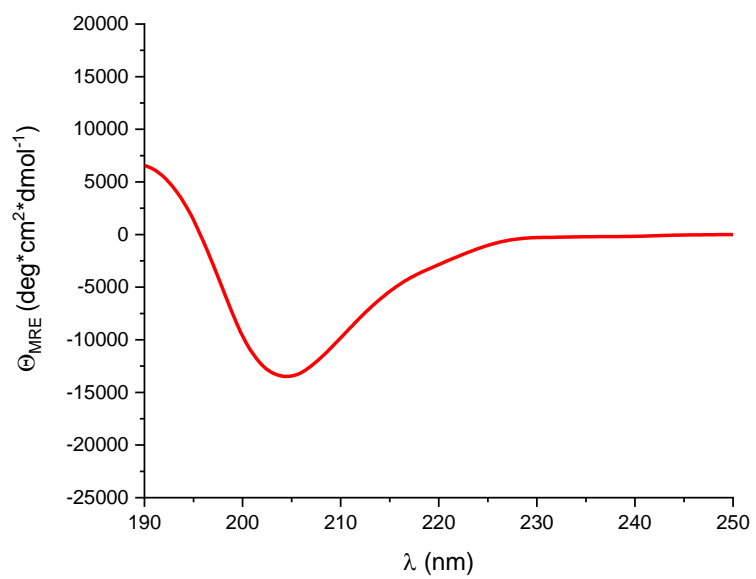
Figure S107. CD spectrum of peptide **21**.
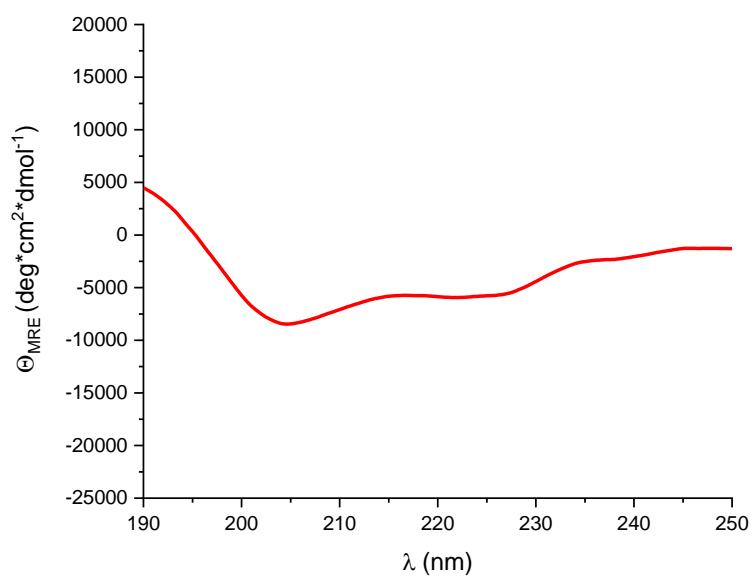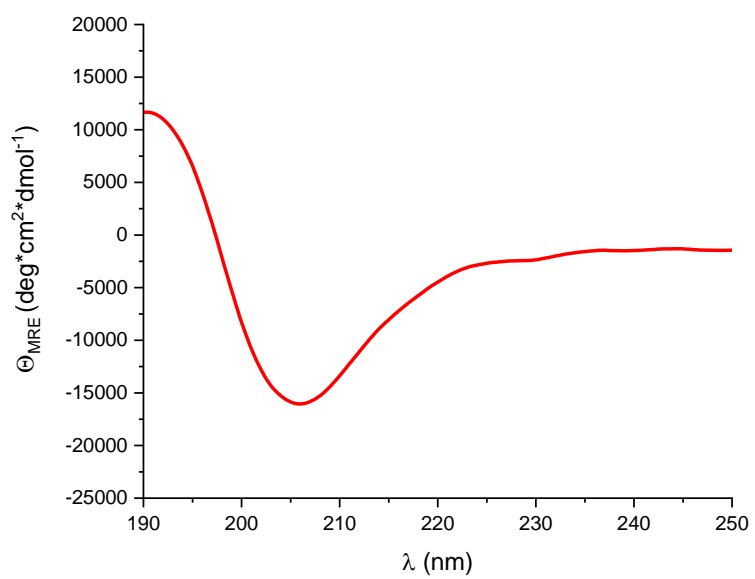
Figure S108. CD spectrum of peptide **22**.
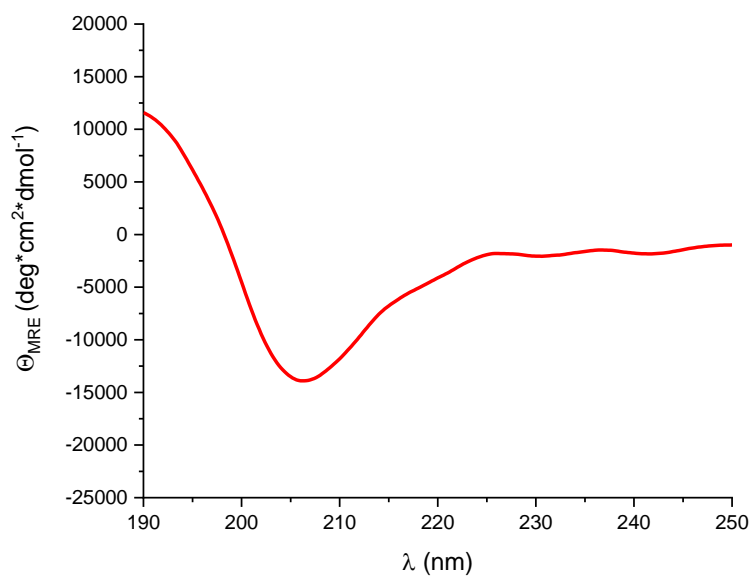
Figure S109. CD spectrum of peptide **23**.
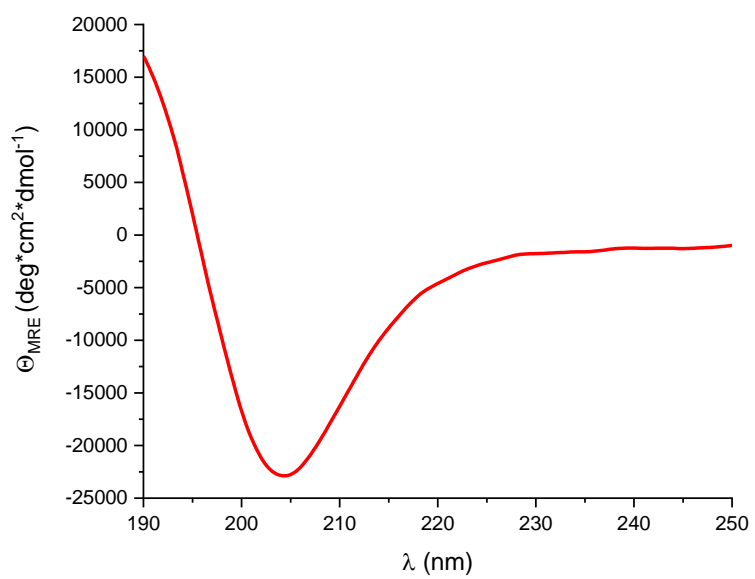
Figure S110. CD spectrum of peptide **24**.
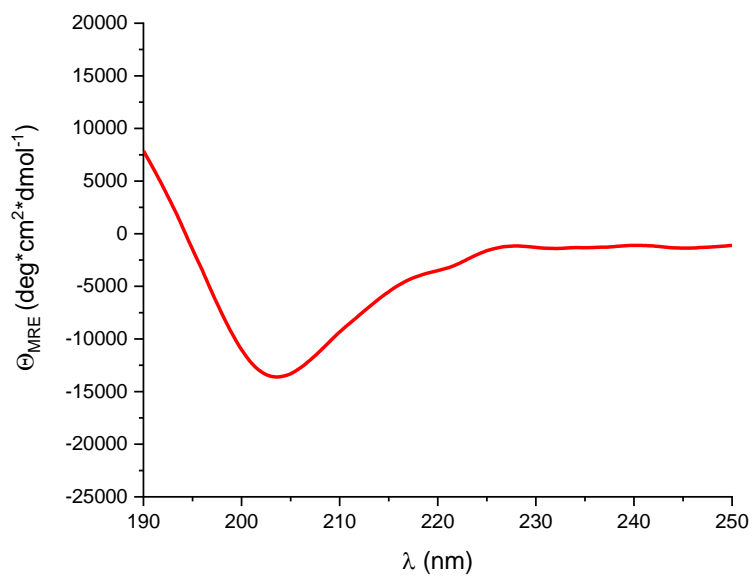
Figure S111. CD spectrum of peptide **25**.
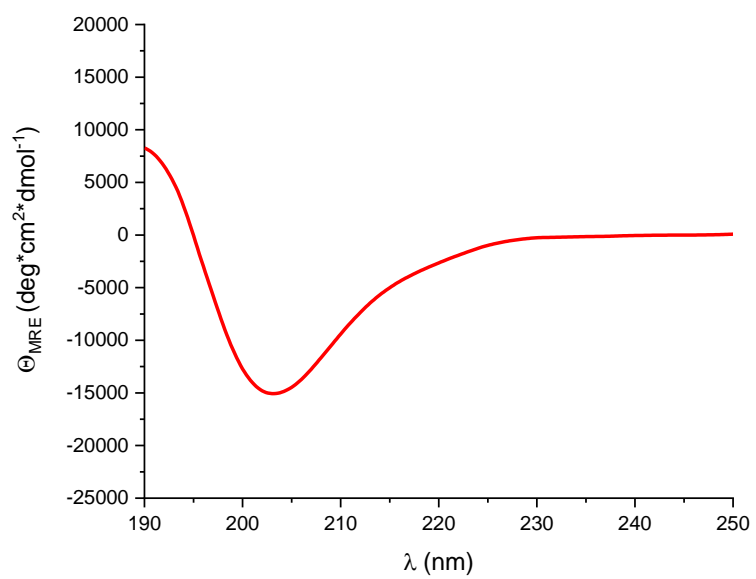
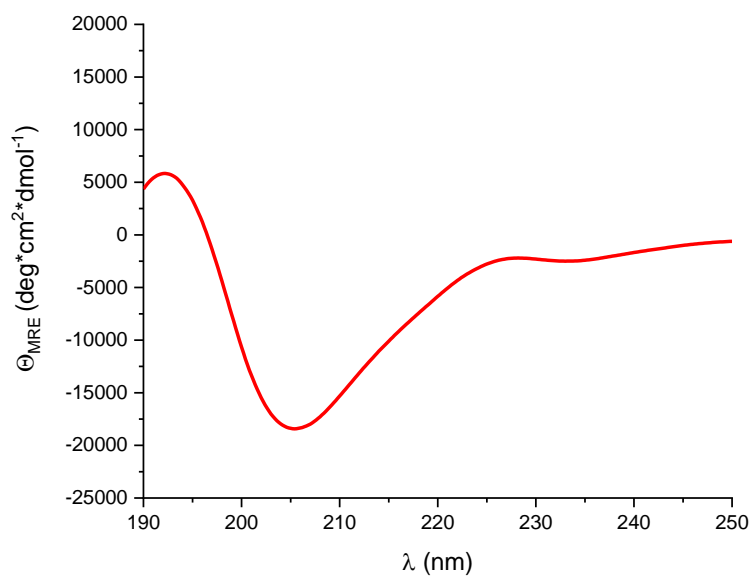**Figure S112**. CD spectrum of peptide **26**.
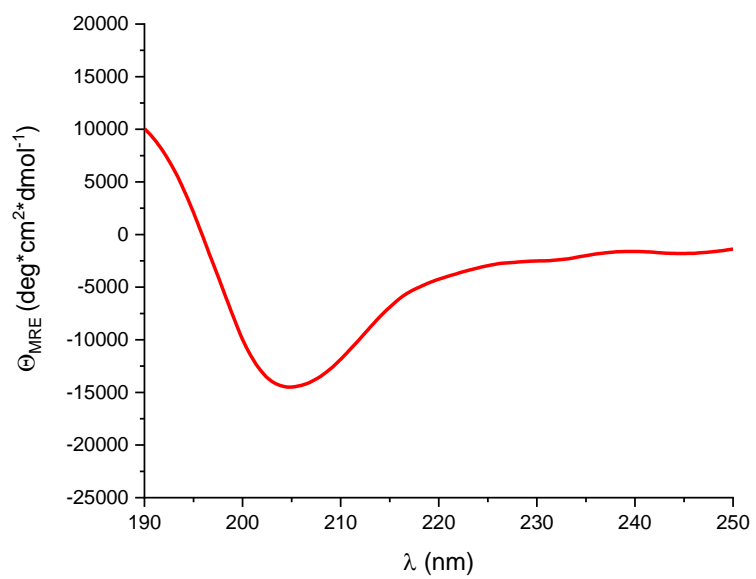
Figure S113. CD spectrum of peptide **27**.
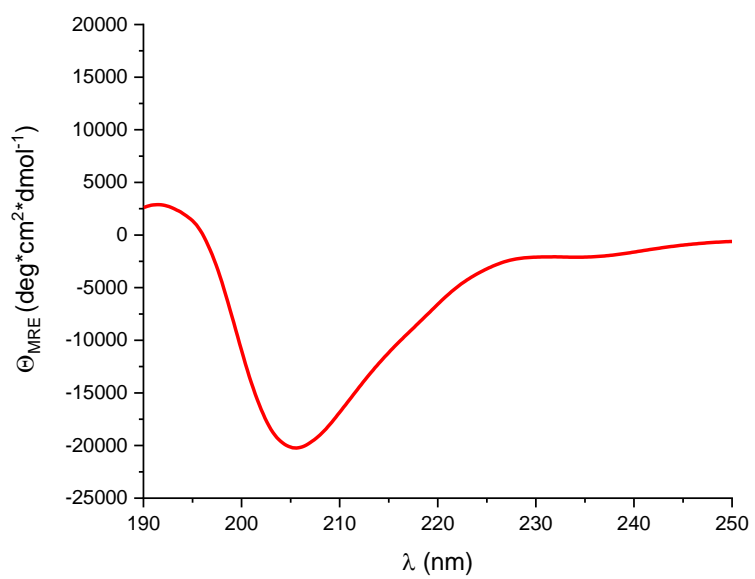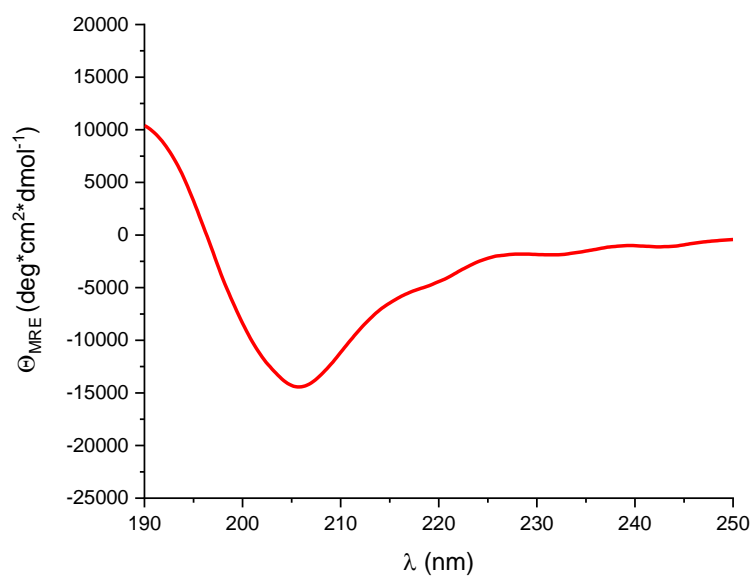
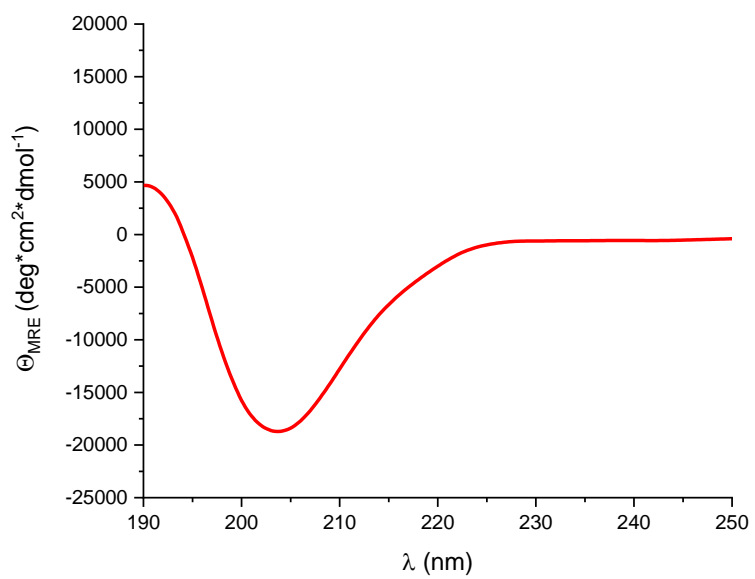**Figure S114**. CD spectrum of peptide **28**.
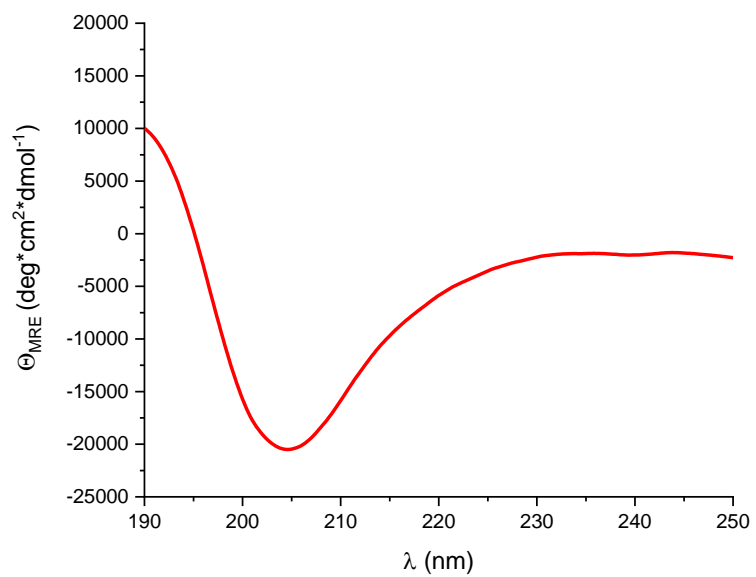
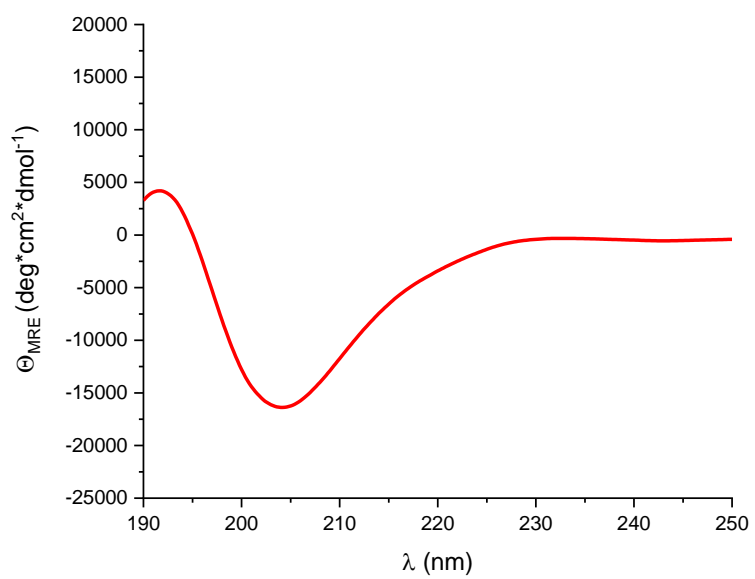**Figure S115**. CD spectrum of peptide **29**.
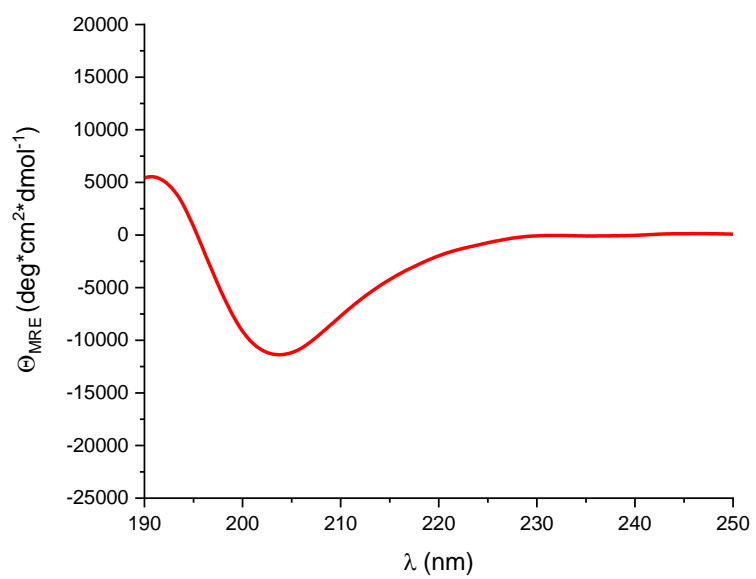
Figure S116. CD spectrum of peptide **30**.
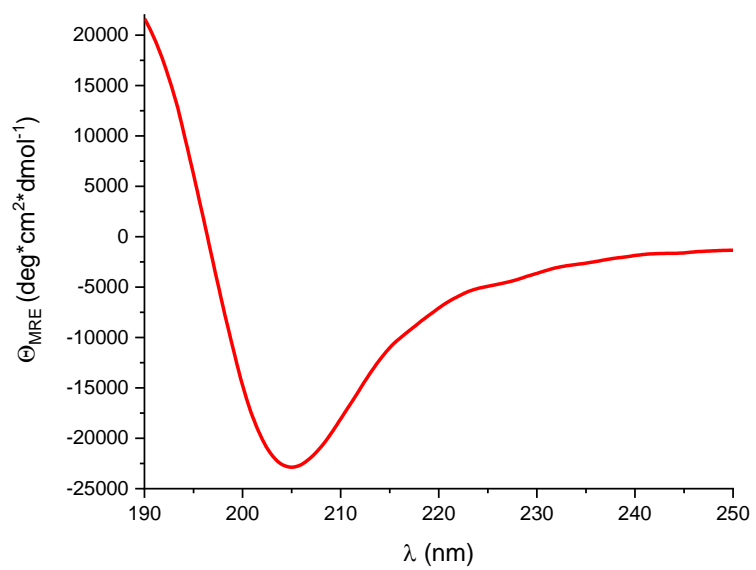
Figure S117. CD spectrum of peptide **31**.
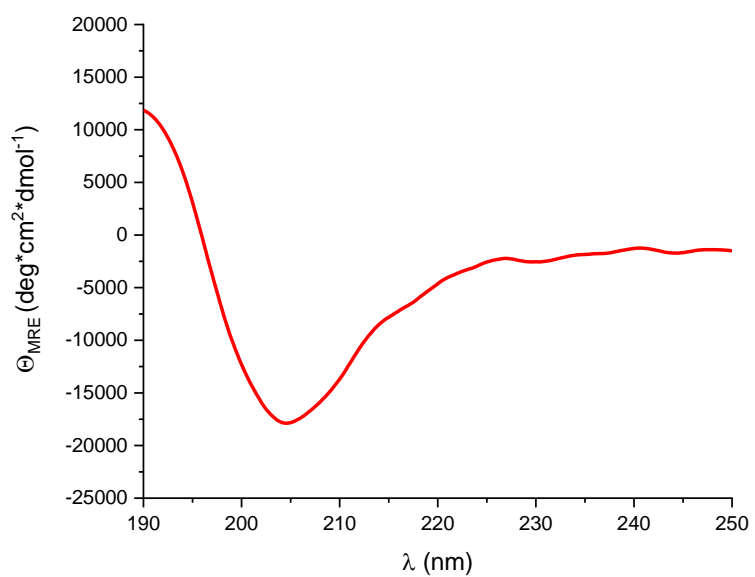
Figure S118. CD spectrum of peptide **32**.
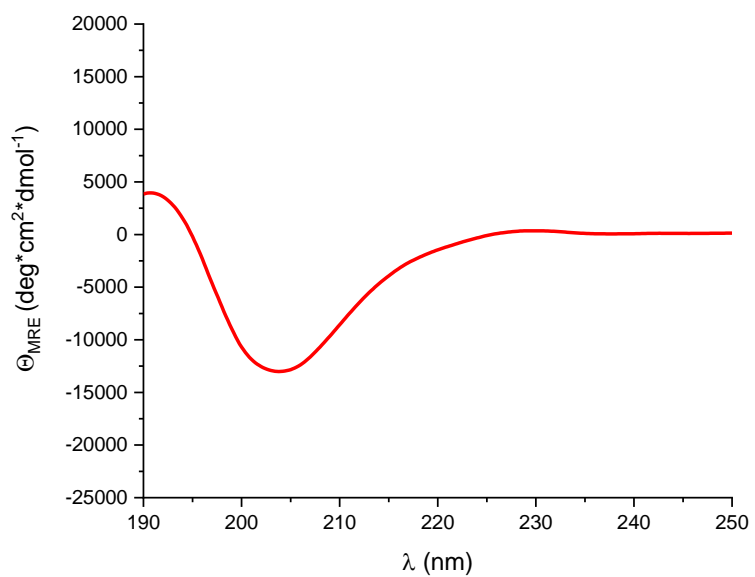
Figure S119. CD spectrum of peptide **33**.
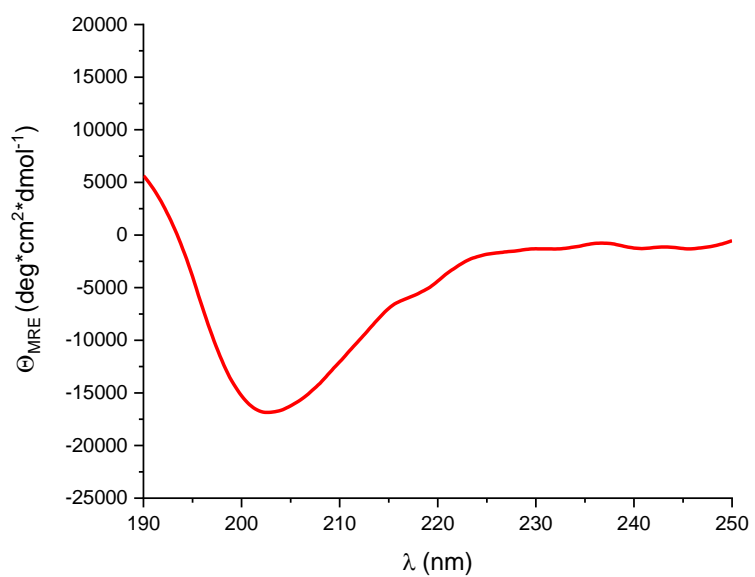
Figure S120. CD spectrum of peptide **34**.
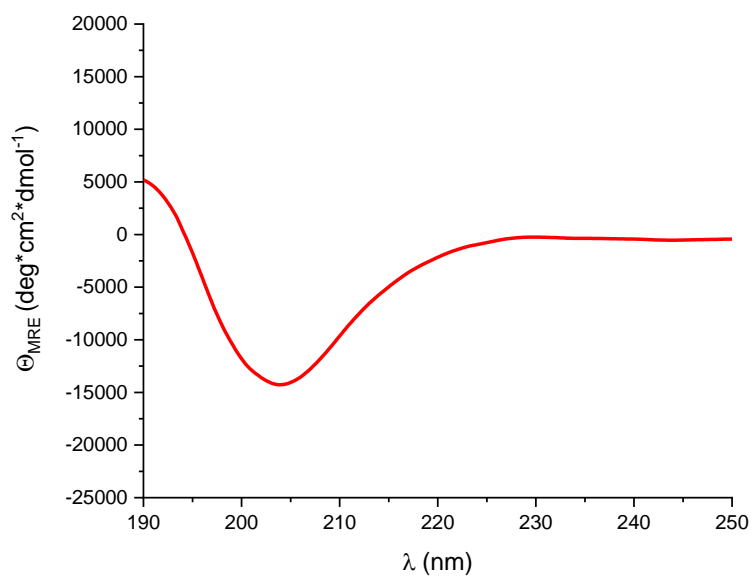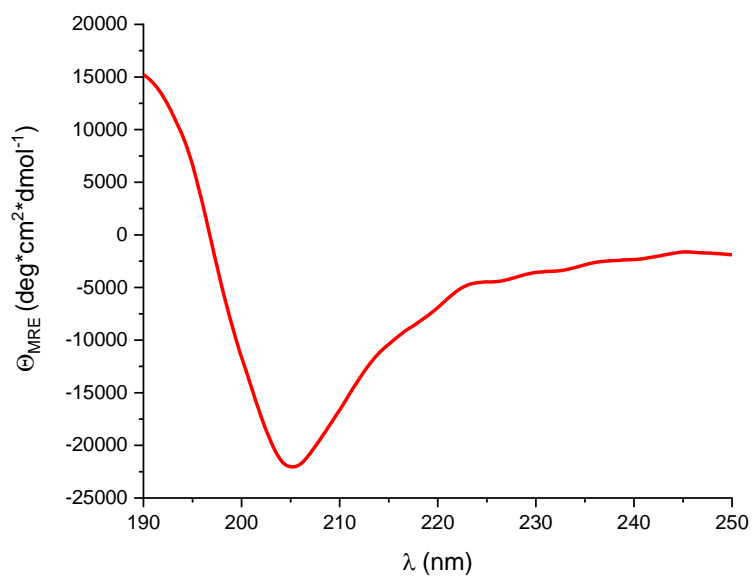

Figure S121. CD spectrum of peptide **35**.
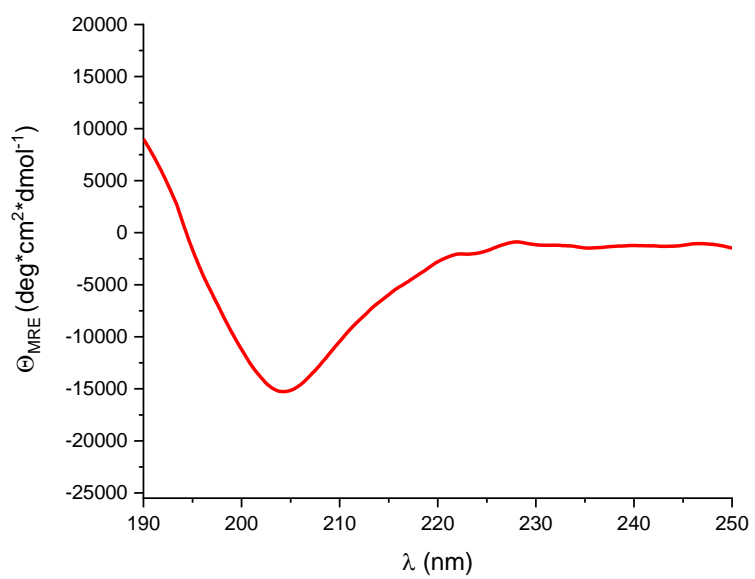
Figure S122. CD spectrum of peptide **36**.
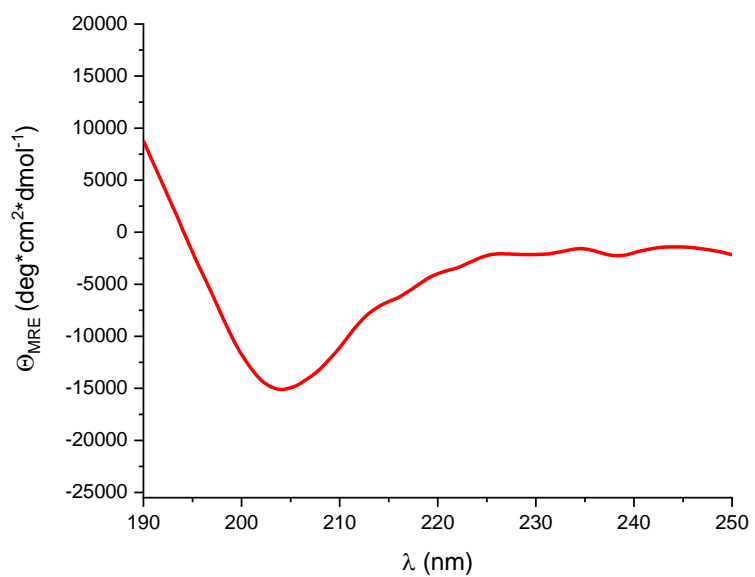
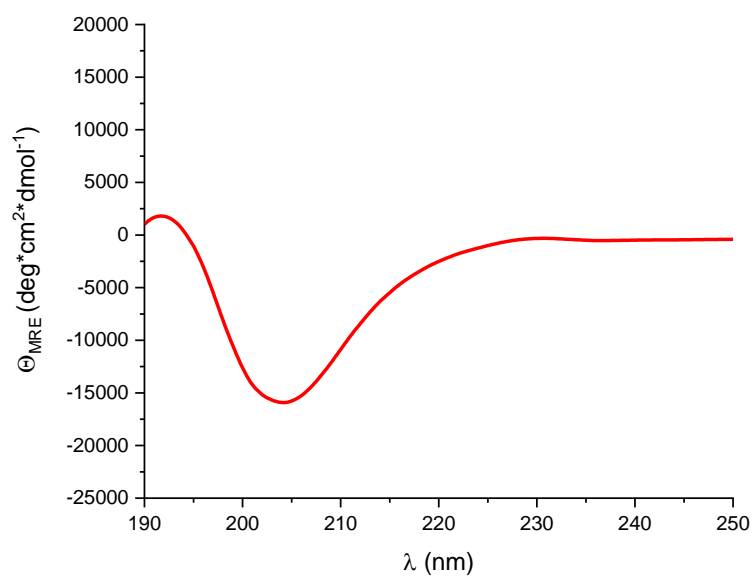**Figure S123**. CD spectrum of peptide **37**.
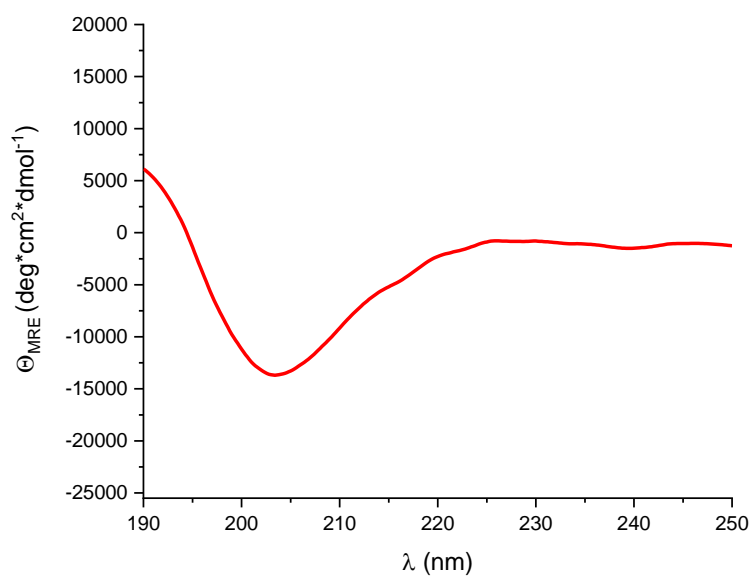
Figure S124. CD spectrum of peptide **38**.
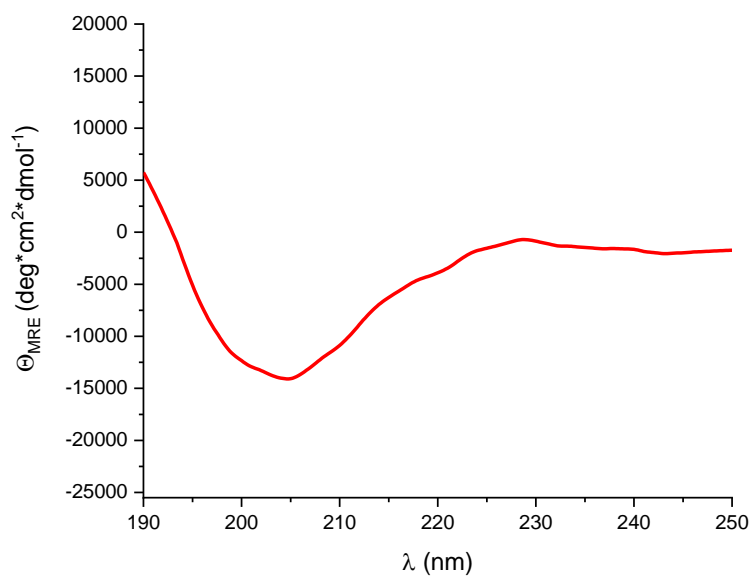
Figure S125. CD spectrum of peptide **39**.
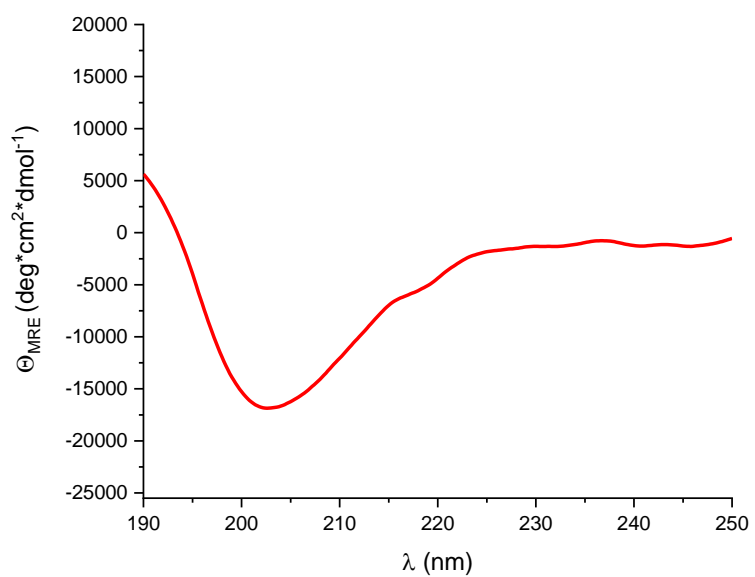
Figure S126. CD spectrum of peptide **40**.
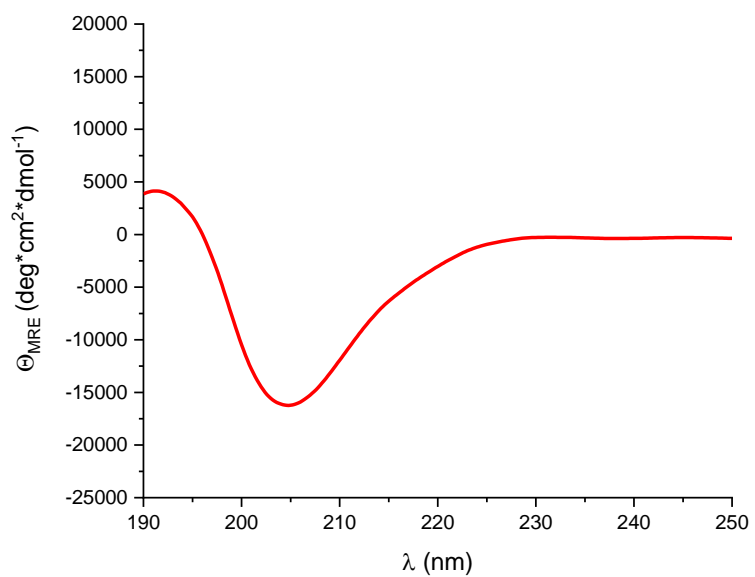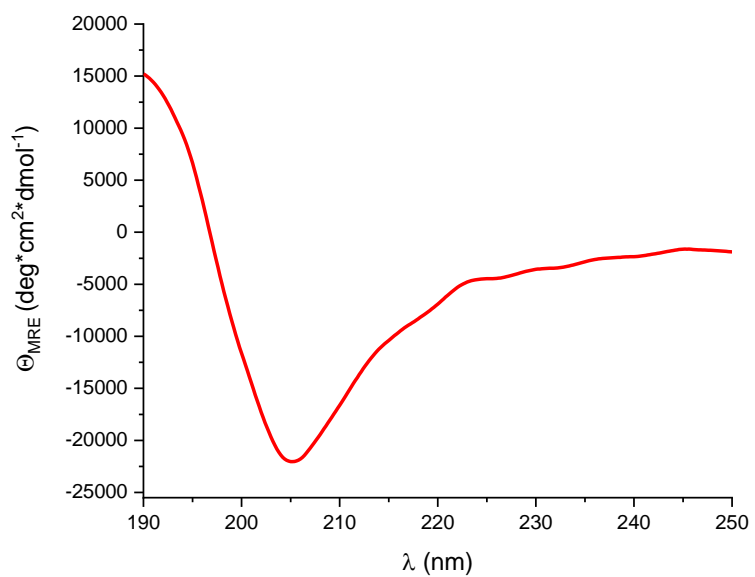

Figure S127. CD spectrum of peptide **41**.
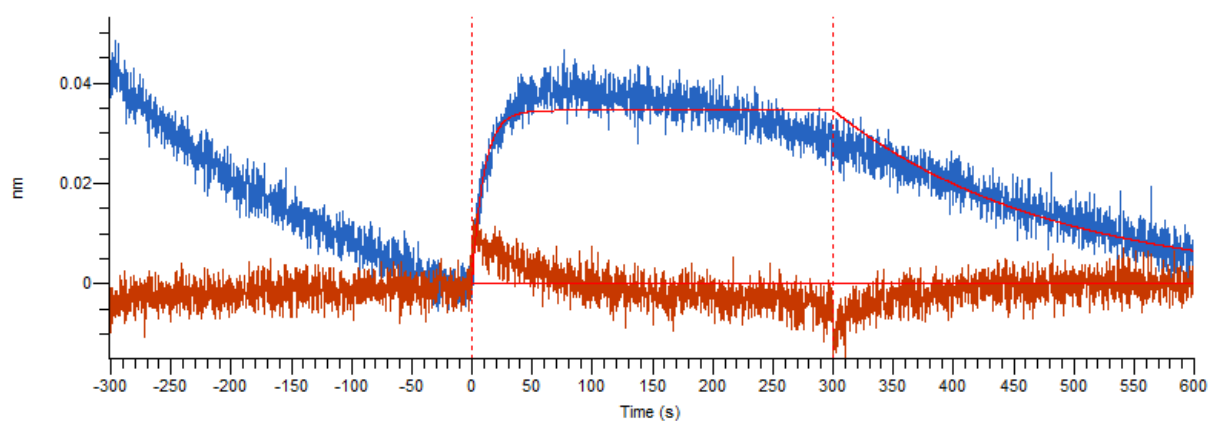
Figure S128. Binding of 50 µM **ACEα1** to the RBD monitored with BLI.
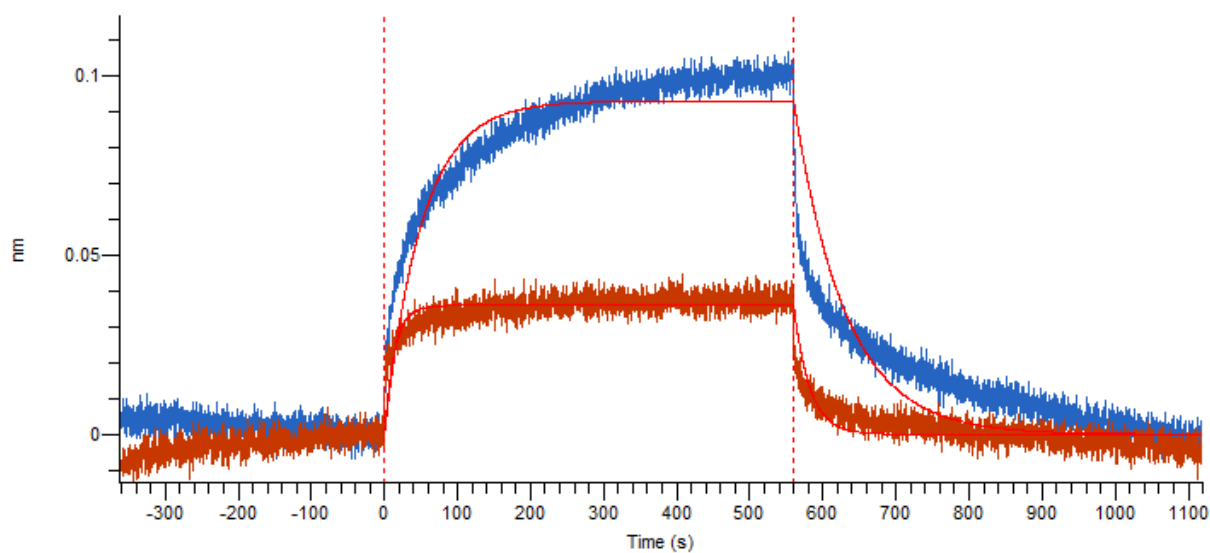
Figure S129. Binding of 50 µM **A1** to the RBD monitored with BLI.
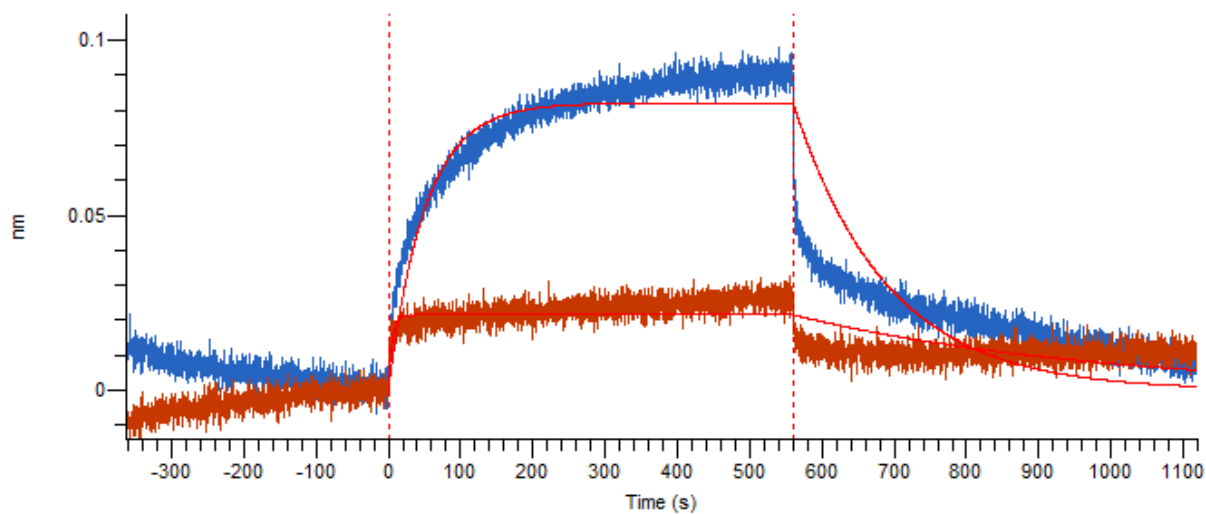
Figure S130. Binding of 50 µM **A1a** to the RBD monitored with BLI.
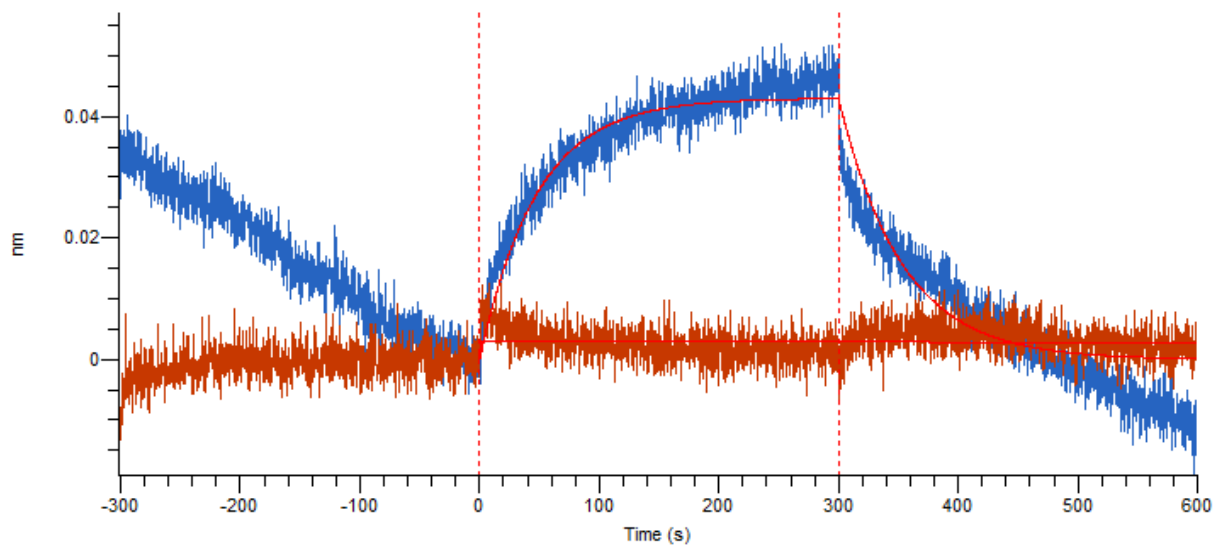
Figure S131. Binding of 50 μM **A1b** to the RBD monitored with BLI.
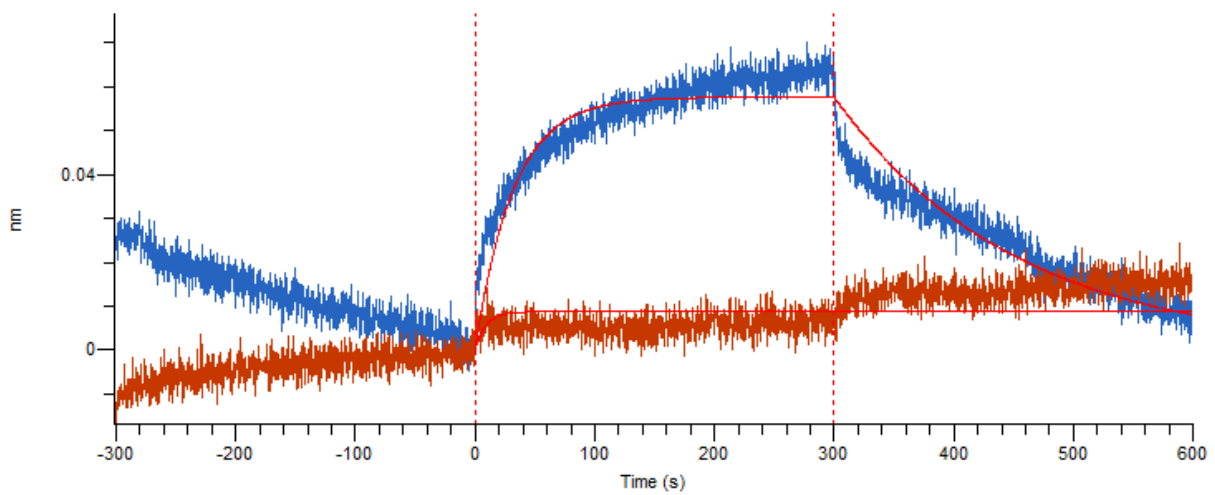
Figure S132. Binding of 50 μM **A1c** to the RBD monitored with BLI.
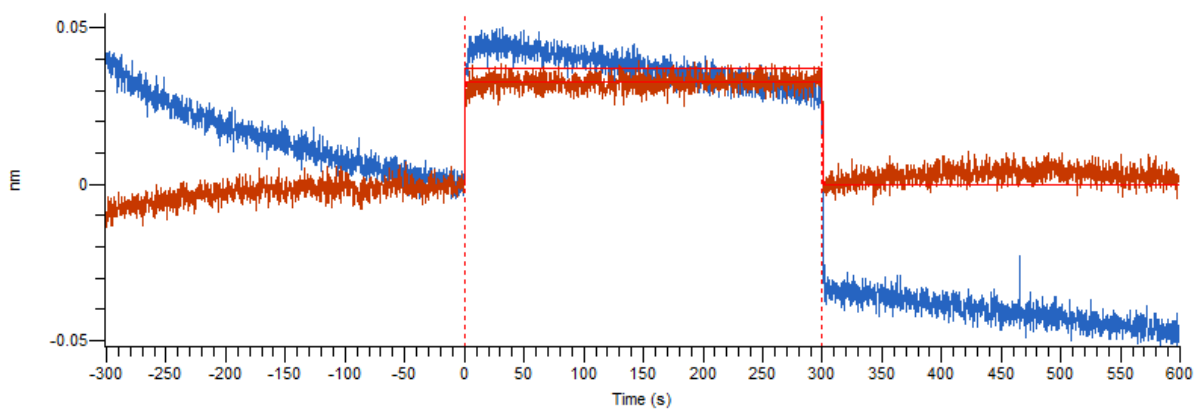
Figure S133. Binding of 50 μM **A1v1** to the RBD monitored with BLI.
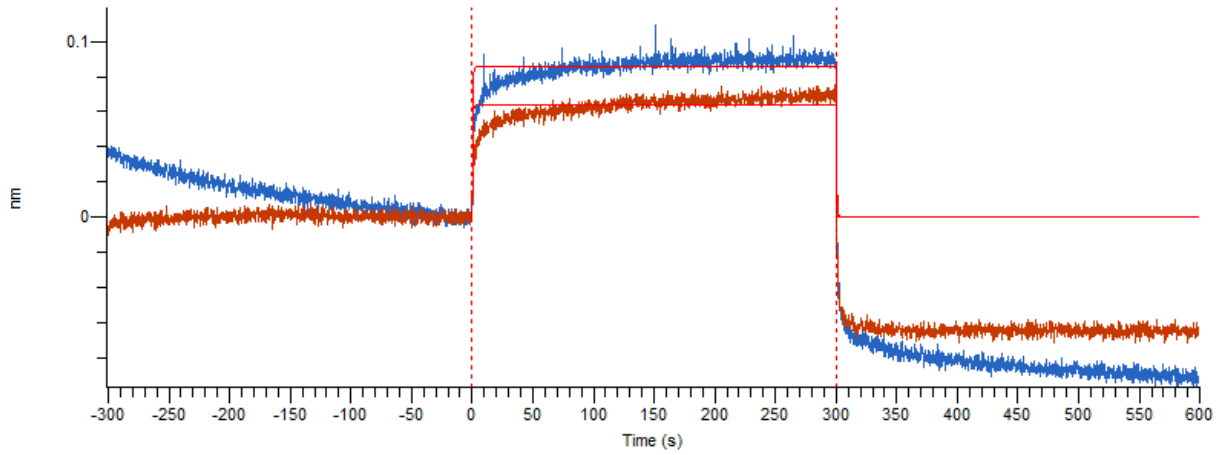
Figure S134. Binding of 50 μM **A1v2** to the RBD monitored with BLI.
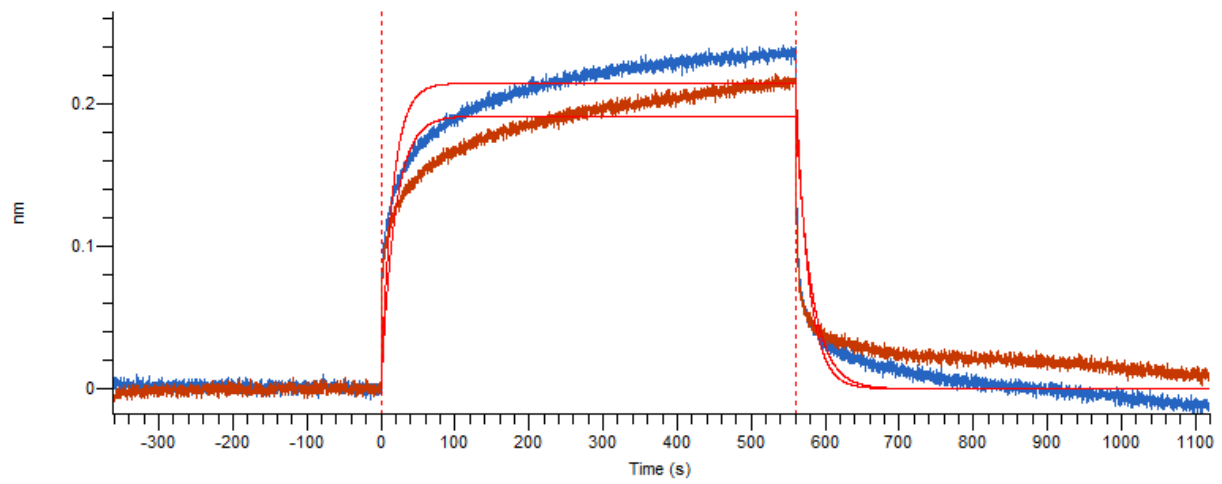
Figure S135. Binding of 50 μM **A1v3** to the RBD monitored with BLI.
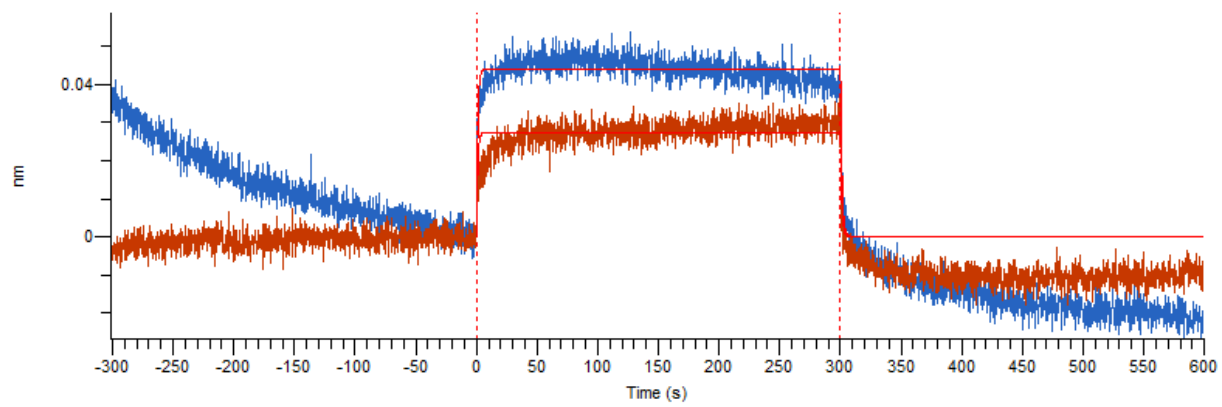
Figure S136. Binding of 50 μM **A1v4** to the RBD monitored with BLI.
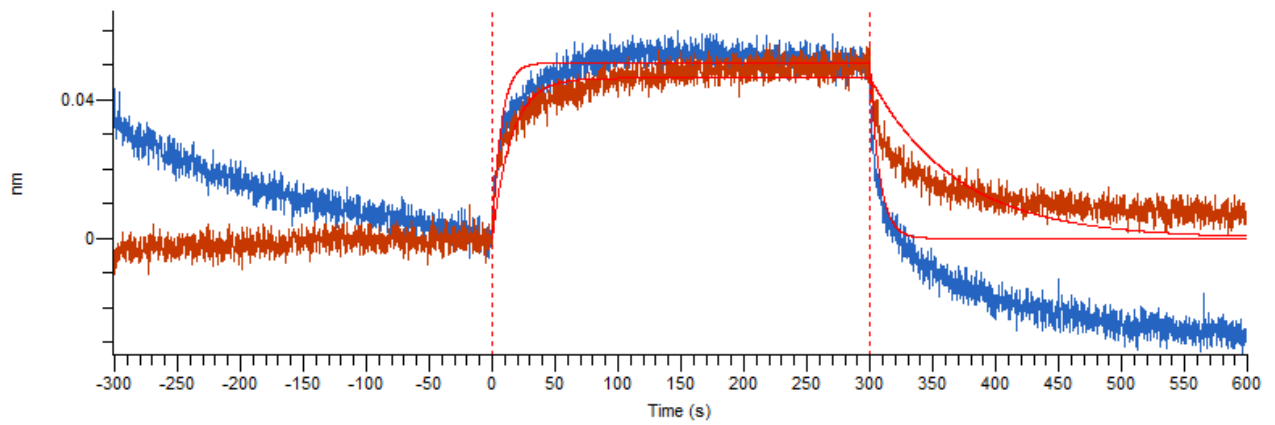
Figure S137. Binding of 50 μM **A2** to the RBD monitored with BLI.
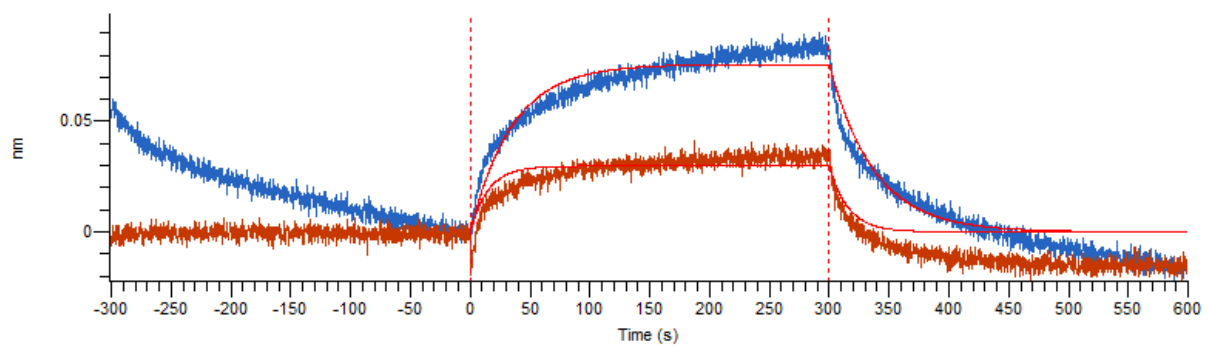
Figure S138. Binding of 50 μM **A2a** to the RBD monitored with BLI.
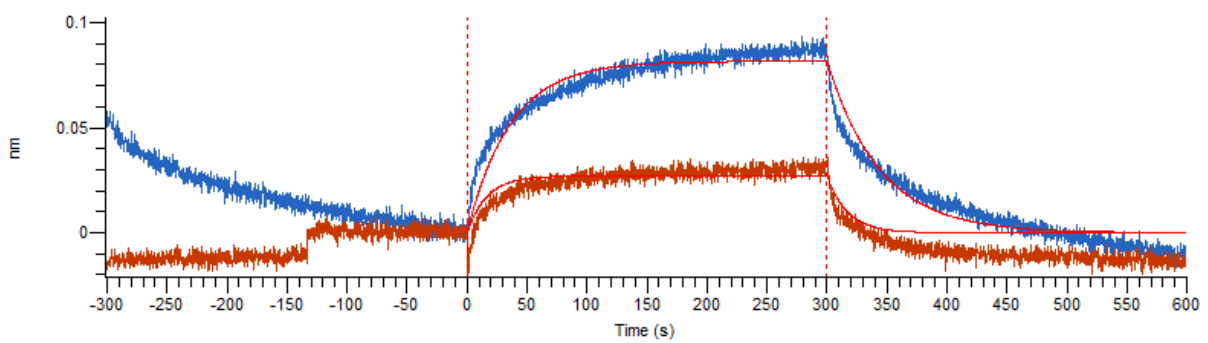
Figure S139. Binding of 50 μM **A2b** to the RBD monitored with BLI.
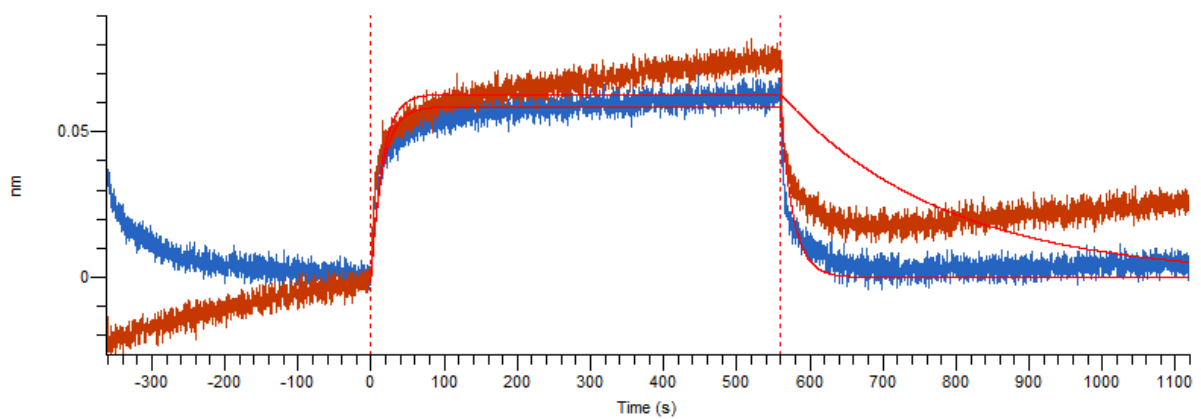
Figure S140. Binding of 50 μM **A2c** to the RBD monitored with BLI.
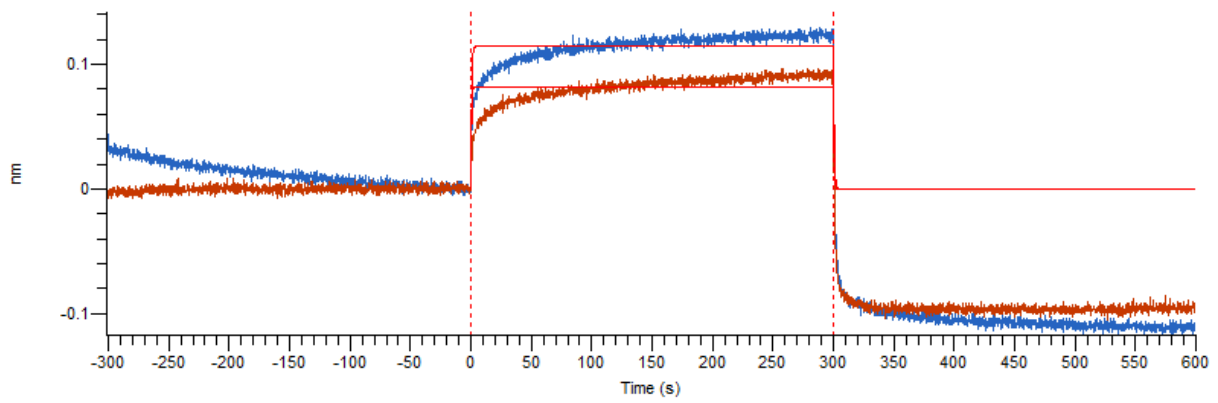
Figure S141. Binding of 50 μM **A2v1** to the RBD monitored with BLI.
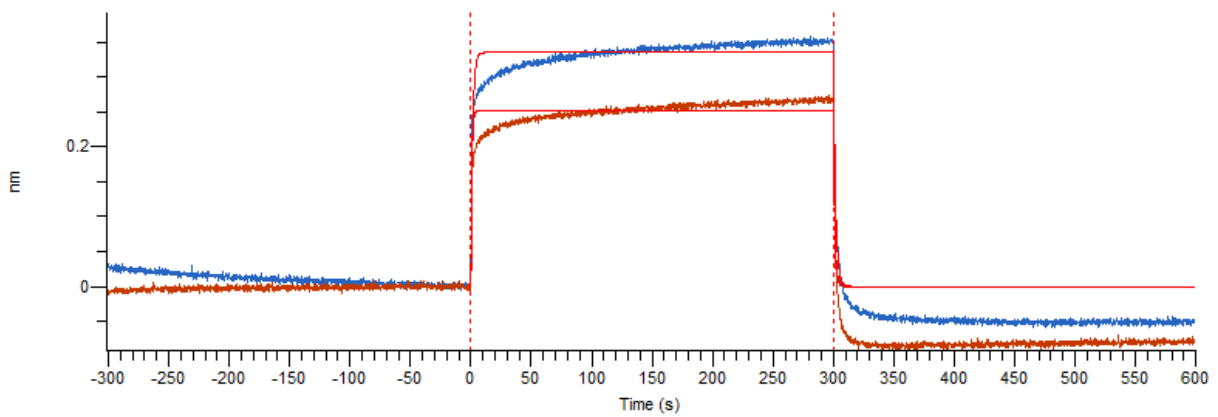
Figure S142. Binding of 50 μM **A2v2** to the RBD monitored with BLI.
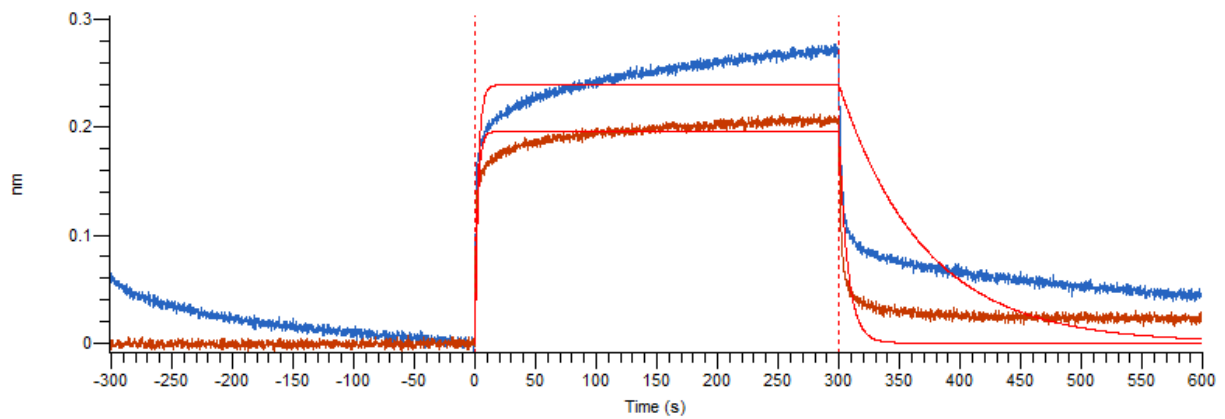
Figure S143. Binding of 50 μM **A2v3** to the RBD monitored with BLI.
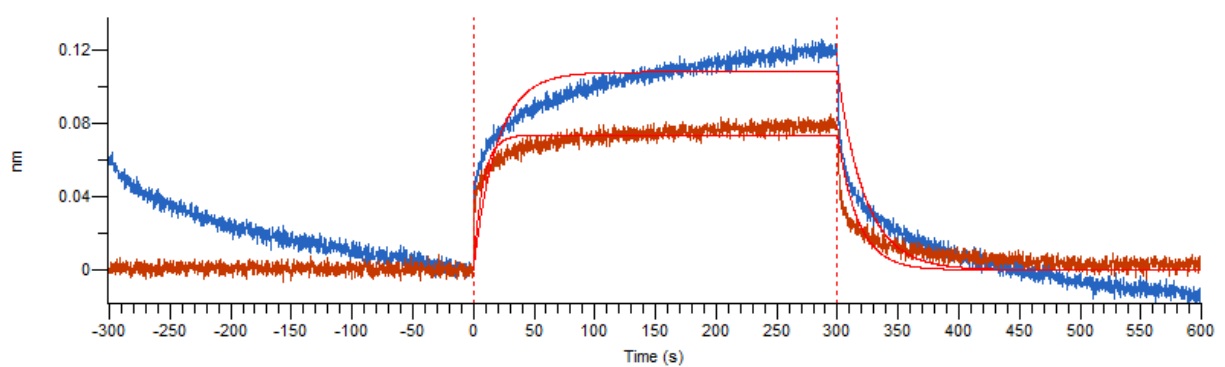
Figure S144. Binding of 50 μM **A2v4** to the RBD monitored with BLI.
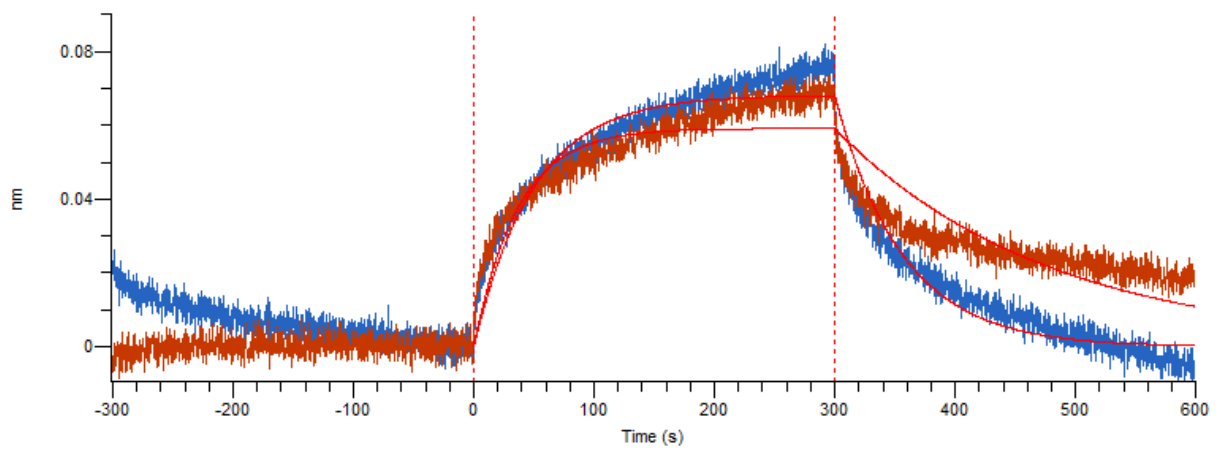
Figure S145. Binding of 50 μM **A3** to the RBD monitored with BLI.
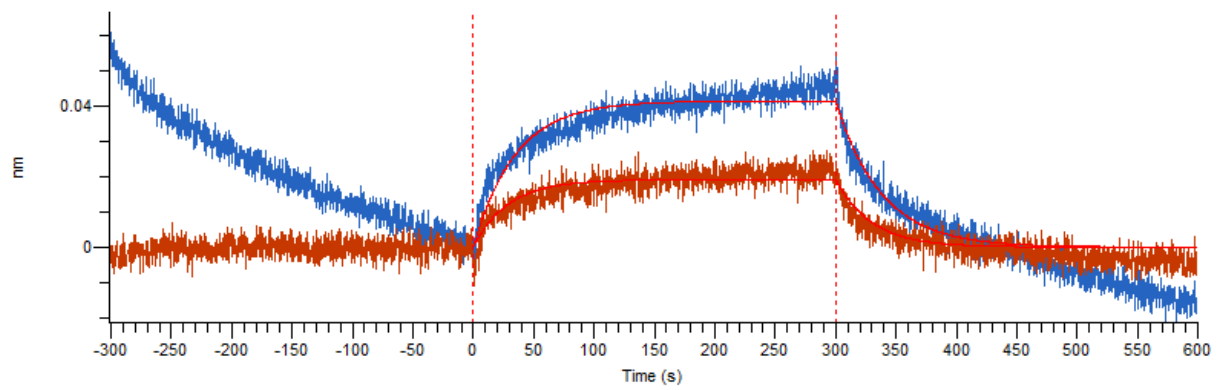
Figure S146. Binding of 50 μM **A3a** to the RBD monitored with BLI.
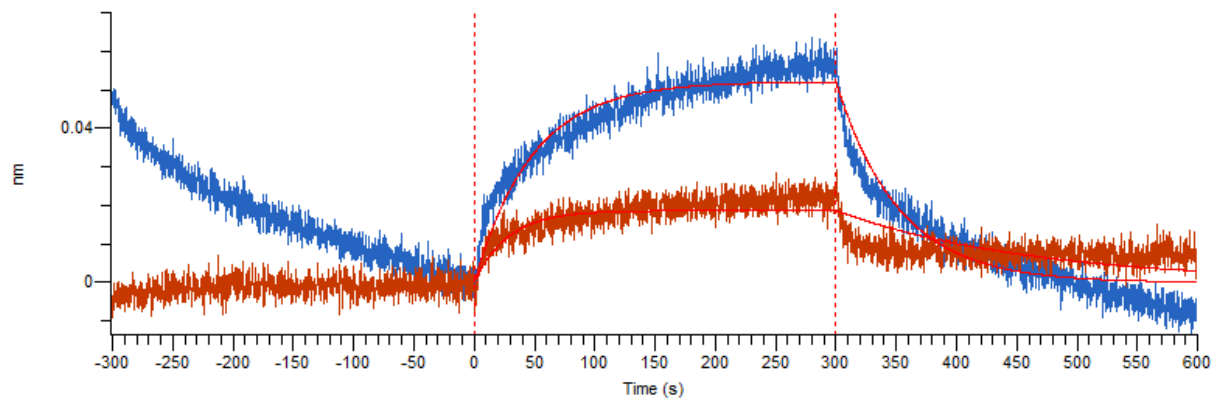
Figure S147. Binding of 50 μM **A3b** to the RBD monitored with BLI.
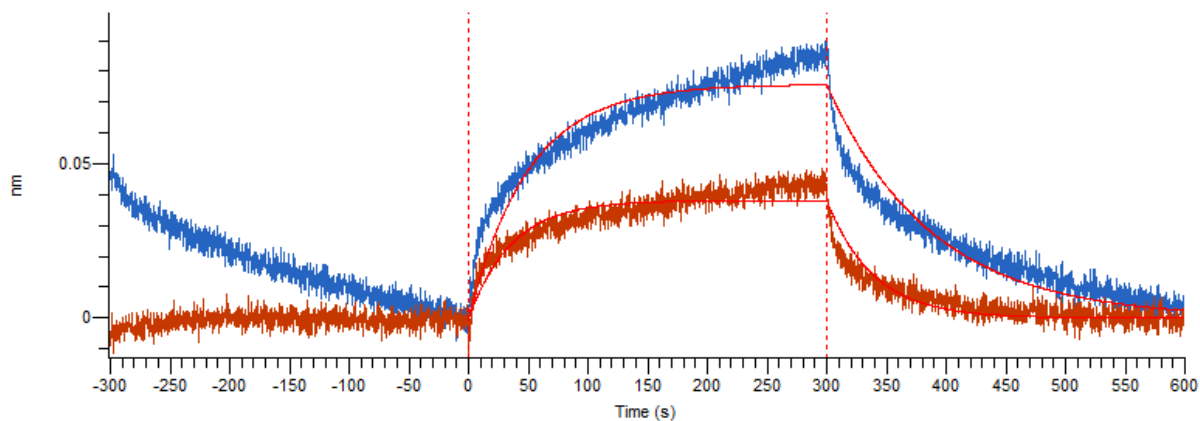
Figure S148. Binding of 50 μM **A3c** to the RBD monitored with BLI.

Figure S149. Binding of 50 μM peptide **1** to the RBD monitored with BLI.

Figure S150. Binding of 50 μM peptide **2** to the RBD monitored with BLI.

Figure S151. Binding of 50 μM peptide **3** to the RBD monitored with BLI.

Figure S152. Binding of 50 µM peptide **4** to the RBD monitored with BLI.

Figure S153. Binding of 50 µM peptide **5** to the RBD monitored with BLI.

Figure S154. Binding of 50 µM peptide **6** to the RBD monitored with BLI.

Figure S155. Binding of 50 μM peptide **7** to the RBD monitored with BLI.

Figure S156. Binding of 50 μM peptide **8** to the RBD monitored with BLI.

Figure S157. Binding of 50 μM peptide **9** to the RBD monitored with BLI.

Figure S158. Binding of 50 μM peptide **10** to the RBD monitored with BLI.

Figure S159. Binding of 50 μM peptide **11** to the RBD monitored with BLI.
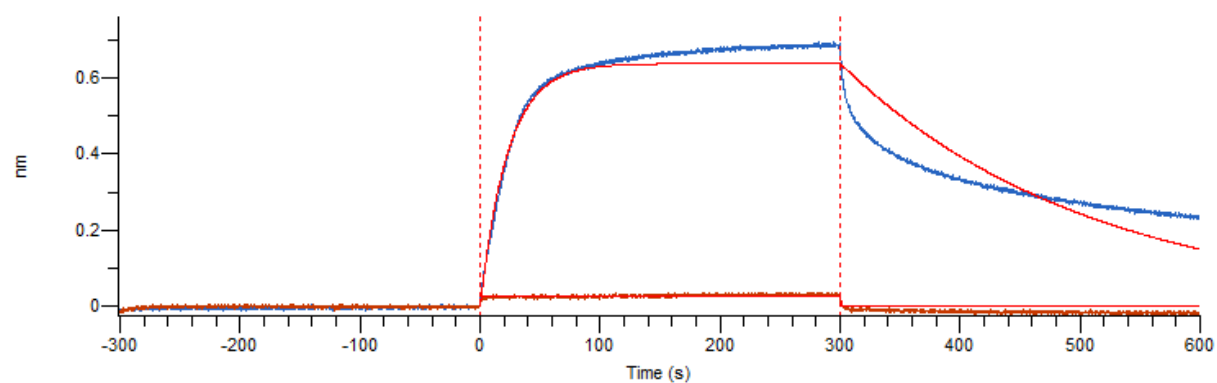
Figure S160. Binding of 50 μM peptide **12** to the RBD monitored with BLI.
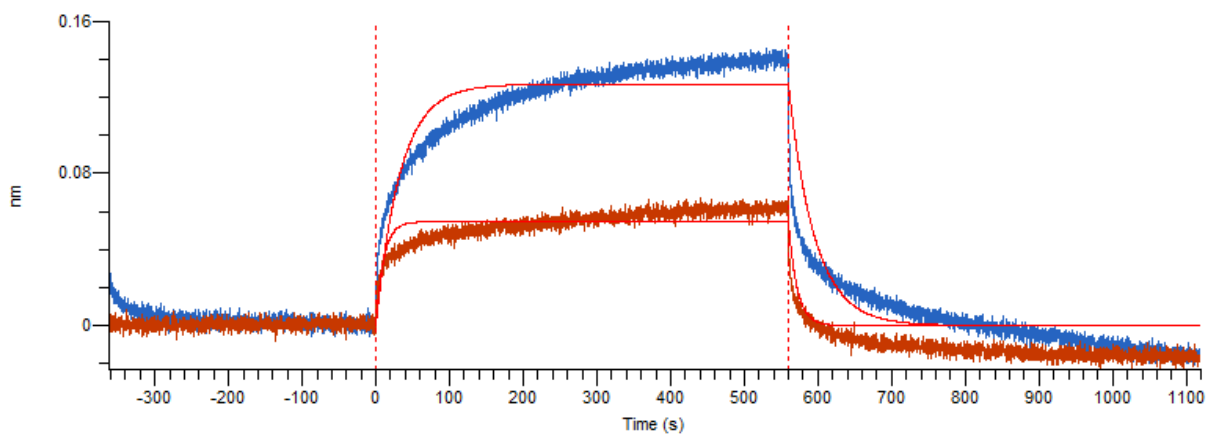
Figure S161. Binding of 50 μM peptide **13** to the RBD monitored with BLI.
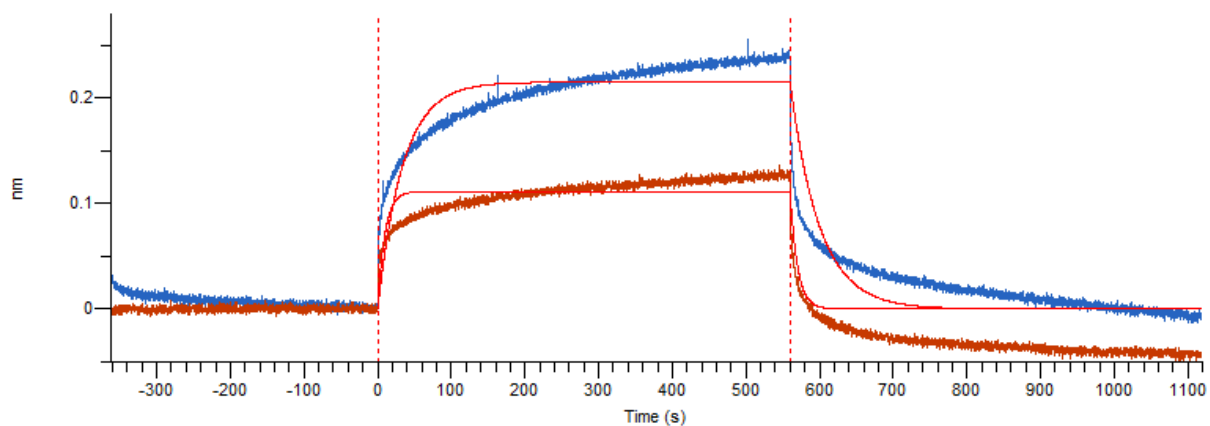
Figure S162. Binding of 50 μM peptide **14** to the RBD monitored with BLI.
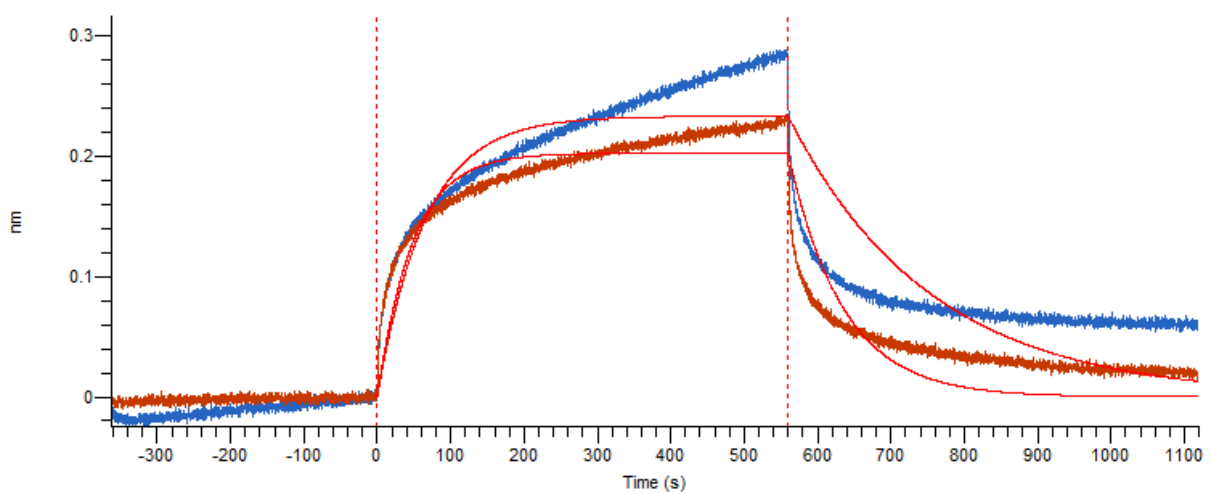
Figure S163. Binding of 50 μM peptide **15** to the RBD monitored with BLI.
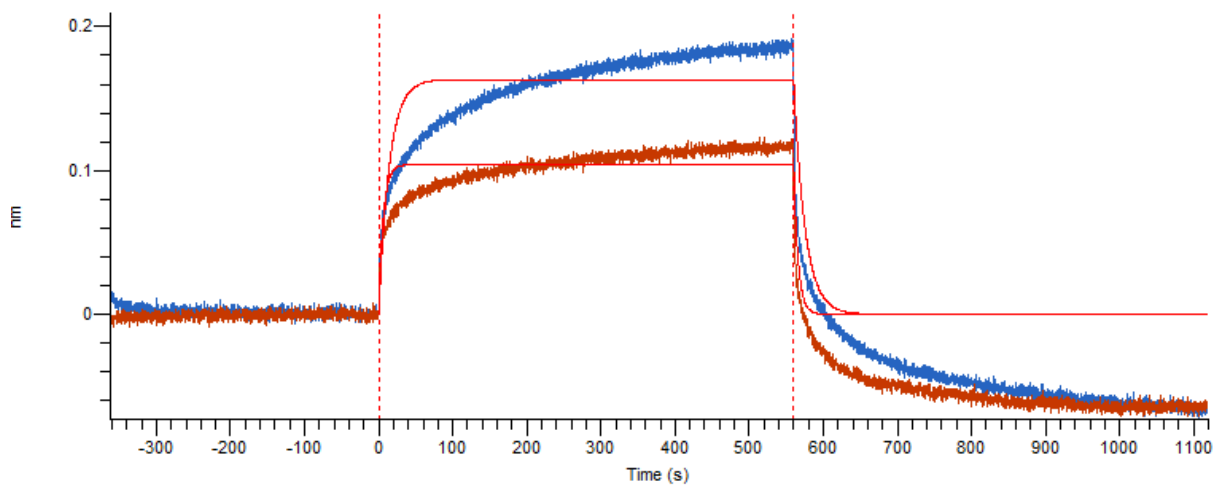
Figure S164. Binding of 50 μM peptide **16** to the RBD monitored with BLI.
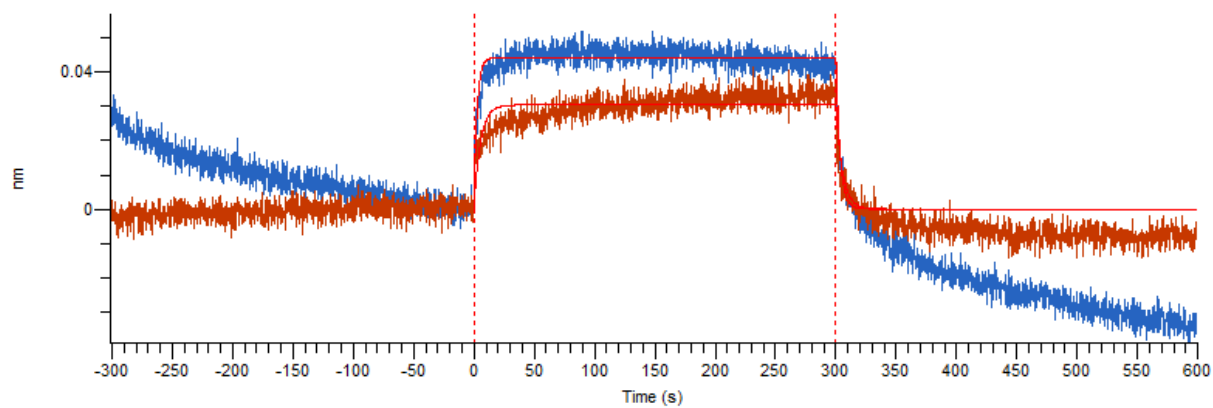
Figure S165. Binding of 50 μM peptide **17** to the RBD monitored with BLI.
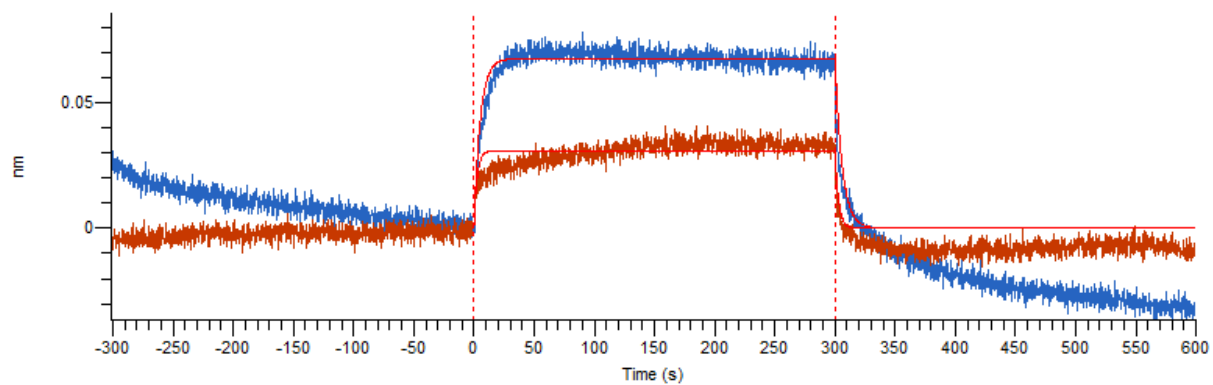
Figure S166. Binding of 50 μM peptide **18** to the RBD monitored with BLI.
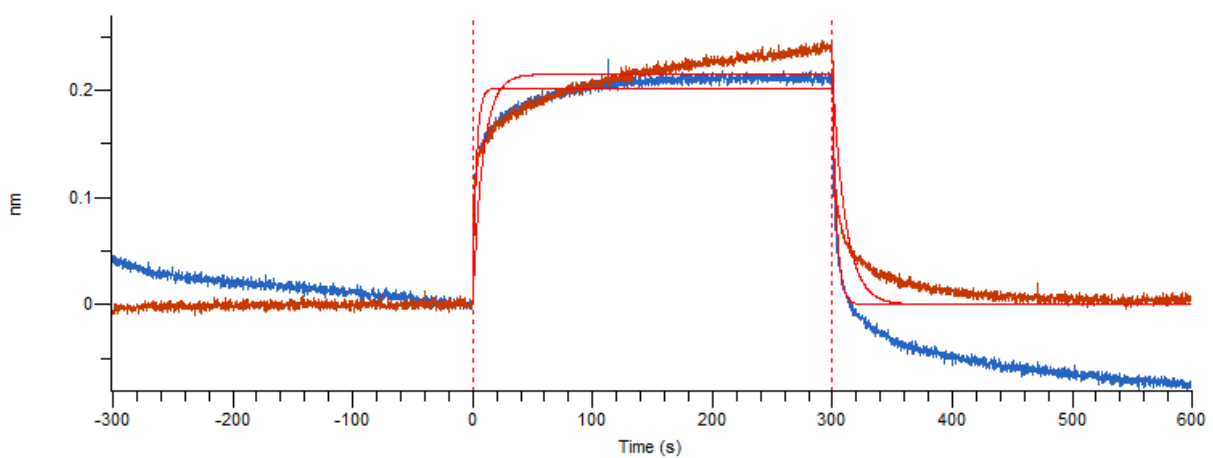
Figure S167. Binding of 50 μM peptide **19** to the RBD monitored with BLI.
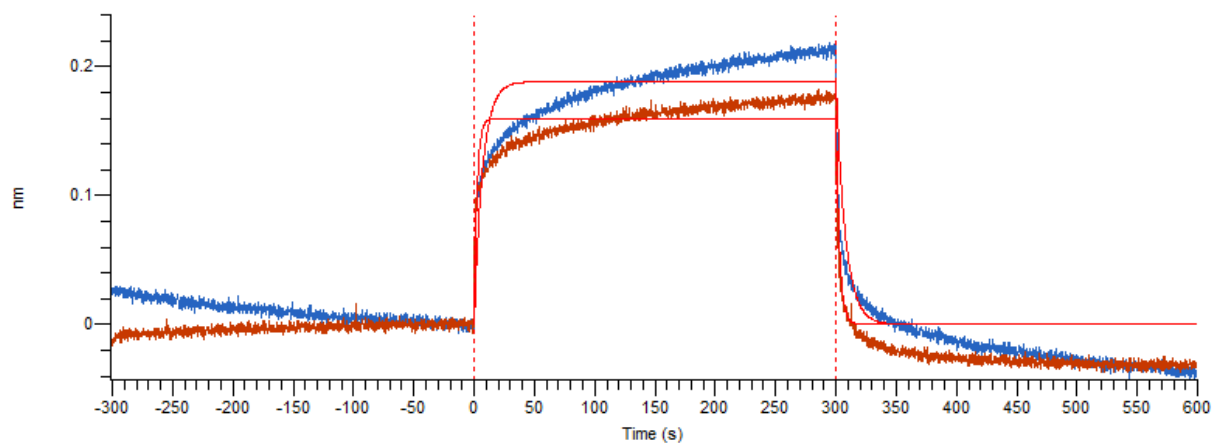
Figure S168. Binding of 50 µM peptide **20** to the RBD monitored with BLI.
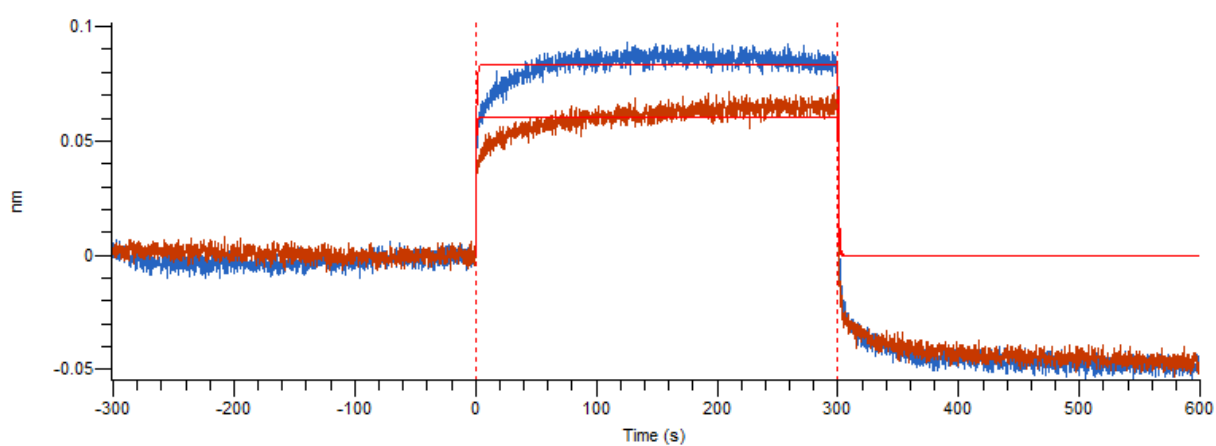
Figure S169. Binding of 50 µM peptide **21** to the RBD monitored with BLI.
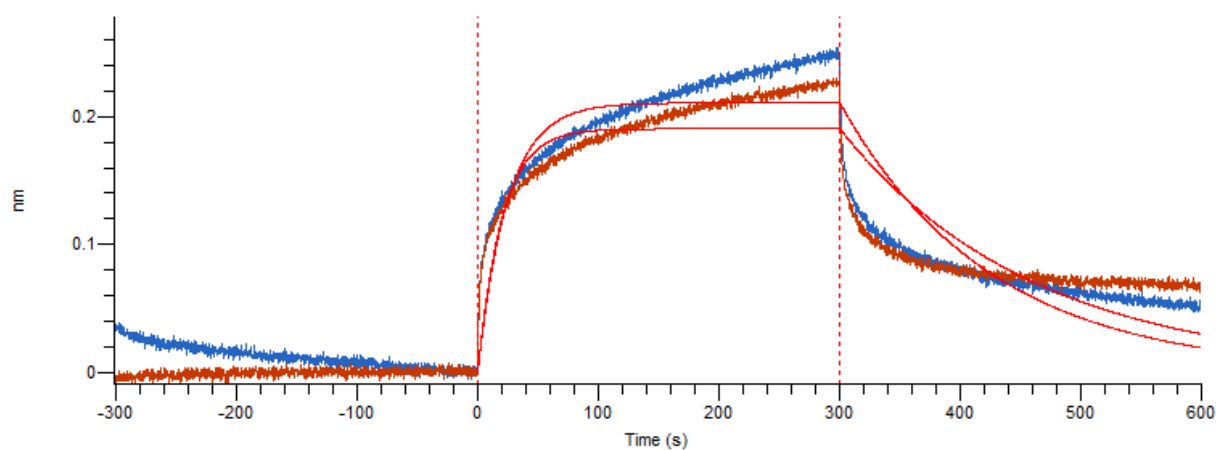
Figure S170. Binding of 50 µM peptide **22** to the RBD monitored with BLI.
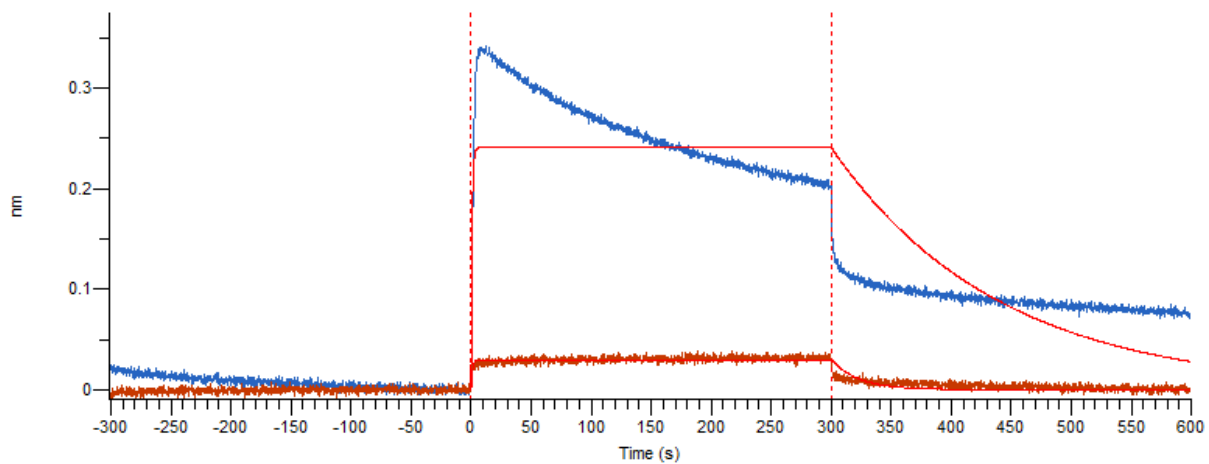
Figure S171. Binding of 50 µM peptide **23** to the RBD monitored with BLI.
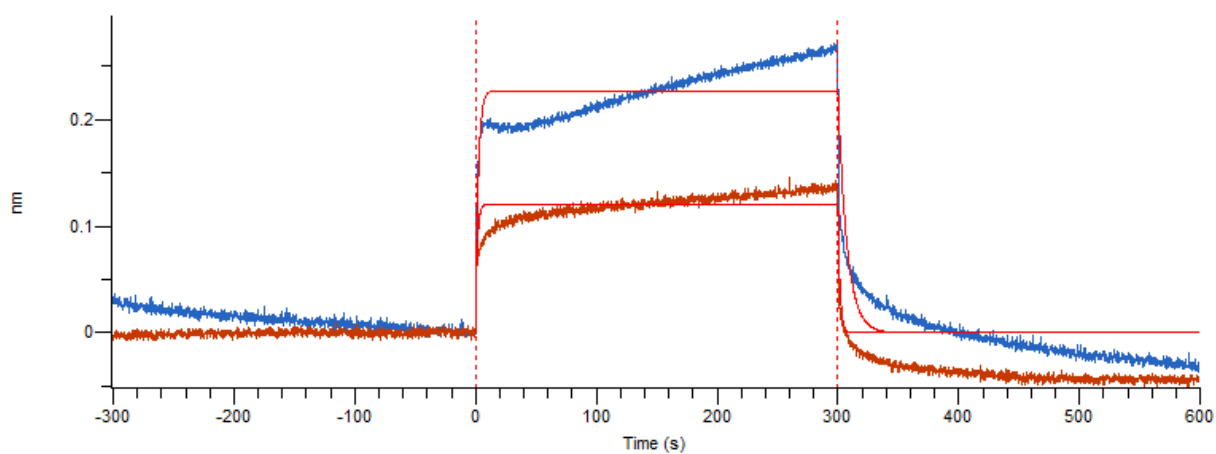
Figure S172. Binding of 50 µM peptide **24** to the RBD monitored with BLI.
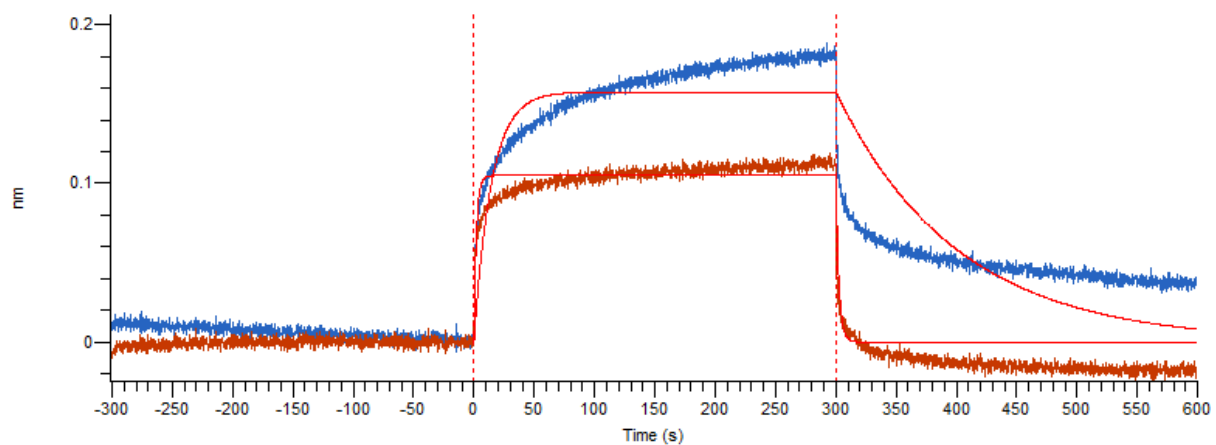
Figure S173. Binding of 50 µM peptide **25** to the RBD monitored with BLI.
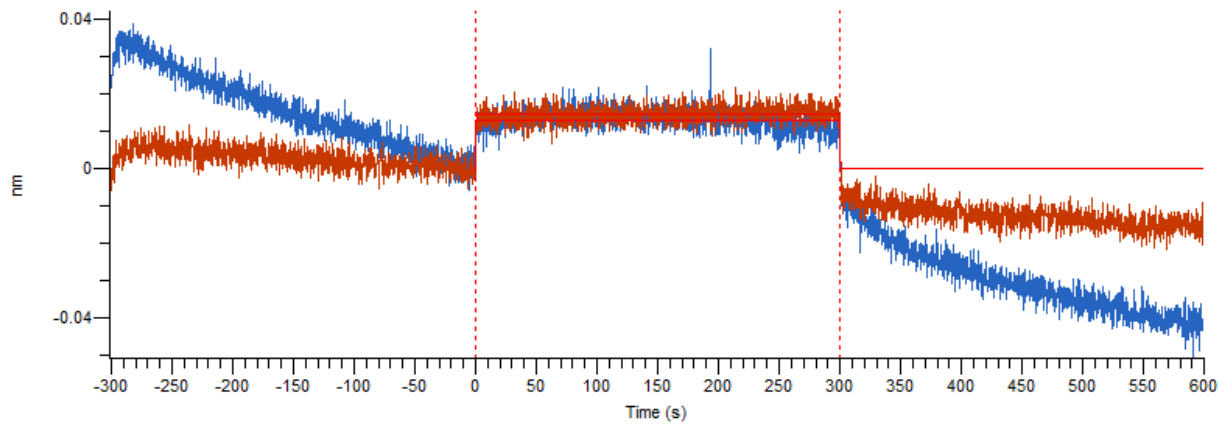
Figure S174. Binding of 50 μM peptide **26** to the RBD monitored with BLI.
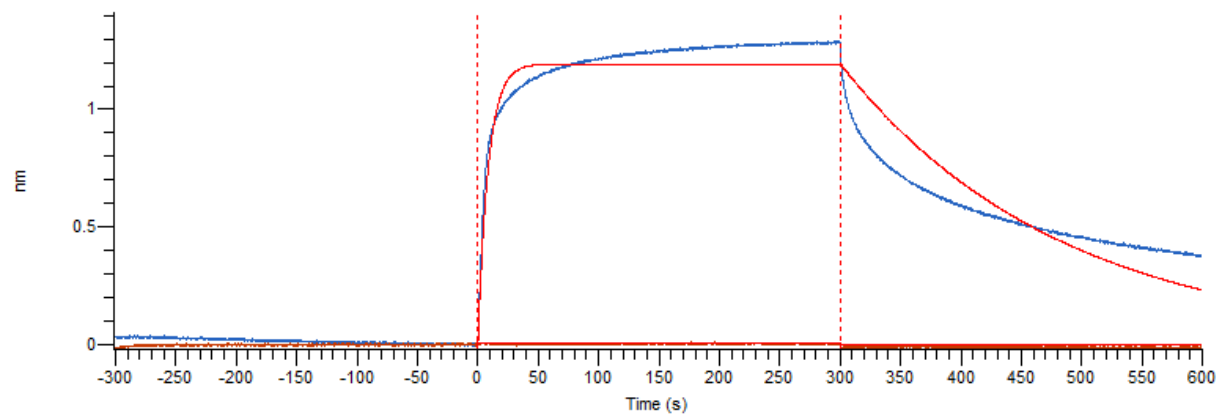
Figure S175. Binding of 50 μM peptide **27** to the RBD monitored with BLI.
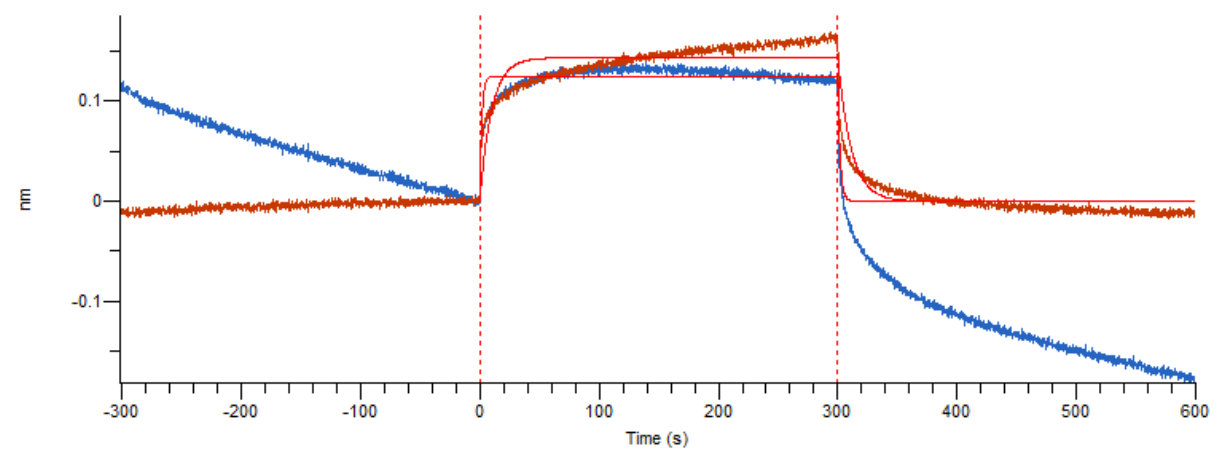
Figure S176. Binding of 50 μM peptide **28** to the RBD monitored with BLI.
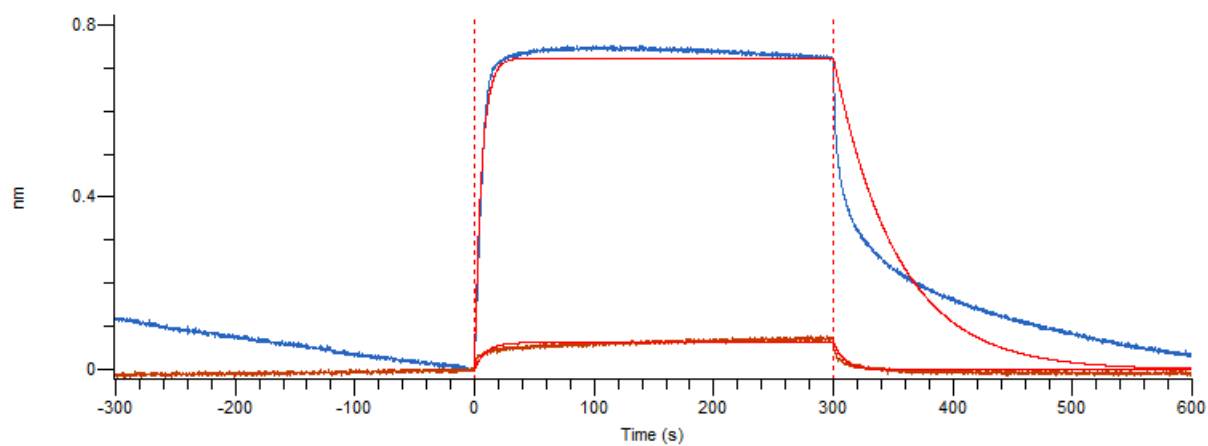
Figure S177. Binding of 50 μM peptide **29** to the RBD monitored with BLI.
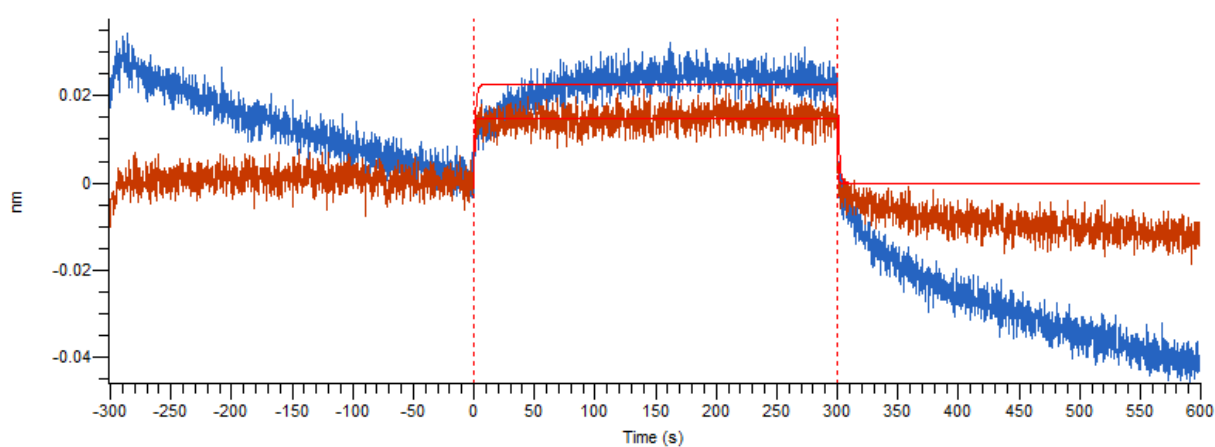
Figure S178. Binding of 50 μM peptide **30** to the RBD monitored with BLI.
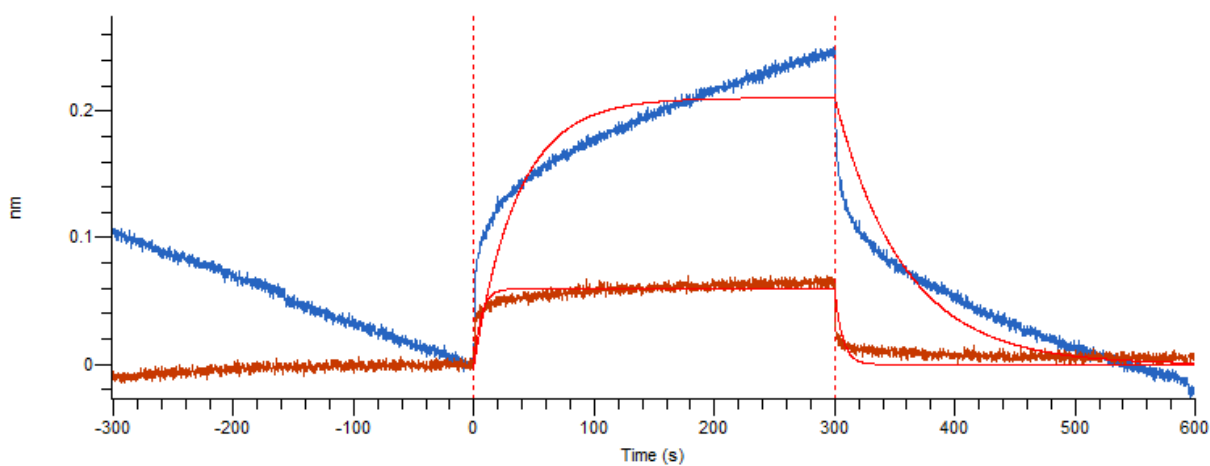
Figure S179. Binding of 50 μM peptide **31** to the RBD monitored with BLI.
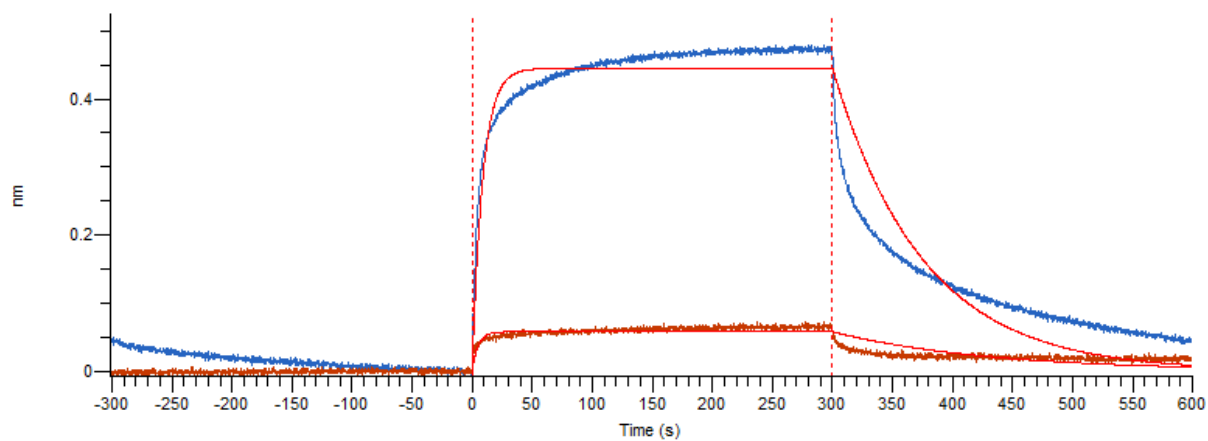
Figure S180. Binding of 50 μM peptide **32** to the RBD monitored with BLI.
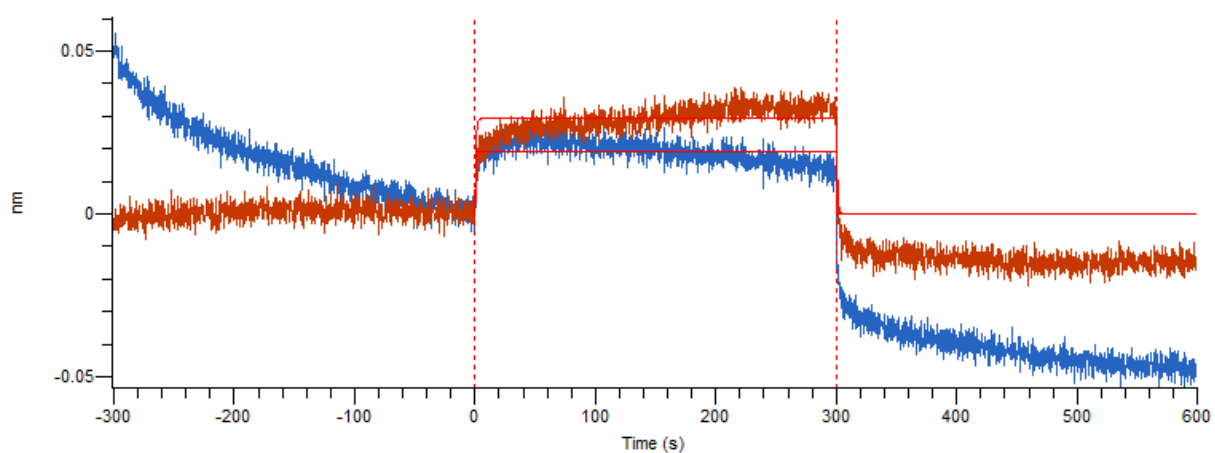
Figure S181. Binding of 50 μM peptide **33** to the RBD monitored with BLI.
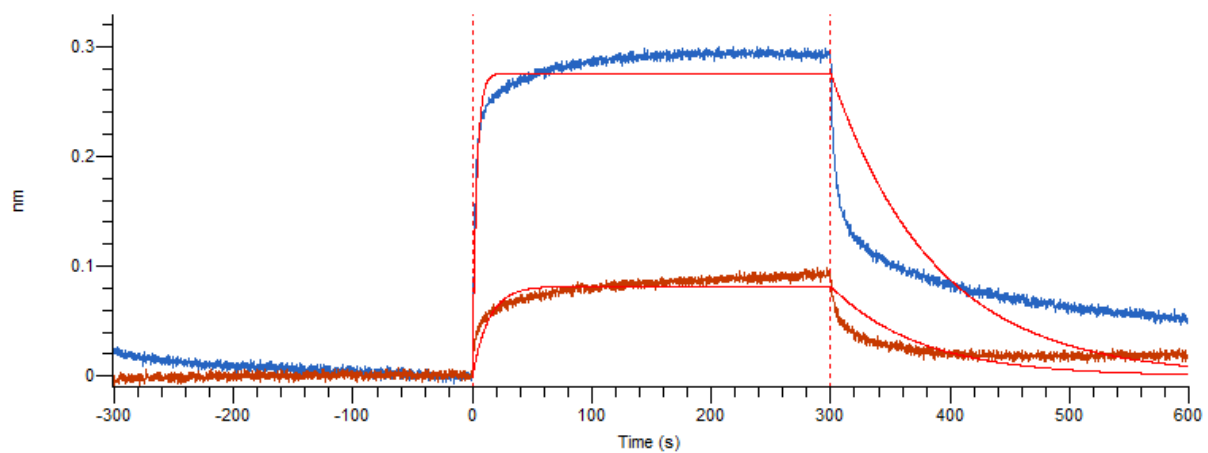
Figure S182. Binding of 50 μM peptide **34** to the RBD monitored with BLI.
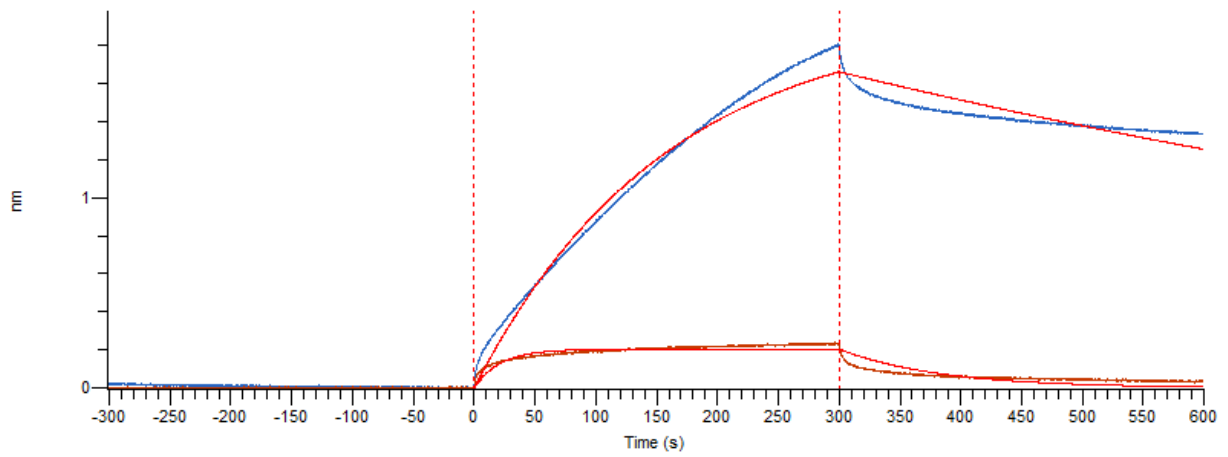
Figure S183. Binding of 50 μM peptide **35** to the RBD monitored with BLI.
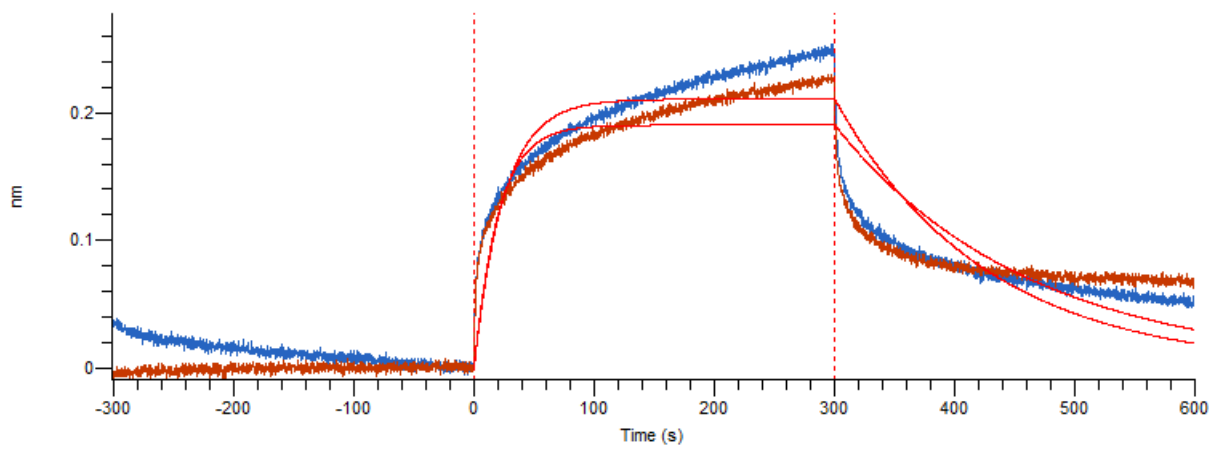
Figure S184. Binding of 50 μM peptide **36** to the RBD monitored with BLI.
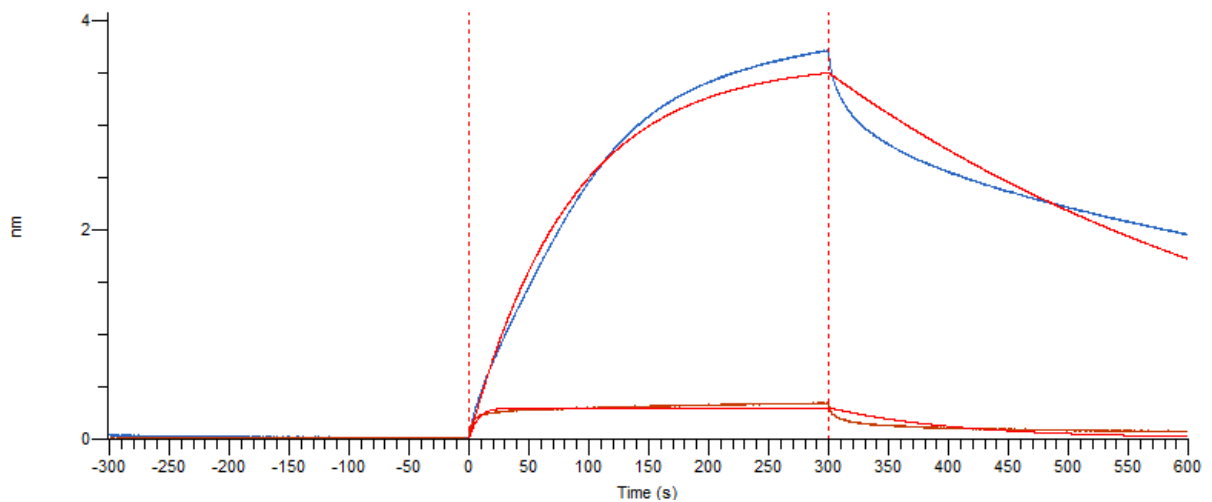
Figure S185. Binding of 50 μM peptide **37** to the RBD monitored with BLI.
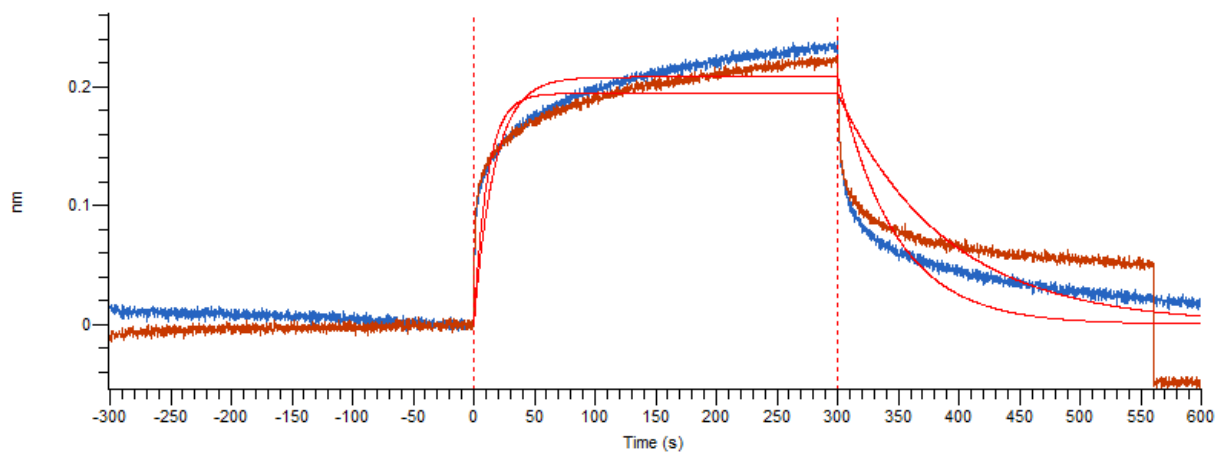
Figure S186. Binding of 50 μM peptide **38** to the RBD monitored with BLI.
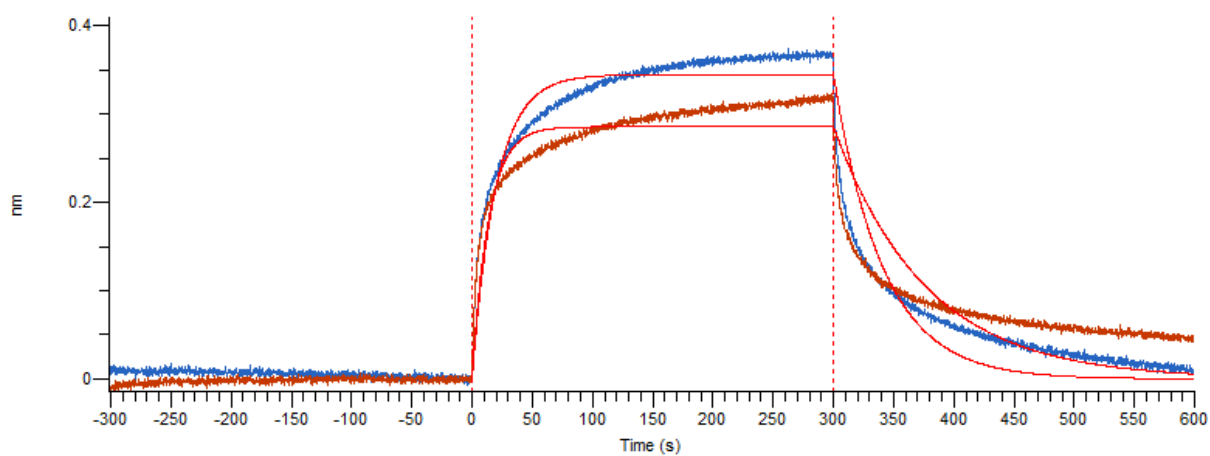
Figure S187. Binding of 50 μM peptide **39** to the RBD monitored with BLI.
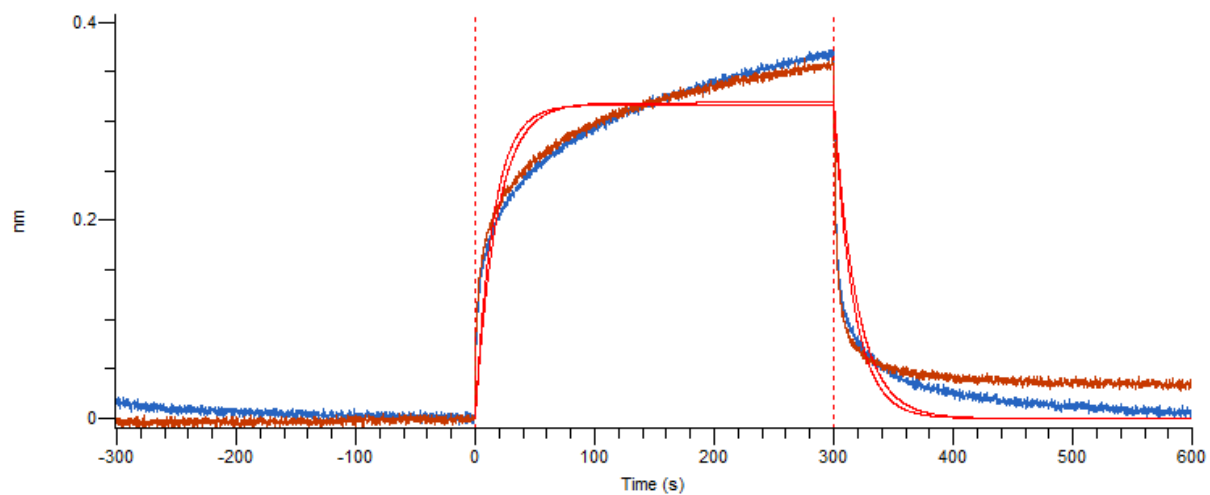
Figure S188. Binding of 50 μM peptide **40** to the RBD monitored with BLI.
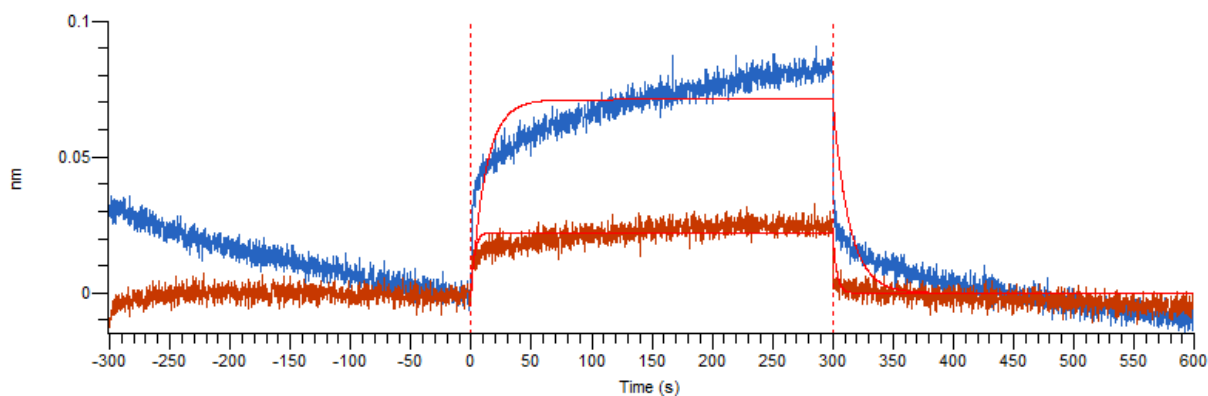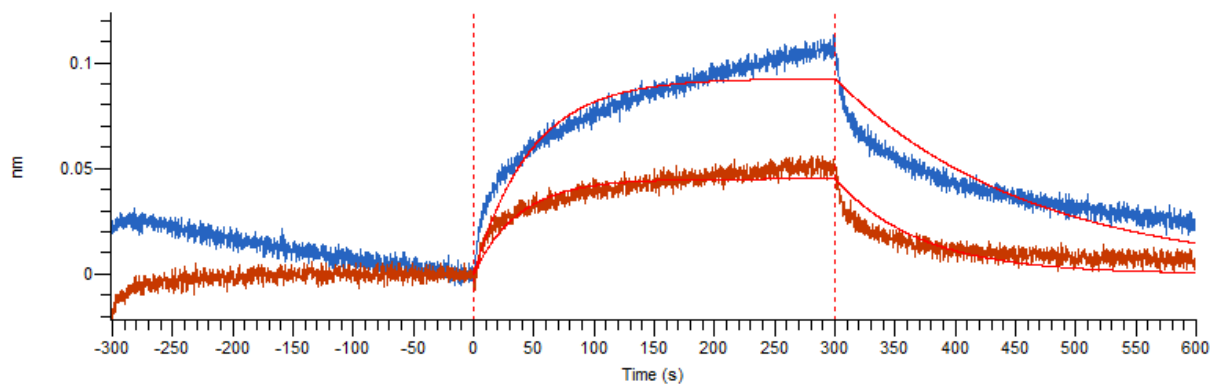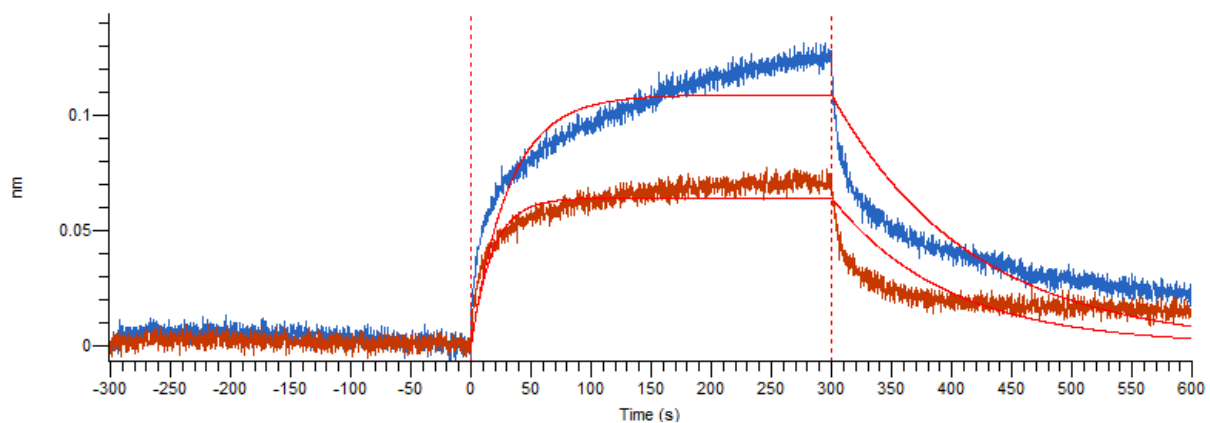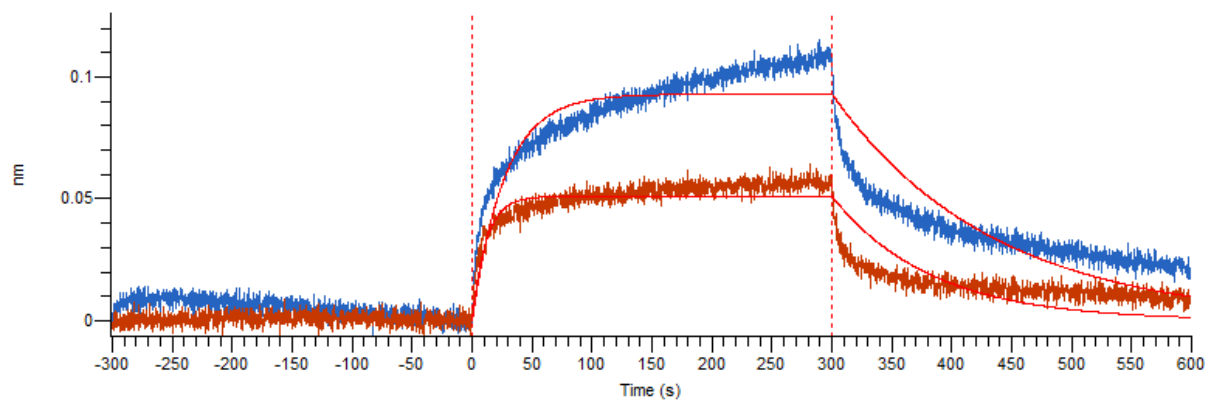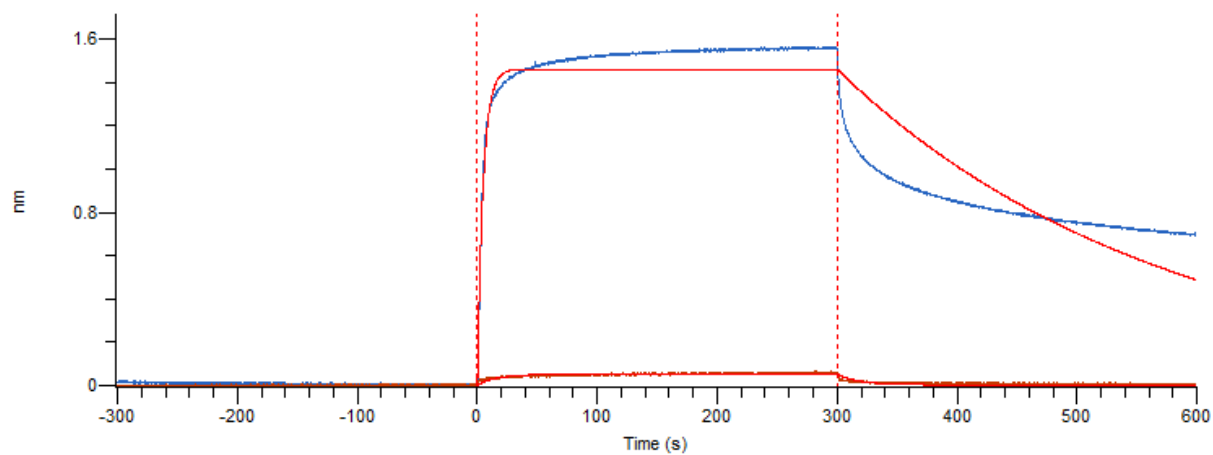
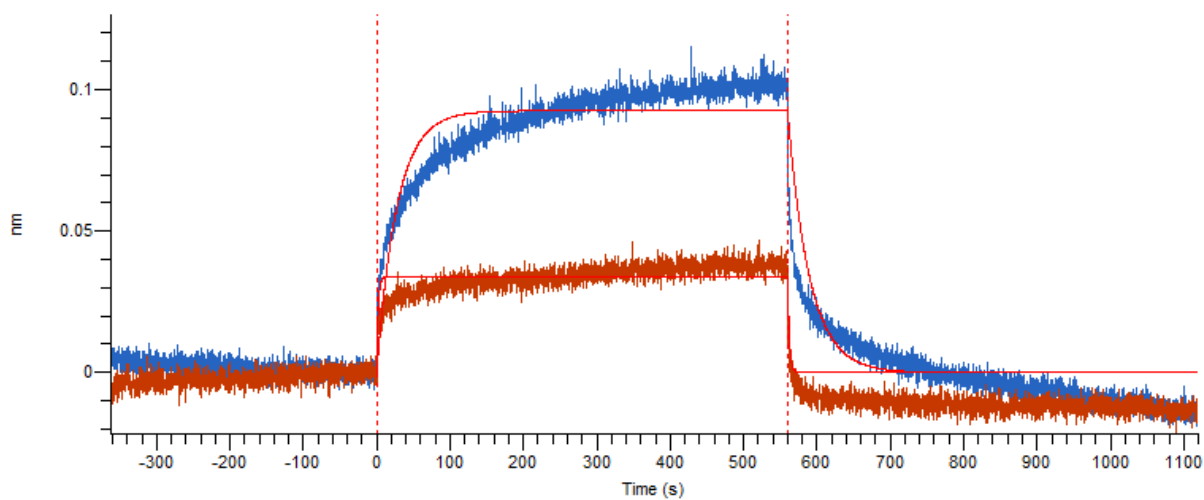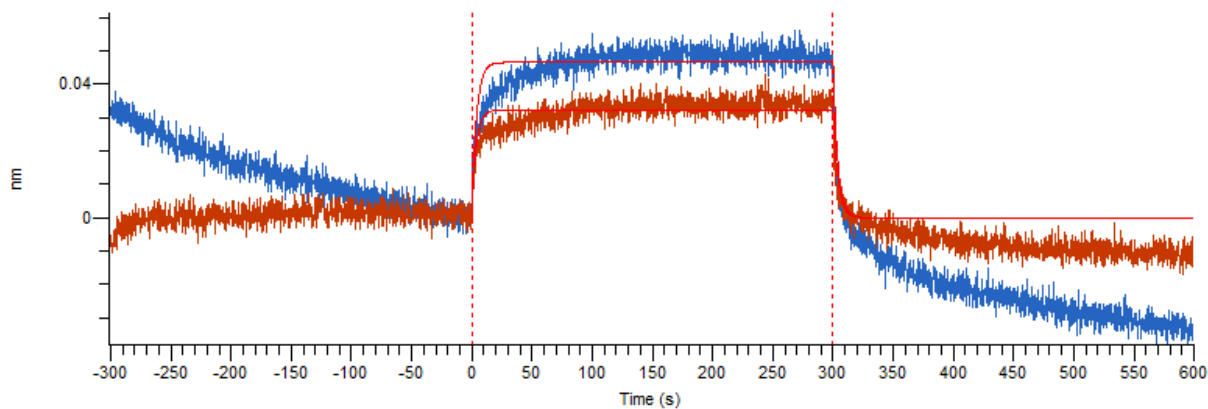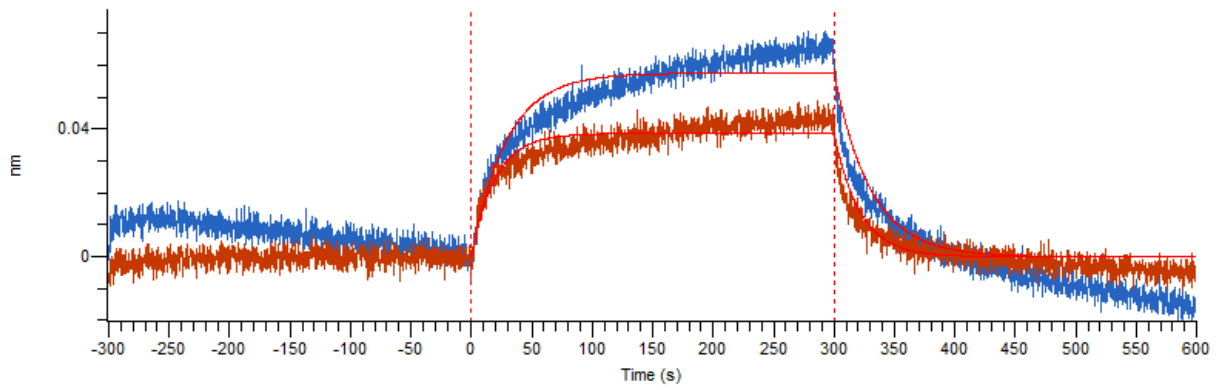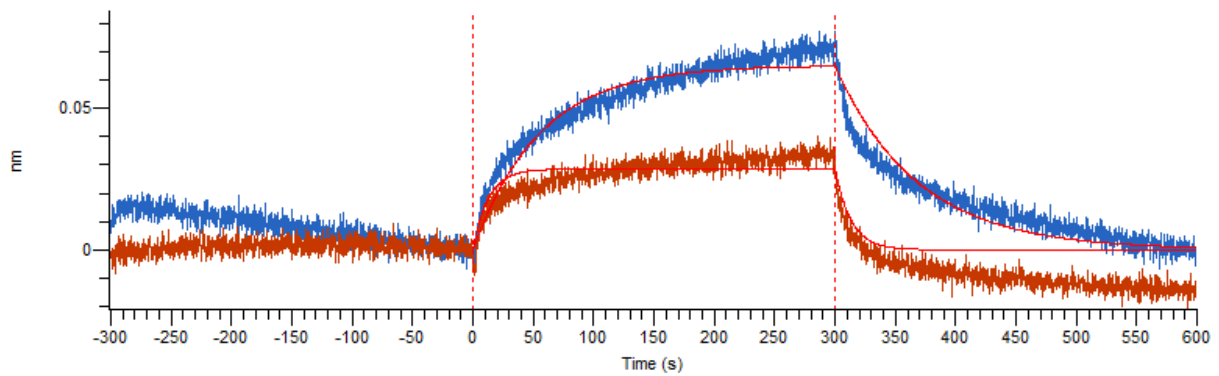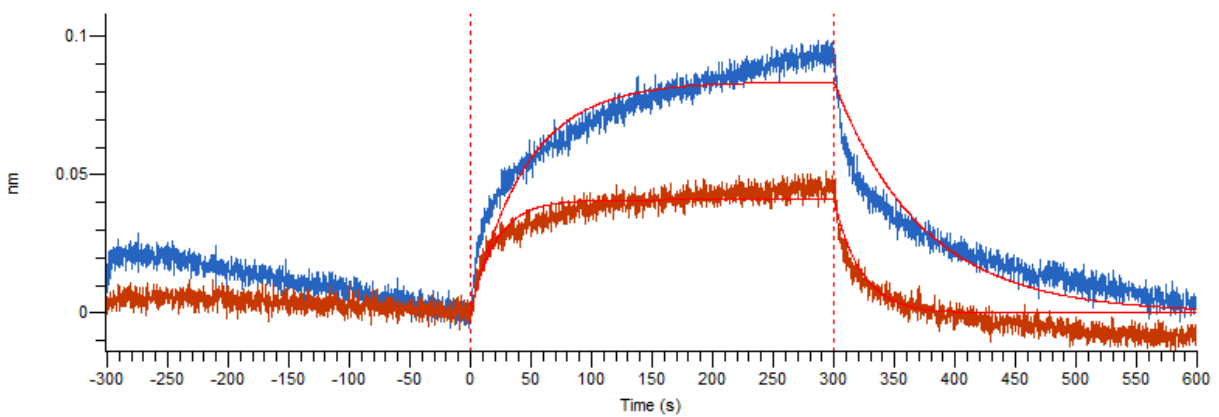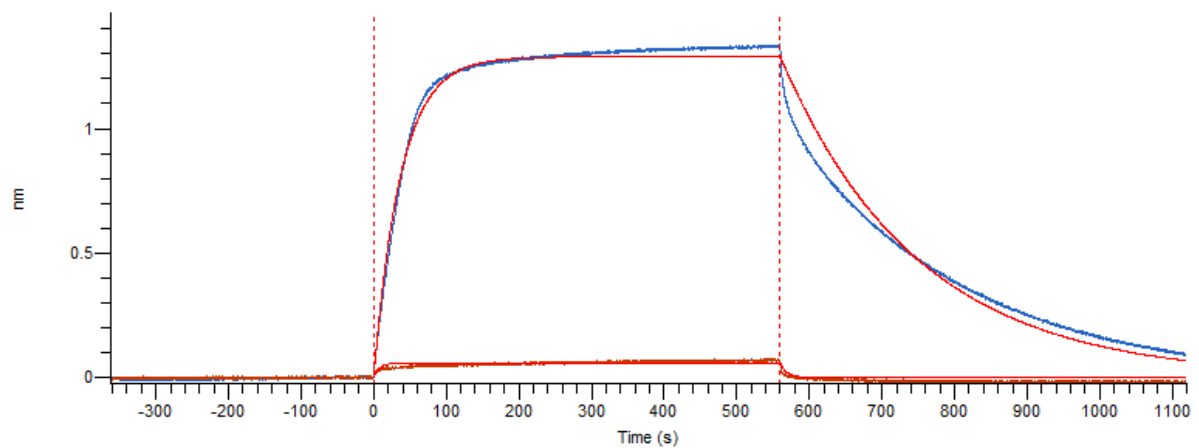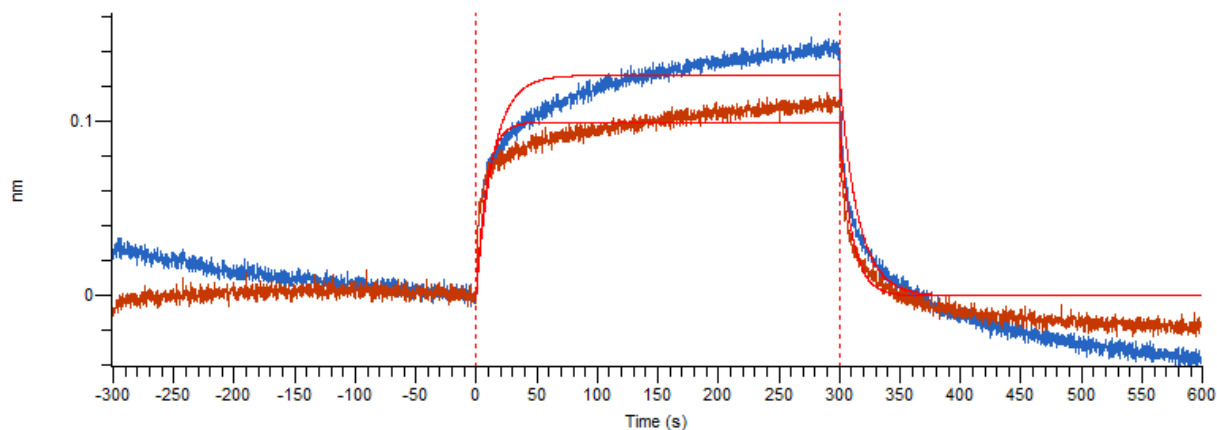**Figure S189**. Binding of 50 μM peptide **41** to the RBD monitored with BLI.

Table S4. Chemical shifts of peptide **27**. Cp stands for *trans*-(1*S*,2*S*)-2-amino-1-cyclopentanecarboxylic acid.

Residue	Proton	Chemical shift [ppm]
Arg1	HN	7.86
	HA	3.93
	HB	1.94 (2) / 1.98 (1)
	HG	1.71
	HD	3.24
Asp2	HN	8.98
	HA	4.80
	HB	2.81 (2) / 2.97 (1)
Asp3	HN	8.87
	HA	4.65
	HB	2.83 (2) / 2.93 (1)
Glu4	HN	8.26
	HA	4.36
	HB	2.09 (2) / 2.25 (1)
	HG	2.41 (2) / 2.48 (1)
Cp5	HN	7.85
	HA	2.58
	HB	4.37
	HG, D, E	1.76 (4) / 1.87 (3) / 1.95 (2) / 2.05 (1)
Arg6	HN	8.30
	HA	3.89
	HB	1.59 (2) / 1.71 (1)
	HG	1.35 (2) / 1.43 (1)
	HD	2.90 (2) / 2.97 (1)
	HE	7.25
Trp7	HN	7.95
	HA	4.67
	HB	3.41 (2) / 3.55 (1)
	HD1	7.26
	HE1	10.27
	HZ2	7.36
	HE3	7.68
	HH2	7.12
	HZ3	7.07
Leu8	HN	8.07
	HA	4.30
	HB	1.65 (2) / 1.73 (1)
	HG	1.64
	HD	0.96
Cp9	HN	7.99
	HA	2.80
	HB	4.38
	HG,D, E	1.73 (4) / 1.79 (3) / 1.91 (2) / 2.00 (1)
Thr10	HN	8.16
	HA	4.40
	HB	3.75
	HG	1.28
Asp11	HN	8.36
	HA	4.55
	HB	2.86 (2) / 3.26 (1)
Cp12	HN	7.98
	HA	2.88
	HB	4.40
	HG,D,E	1.79 (4) / 1.85 (3) / 1.95 (2) / 2.10 (1)
Val13	HN	8.42
	HA	3.47
	HB	2.31
	HG	0.82 (2) / 1.03 (1)
Tyr14	HN	8.42
	HA	4.36
	HB	3.27 (2) / 3.46 (1)
	HD	6.66
	HE	7.14
Glu15	HN	8.49
	HA	4.08
	HB	2.17
	HG	2.50 (2) / 2.72 (1)
Cp16	HN	8.23
	HA	2.95
	HB	4.32
	HG,D,E	1.70 (4) / 1.73 (3) / 1.84 (2) / 1.99 (1)
Trp17	HN	8.35
	HA	4.41
	HB	3.18 (2) / 3.22 (1)
	HD1	7.15
	HE1	10.27
	HZ2	7.34
	HE3	7.53
	HH2	7.10
	HZ3	7.01
His18	HN	7.81
	HA	4.59
	HB	3.25 (2) / 3.47 (1)
	HD2	7.32
	HE	7.31 (2) / 8.38 (1)
NH$_2$	HN1	7.30
	HN2	7.08

Table S5. Interproton contacts of peptide **27**, Cp stands for *trans*-(1*S*,2*S*)-2-amino-1-cyclopentanecarboxylic acid.

Sequential (*i, i+1*)	Intensity
Arg1HA-Asp2HN	s
Arg1HG-Asp2HN	w
Asp2HA-Asp3HN	s
Asp3HA-Glu4HN	s
Asp3HB1-Glu4HN	m
Asp3HB2-Glu4HN	m
Cp5HA-Arg6HN	s
Cp5HB-Arg6HN	m
Arg6HA-Trp7HN	m
Arg6HB2-Trp7HN	m
Arg6HG1-Trp7HN	w
Arg6HG2-Trp7HN	w
Trp7HA-Leu8HN	m
Trp7HB1-Leu8HN	s
Trp7HB2-Leu8HN	m
Leu8HA-Cp9HN	m
Leu8HD-Cp9HB	w
Leu8HD-Cp9HN	w
Leu8HG-Cp9HN	m
Cp9HA-Thr10HN	s
Cp9HB-Thr10HN	s
Thr10HA-Asp11HN	s
Thr10HB-Asp11HN	m
Thr10HG-Asp11HN	m
Asp11HA-Cp12HN	m
Asp11HB1-Cp12HN	s
Cp12HA-Val13HN	s
Cp12HB-Val13HN	m

Cp12HA-Val13HB1	w
Val13HG2-Tyr14HE	m
Val13HN-Tyr14HE	w
Tyr14HA-Glu15HN	m
Tyr14HB1-Glu15HN	s
Tyr14HB2-Glu15HN	m
Tyr14HE-Glu15HN	m
Tyr14HE-Glu15HA	m
Tyr14HE-Glu15HG1	m
Tyr14HE-Glu15HG2	w
Tyr14HN-Glu15HB	w
Glu15HA-Cp16HN	m
Glu15HB-Cp16HN	s
Glu15HN-Cp16HA	w
Cp16HA-Trp17HN	s
Cp16HN-Trp17HA	w
Trp17HA-His18HN	m
Trp17HN-His18HB1	m
His18HE-HN2HN1	m
His18HA-NH2HN2	w

Sequential (*HN-HN*)	Intensity
Asp3HN-Glu4HN	s
Glu4HN-Cp5HN	s
Cp5HN-Arg6HN	m
Arg6HN-Trp7HN	m
Trp7HN-Leu8HN	m
Cp9HN-Thr10HN	m
Thr10HN-Asp11HN	m
Asp11HN-Cp12HN	s

Cp12HN-Val13HN	m
Tyr14HN-Glu15HN	m
Glu15HN-Cp16HN	s
Trp17HN-His18HN	s
His18HN-HN2HN1	s
His18HN-HN2HN2	m

Medium range (*i, i+2*)	Intensity
Asp2HA-Glu4HN	m
Asp3HA-Cp5HN	m
Cp5HA-Trp7HN	w
Cp5HB-Trp7HE3	m
Arg6HA-Leu8HN	w
Leu8HA-Thr10HN	w
Asp11HN-Val13HG1	w
Cp12HA-Tyr14HN	w
Tyr14HB1-Cp16HN	m
Cp16HA-His18HN	w
Cp16HB-His18HN	m
Cp16HB-His18HD2	m
Trp17HA-HN2HN1	w

Medium range (*i, i+3*)	Intensity
Glu4HA-Trp7HD1	m
Glu4HA-Trp7HN	s
Cp5HG-Leu8HD	w
Cp5HB-Leu8HN	s
Cp5HN-Leu8HD	w
Arg6HA-Cp9HA	s
Arg6HA-Cp9HN	m
Arg6HA-Cp9HG	m

Trp7HA-Thr10HN	s
Trp7HE3-Thr10HG	m
Leu8HA-Asp11HB2	s
Leu8HA-Asp11HN	s
Leu8HA-Asp11HB1	s
Asp11HA-Tyr14HN	w
Asp11HA-Tyr14HD	s
Cp12HB-Glu15HN	s
Cp12HB-Glu15HB	s
Val13HA-Cp16HA	s
Val13HA-Cp16HN	m
Tyr14HA-Trp17HD1	s
Tyr14HA-Trp17HN	s
Glu15HA-His18HN	m
Glu15HA-His18HB2	s
Glu15HA-His18HD2	w
Medium range (*i*, *i*+4)	**Intensity**
Asp3HA-Trp7HN	s
Glu4HA-Leu8HN	w
Glu4HB1-Leu8HN	w
Glu4HB2-Leu8HN	w
Arg6HA-Thr10HN	w
Trp7HA-Asp11HN	s
Asp11HA-Glu15HN	m
Val13HG2-Trp17HE1	m
Tyr14HA-His18HD2	w
Tyr 14HD-His18HE	w
Tyr14HE-His18HE	w
Glu15HA-HN2HN1	w

Table S6. Vicinal coupling constants (^3JHNHA) determined from ^{1}H NMR spectrum for peptide **27**.

NH	^3J [Hz]
HN1	**
HN2	7.09
HN3	6.50
HN4	6.15
HN5	7.66
HN6	2.3
HN7	7.35
HN8	5.83
HN9	9.33
HN10	2.88
HN11	4.17
HN12	9.10
HN13	~3.3*
HN14	~4*
HN15	5.25
HN16	9.02
HN17	4.63
HN18	8.84

Table S7. NMR calculation statistics for peptide **27**

average number of NOE violations	2.9
average amount of NOE violations [Å]	2.019
number of different VdW violations	15
average number of VdW violations	8.7
average amount of VdW violations [Å]	2.371
average RMSD [Å]	1.428

Interaction Energy Calculations. Interaction Energies were calculated using MMGBSA [S5] method implemented in Amber 22 software [S6]. The forcefield ff5ipq-m extended with parameters for β-residues was applied [S7]. Peptide-protein complex were neutralized with Cl⁻ ions and solvated with TIP3P waters in a rectangular box with a 12 Å buffer distance. The system was subjected to molecular dynamic calculatins including: (a) minimization; (b) heating (50 ps); (c) density equilibration (50 ps) and (d) constant pressure equilibration (500 ps) at 300K. Subsequently, the production MD simulation were performed (500 ps) at 300K. The interaction energies (MMGBSA algorithm) were calculated using MMPBSA.py script included in Amber22 software.

Table S8. Peptide-RBD of S protein interaction energies calculated using MMGBSA method

Peptide no	calculated ΔG [kcal/mol]
7	-31.6 ± 4.0
10	-31.4 ± 4.3
12	-35.6 ± 5.6
27	-44.4 ± 6.6

Molecular Dynamics simulations. Calculations were performed using GROMACS [S8] software. The PDB file, of the RBD protein in complex with the inhibitor, was processed with pdb2gmx to generate the topology file using Amber03ff [S9] force field which includes parametrization of trans-(1*S*-2*S*)-2-aminocyclopentanecarboxylic acid (*trans*-ACPC) under the three letter code SS5. The protein complex was then placed in a cubic box with 10 Å distance from any box edge, and the box was filled with water molecules using spc216.gro, a 3-point solvent model. The solvated complex was neutralized substituting water molecules by the corresponding ions to achieve neutral charge of the box. Subsequently, the system was energy minimized using steepest descent minimization with maximum 50000 steps and maximum force of < 1000 kJ/mol/nm. Long range electrostatic interactions were treated with Particle Mesh Ewald (PME). Next the system was allowed to equilibrate in two stages: (a) Heating equilibration phase (NVT equilibration): The temperature was set at 300 K, over 100 ps simulation in 50000 steps at 2 fs per step, applying Periodic Boundary Conditions and modified Berendsen thermostat, with position restrains on the protein complex; (b) pressure equilibration phase (NPT equilibration): The pressure equilibration used the same molecular dynamic parameters as the NVT phase using pressure coupling, controlled by Parrinello-Rahman with a reference pressure of 1.0 bar and tau_p 2ps. The equilibration was run over 100 ps. Finally, MD production was done. A 100 ns simulation was run. From the trajectory we extracted the radios of gyration of the complex for the most potent and less potent inhibitors towards RBD-protein.
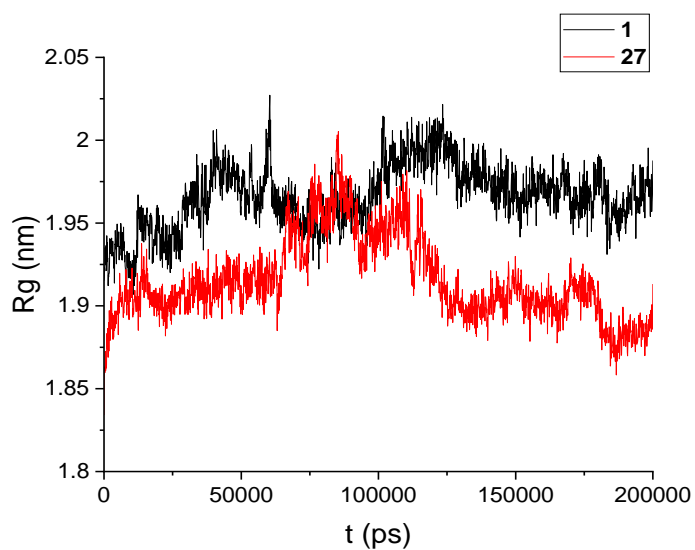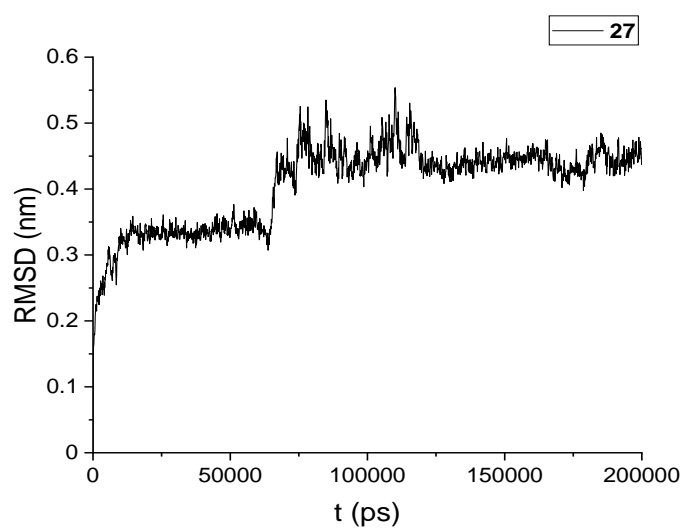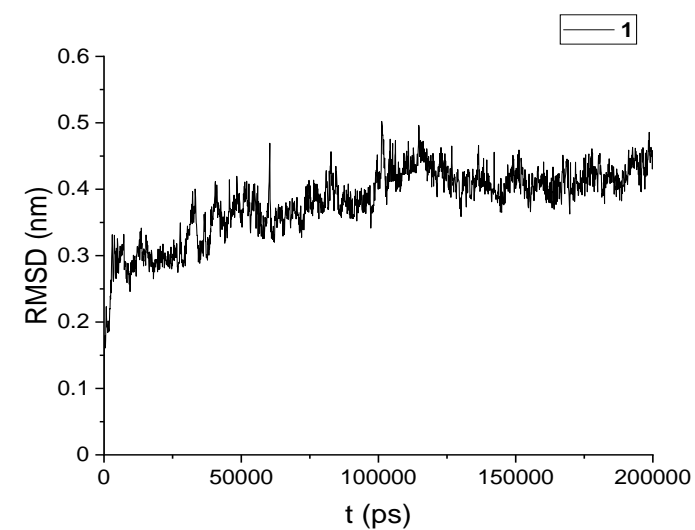
Figure S190. RMSD and radius of gyration (R_g) for complexes of peptides **1** and **27** with RBD of the S protein during MD simulations.

References

[S1] C.D. Schwieters, J.J. Kuszewski, and G.M. Clore, Progr. NMR Spectroscopy, 2006, 48, 47-62.

[S2] R. Yan, Y. Zhang, Y. Li, L. Xia, Y. Guo, Q. Zhou, Science, 2020, 367, 1444−1448.

[S3] L. Cao, I. Goreshnik, B. Coventry, J. B. Case, L. Miller, L. Kozodoy, R. E. Chen, L. Carter, A. C. Walls, Y.-J. Park, E.-M. Strauch, L. Stewart, M. S. Diamond, D. Veesler, D. Baker, Science, 2020, 370, 426–431.

[S4] W. S. Horne, L. M. Johnson, T. J. Ketas, P. J. Klasse, M. Lu, J. P. Moore, S. H. Gellmana, Proc. Natl. Acad. Sci. U. S. A. 2009, 106, 14751–14756.

[S5] B. R. Miller III, T. D. McGee Jr., J. M. Swails, N. Homeyer, H Gohlke, A. E. Roitberg, J. Chem. Theory Comput., 2012, 8, 3314-3321.

[S6] D.A. Case, H.M. Aktulga, K. Belfon, I.Y. Ben-Shalom, J.T. Berryman, S.R. Brozell, D.S. Cerutti, T.E. Cheatham, III, G.A. Cisneros, V.W.D. Cruzeiro, T.A. Darden, N. Forouzesh, G. Giambaşu, T. Giese, M.K. Gilson, H. Gohlke, A.W. Goetz, J. Harris, S. Izadi, S.A. Izmailov, K. Kasavajhala, M.C. Kaymak, E. King, A. Kovalenko, T. Kurtzman, T.S. Lee, P. Li, C. Lin, J. Liu, T. Luchko, R. Luo, M. Machado, V. Man, M. Manathunga, K.M. Merz, Y. Miao, O. Mikhailovskii, G. Monard, H. Nguyen, K.A. O'Hearn, A. Onufriev, F. Pan, S. Pantano, R. Qi, A. Rahnamoun, D.R. Roe, A. Roitberg, C. Sagui, S. Schott-Verdugo, A. Shajan, J. Shen, C.L. Simmerling, N.R. Skrynnikov, J. Smith, J. Swails, R.C. Walker, J. Wang, J. Wang, H. Wei, X. Wu, Y. Wu, Y. Xiong, Y. Xue, D.M. York, S. Zhao, Q. Zhu, and P.A. Kollman (2023), Amber 2023, University of California, San Francisco.

[S7] A. T. Bogetti, H. E. Piston, J. M. G. Leung, C. C. Cabalteja, D. T. Yang, A. J. DeGrave, K. T. Debiec, D. S. Cerutti, D. A. Case, W. S. Horne, L. T. Chong, J. Chem. Phys. 2020, 14, 153, 064101.

[S8] M.J. Abraham, T. Murtola, R. Schulz, S. Páll, J.C. Smith, B. Hess, and E. Lindahl, SoftwareX, 2015, 1–2, 19–25.

[S9] E. J. Sorin, V. S. Pande, Biophys. J. 2005, 88, 2472-2493.